Studies on CO_2 capture using adsorption from simulated refinery flue gas

Thesis

submitted for the award of degree

of

Doctor of Philosophy

By

Surajit Sengupta
(Roll No.: 950901001)

Department of Chemical Engineering
Thapar University
(Formerly known as Thapar Institute of Engineering & Technology)
Patiala-147004, Punjab, India
URL: www.thapar.edu

March 2015

CERTIFICATE

This is to certify that the thesis entitled "**Studies on CO_2 capture using adsorption from simulated refinery flue gas**" being submitted by **Mr. Surajit Sengupta** to the Department of Chemical Engineering, Thapar University, Patiala for the award of degree of **Doctor of Philosophy**, is a record of bonafide research work carried out by him. Mr. Surajit Sengupta has worked under our guidance and supervision and has fulfilled the requirements for the submission of this thesis, which to our knowledge has reached the requisite standard.

The results embodied in the thesis have not been submitted in part or full to any other University or Institute for the award of any degree or diploma.

Dr. Pramod Kumar Bajpai
Distinguished Professor
Department of Chemical Engineering
Thapar University, Patiala

Dr. Haripada Bhunia
Associate Professor
Department of Chemical Engineering
Thapar University, Patiala

Dr. Asit Kumar Das
Head
Refining R&D,
Reliance Technology Group
Reliance Industries Limited

ACKNOWLEDGEMENTS

I am highly grateful to the authorities of Thapar University, Patiala for providing this opportunity to carry out the present research work. I have got the opportunity to associate myself with Prof. Pramod Kumar Bajpai, Distinguished Professor and Dr. Haripada Bhunia, Associate Professor, Department of Chemical Engineering, Thapar University, Patiala as my supervisors. They have given me their invaluable encouragement, helpful suggestions and supervision throughout the course of this work.

I am highly grateful to Dr. Asit Kumar Das, Head, Refining R&D, RIL Jamnagar as one of my Supervisors for his invaluable supervision during this research work. He has always given me his valuable guidance, suggestions and knowledge throughout this research work. He has inspired me to become an independent researcher and helped me by providing the lot of research facilities in R&D Jamnagar and the foremost thing is that he has made me realize the power of critical reasoning. He also provided me constructive criticism, which helped me develop a broader perspective to my thesis.

I am also highly thankful to the Management, Reliance Industries Limited for allowing me to do this work at Refining R&D division in RIL Jamnagar with excellent research facilities.

I am grateful to all my supervisors for showing me all the angles of research life. Their deep insight into the problem and ability to provide constructive suggestions have been of immense value in improving the quality of my research work at all stages.

Heartiest thanks to Prof. Prakash Gopalan, Director, Thapar University, Patiala, and Dr. Raj Kumar Gupta, Associate Professor and Head, Department of Chemical Engineering, Thapar University, Patiala, and all faculty members for their encouragement and support during this research work.

My sincere thanks also go to the doctoral committee members for their valuable suggestions during this research work.

I am also thankful to Dr. Vinay Amte, Dr. Satyanarayana Reddy, and other colleagues of RIL Jamnagar for their full support, constant inspiration and encouragement during the course of this study. I am also thankful to all the authors whose research work has been referred to by me.

I am also thankful to some of the fellow researchers at Thapar University for the valuable support extended during research work. These include Ms. Chitrakshi Goel, Ms. Kimi Jain and Mr. Gaurav Madhu.

I acknowledge with thanks the help rendered by my colleagues while carrying out laboratory analysis and pilot plant trial experiments.

I express my gratitude to my wife Priyanka Sengupta, son Shubhayus Sengupta and my parents and other family members for their patience, sacrifice, and support throughout the research work. In particular, my wife and son have been my best companion and supported, encouraged and helped me go through this period in the most positive way. I would like to thank the God for giving me the inspiration and strength to complete my study in good health.

Date: 16/03/2015
Place: Patiala

Surajit Sengupta
(Surajit Sengupta)

ABSTRACT

Carbon dioxide (CO_2) capture is a major concern around the world because of its detrimental impacts on the Earth. As a mitigation measure, solid-based adsorbents have been extensively investigated to capture CO_2 from dilute flue gas streams. It has been observed, in general, that CO_2 adsorption-regeneration studies have been carried out on different types of adsorbents based on alkali metal carbonates as active precursor. So far, a great amount of work has been progressed with K_2CO_3-based adsorbents, still there is huge scope to improve the adsorption-regeneration characteristics of CO_2 adsorbents; particularly to increase the capture capacity, effective dispersion of active phase (like K_2CO_3) inside the porous structure and stability after multiple tests. Moreover, activity of these K-based adsorbents in continuous CO_2 removal is merely reported so far. The development of low cost, energy efficient CO_2 capture process is also needed to minimize CO_2 emissions into the atmosphere.

The present work intends to bridge the gaps related with the improvement in both adsorbent and process development. CO_2 adsorption studies were performed using a series of adsorbents prepared by incipient wet impregnation method. Several adsorbents using alumina-clay as support and sodium carbonate (Na_2CO_3) as active component were prepared and characterized for textural properties with the objective to correlate with CO_2 adsorption and desorption. The effects of adsorption temperature, Na_2CO_3 loading on the support material and feed CO_2 concentration were evaluated using simulated flue gas with 3 – 9 vol% CO_2, 2.5 vol% H_2O and balance N_2 at 55 °C in a fixed bed reactor. 20-wt% Na_2CO_3 based adsorbent showed maximum CO_2 adsorption capacity of 0.39 mmol/g of adsorbent at flue gas temperature of 55 °C and CO_2 content of about 8 v/v %. At increased adsorption temperature, CO_2 adsorption capacity of this adsorbent decreases. The best fitted parameters, V_m of 0.875 mmol/g and k of 0.148 bar^{-1} using the Langmuir equation are estimated. The estimated activation energy of this adsorbent system is 42 kJ/mol. The lower CO_2 adsorption capacity with these adsorbent systems is due to the effect of water content in flue gas streams. That is why the role of water content in feed simulated flue gas needs to be examined. Similarly, textural properties of the support material play an important role to achieve higher CO_2 adsorption capacity. Homogeneous dispersion of active phase needs to be assured to produce available active sites for CO_2 adsorption.

This work particularly focuses on the effect of adsorbent preparation by single- and multi-step impregnation of K_2CO_3 on alumina support and their adsorption/regeneration performance in a fixed bed reactor system. It also highlights the role of physico-chemical properties of

adsorbents prepared by both methods on adsorption and regeneration characteristics. The multi-step impregnation (MI) method enables uniform dispersion of active species (K_2CO_3) in the broad macro-pores without blocking narrower meso-pores. This facilitates higher loading of accessible K_2CO_3 for CO_2 adsorption and hence, higher adsorption capacity. The single-step impregnation (SI) method suffers from blockage of narrower meso-pores by excessive growth of K_2CO_3. This limits the CO_2 accessibility towards active species in the porous structure due to formation of larger active species aggregates. For 50-wt% K_2CO_3/Al_2O_3 prepared by MI and SI method, the maximum CO_2 adsorption capacity at 8 vol% CO_2 is found to be 3.12 and 2.1 mmol/g respectively. The regeneration efficiency of 50MI and 50SI are observed to be nearly 65% and 56% respectively, at 130 ^oC in multi-cycle testing. From the results, it is concluded that adsorbent prepared by MI method shows better performance due to its tunable textural and morphological properties to achieve higher CO_2 adsorption capacity.

Another objective of this study is to develop new K_2CO_3-based adsorbents having improved regeneration properties with stable adsorption capacity during multiple cycle studies. The acidity of alumina support is presumed to be responsible for preferential formation of $KAl(CO_3)_2(OH)_2$, which in turn requires high temperature for regeneration (>300 ^oC) as reported in literatures. Keeping this in view, the alumina support has been modified by (i) applying heat treatment, (ii) treatment with alkali hydroxide followed by calcination, etc. so as to reduce the surface hydroxyl concentration/ acid sites. The modified adsorbents were evaluated in a fixed bed reactor system over a temperature range of 55-75 ^oC with 8 vol% of CO_2 in a simulated flue gas mixture. Various physico-chemical properties were studied to explain the adsorption as well as regeneration of such adsorbents. The effects of operating parameters such as adsorption temperature, thermal dehydration of support material, gas-hourly space velocity (GHSV) during regeneration have also been studied. The CO_2 adsorption capacities are found to be in the range of 2.3 - 2.6 mmol CO_2/g of adsorbent, which also shows good stability after multi-cycle tests. There is a significant reduction of regeneration temperature (from 350 ^oC to 130 ^oC) of these K_2CO_3/Al_2O_3 adsorbents. The developed adsorbents also show high attrition resistance and thus can be effectively used in commercial application for CO_2 capture.

This study also focused on carbonation-regeneration characteristics of 35-wt% K_2CO_3/ Al_2O_3 adsorbents in both non-circulating fluidization and continuous circulation between two inter-connected fluidized-bed reactor systems. The key interest of this study is to highlight the effect of process parameters such as adsorption temperature, water content in inlet flue gas, GHSV

and nature of sweep gas used for desorption. The work attempts to bring out the important results of pilot scale trials using an existing FCC pilot unit. In particular, it presents results which are critical for transitioning from lab scale to the most efficient industrial scale in the development of low cost CO_2 capture process with lower regeneration temperature and multi-cycle stability. The adsorption capacity was found to be 1.42 mol CO_2/kg of adsorbent in non-circulating fluid bed at Pilot scale, which is 71% of the adsorption capacity achieved in fixed-bed adsorption at Lab scale. Multiple adsorption-regeneration cycles were done in two separate fluidized beds, with continuous circulation of the adsorbent between the two beds, in order to investigate the effect of adsorption and regeneration temperature, water vapor content in simulated inlet flue gas stream, gas-hourly space velocity (GHSV) and mode of adsorbent regeneration. More than 80% CO_2 removal was achieved from a simulated flue gas stream having 8.3 vol% CO_2, 15.8 vol% H_2O and rest N_2. The adsorbent showed excellent structural stability after 144 hours of continuous operation. It was found that the performance of the CO_2 removal was very sensitive to the water vapour content in the inlet simulated flue gas and the gas velocity in the adsorber bed (gas-solid contact time in the adsorber). The performance evaluation results from the CO_2 capturing adsorbent in fluidized bed system at pilot scale were very promising and encouraging to scale up the trials further to demonstration level.

There is an increased interest in developing less expensive and/or energy integrated processes for capturing CO_2 as the present capture cost using conventional amine absorption process is high (nearly 100 \$/Ton CO_2). The adsorption processes, generally employing solid adsorptive material that fall under the post combustion category, serve as an alternative to the absorption based process. This is because replacing water by solid support greatly reduces the energy required for CO_2 capture due to the lower heat capacity of solid supports as compared to water. The proposed energy-integrated process for CO_2 capture from flue gas stream is very cost-effective, energy-intensive process. The estimated cost per ton of CO_2 captured is found to be one third of the cost associated with conventional amine absorption process. Significant improvements on utility and power requirement helps to make heat integrated based CO_2 capture more economically competitive. An important feature of the study is analysis of key performance parameters that influence the cost economics. Understanding the nature of these impact, and the potential for reducing them, is crucial to projecting future costs and capabilities of new technologies for carbon capture.

PUBLICATIONS/ PATENTS

Publications in SCI journals

1. **Sengupta, S**., Amte, V., Dongara, R., Das, A.K., Bhunia, H., Bajpai, P.K. Effects of adsorbent preparation method for CO_2 capture from flue gas using K_2CO_3/Al_2O_3 adsorbents. *Energy & Fuels.* **2015**, 29, 287-297.

2. **Sengupta, S.**, Reddy, S.A, Dongara, R., Das, A.K., Bhunia, H., Bajpai, P.K. Improvement in regeneration properties and multi-cycle stability for K_2CO_3/Al_2O_3 adsorbents for CO_2 removal from flue gas. *Energy & Fuels*. **2014**, 28(8), 5354-5362.

Publication in Conference Proceedings

1. **Sengupta, S.**, Yadav, H., Dinda, S., Dongara, R., Das, A.K., Bhunia, H., Bajpai, P.K. Low temperature regenerable sorbent for carbon dioxide capture from flue gas. Proc. Advances in Chemical Engineering-II, *Macmillan Publisher India Ltd.* **2011**, 295-301.

Patents applied

1. Reddy, S.A., **Sengupta, S.**, Dongara, R., Das, A.K., Amte, V., Yadav, A.H., Bajpai, P.K., Bhunia, H. Stabilized inorganic oxide supports and adsorbents derived therefrom for carbon dioxide capture. (Patent Application No.: 866/MUM/**2014**).
2. Amte, V., Das, A.K., **Sengupta, S.**, Yadav, M., Mandal, S., Pal, A., Gupta, A., Bhujade, R., Reddy, S.A., Dongara, R. A single compression system and process for capturing carbon dioxide (Patent Application No.: 3190/MUM/**2013**).
3. Amte, V., Das, A.K., **Sengupta, S.**, Yadav, M., Mandal, S., Pal, A., Gupta, A., Bhujade, R., Reddy, S.A., Dongara, R. A single compression system and process for capturing carbon dioxide (Patent Application No.: PCT/IN/**2014**/000628).
4. Reddy, S.A., **Sengupta, S.**, Dongara, R., Das, A.K., Amte, V., Yadav, A.H., Bajpai, P.K., Bhunia, H. Stabilized inorganic oxide supports and adsorbents derived therefrom for carbon dioxide capture (Patent Application No.: PCT/IB**2015**/050636).
5. **Sengupta, S.**, Amte, V., Das, A.K., Reddy, S.A., Mandal, S., Yadav, M., Gohel, A., Nerivetla, S., Nath, K. Process for CO_2 capture from flue gases using K_2CO_3-Al_2O_3 adsorbent in circulating fluidized reactor system (Patent Application No.: 1963/MUM/**2015**).

DEDICATION

To

My Dear Wife

Mrs. Priyanka Sengupta

My Parents

Mr. Sukumar Sengupta and Mrs. Krishna Sengupta

Our Beloved Son

Mast. Shubhayus Sengupta

TABLE OF CONTENTS

LIST OF FIGURES

LIST OF TABLES

LIST OF SYMBOLS

Symbol	Description	Unit
$	US dollar	-
%T	Percent transmission	%
b	Adsorption equilibrium constant	-
C	BET constant	-
$C_{CO_2 in}$	Inlet CO_2 concentration in feed simulated gas	vol%
$C_{CO_2 out}$	Outlet CO_2 concentration in treated simulated gas	vol%
d	Space between diffracting planes	Å
E	Activation energy	kJ/mol
ΔH	Isosteric heat of adsorption	kJ/mol
ΔH_r	Heat of reaction	kJ/mol
K	Freundlich constant	-
K	Affinity constant	-
k_a	Adsorption rate constant	$s^{-1}bar^{-1}$
k_d	Desorption rate constant	s^{-1}
K_e	Equilibrium constant	bar^{-1}
m	Mass of adsorbent	mg
n	constant	-
nm	Nanometer	-
P	Partial pressure	bar
p_{CO2}	Partial pressure of CO_2 at inlet	bar
P_o	Saturation pressure	bar
q	Adsorbed amount of adsorbate	mmol/g
Q	Heat of adsorption	kJ/mol
q_m	Maximum adsorption capacity	mmol/g
$q_{m,o}$	Maximum adsorption capacity at 298 K	mmol/g
q_t	Adsorption capacity at any given time '*t*'	mmol/g
R	Universal rate constant	$J/mol.K^{-1}$
T	Temperature	K

T_{ads}	Adsorption temperature in adsorber	^{o}C
t_{gas}	Gas residence time	sec
T_o	Temperature at 298 K	K
T_{reg}	Desorption temperature in desorber	^{o}C
t_{solid}	Adsorbent residence time	min
U_o	Superficial gas velocity	m/s
V	Adsorbed gas quantity	mmol/g
$V_{A\ or\ D}$	Volume of adsorber (A) or desorber (D)	m^3
$v_{A\ or\ D}$	Volumetric flow in adsorber and desorber	m^3/h
V_{ads}	CO_2 adsorption capacity	mmol/g
V_m	Monolayer capacity	mmol/g
V_m	Maximum capacity CO_2 adsorbed	mmol/g
W_{solid}	Weight of adsorbent	kg
Greek letters		
x	Mass of adsorbate	mg
α	Alpha phase of alumina (Al_2O_3)	-
β	Beta zeolite	-
γ	Gamma phase of alumina (Al_2O_3)	-
δ	Delta phase of alumina (Al_2O_3)	-
η	CO_2 removal efficiency	%
θ	Theta phase of alumina (Al_2O_3)	-
θ	Bragg's angle	^{o}
θ	Fractional coverage	mol/mol
λ	Wavelength of X-ray	nm
μm	Micrometer	-
φ	Dimensionless parameter	-

LIST OF ABBREVIATIONS

Abbreviations	Description
AI	Attrition index
ALC	Alumina-clay composite
BET	Brunauer-Emmett-Teller
EDX	Energy-dispersive X-ray spectroscopy
FTIR	Fourier transform infrared spectroscopy
GC	Gas chromatography
GHG	Greenhouse gas
GHSV	Gas-hourly space velocity
MEA	Monoethanol amine
MFC	Mass flow controller
MI	Multi-step impregnation
HeX	Heat exchanger
LL	Lean loading
PEI	Polyethyleneimine
PSD	Pore size distribution
RL	Rich loading
SA	Surface area
SAED	Selected area electron diffraction
SC	Sodium carbonate
SCR	Solid circulation rate
SEM	Scanning electron microscopy
SI	Single-step impregnation
TCD	Thermal conductivity detector
TEM	Transmission electron microscopy
TGA	Thermo gravimetric analysis
TPD	Temperature programmed desorption
TPV	Total pore volume
WPV	Water pore volume
XRD	X-Ray diffraction

Chapter 1

Introduction

1.1 Greenhouse gases and global warming

Earth's average temperature is increasing significantly since last three decades, which is affecting detrimental changes on climate. In one side rapid industrial growth has helped to meet the global energy demand, but on the other side mother Earth is in danger due to its significant impacts on the environment. Figure 1.1 shows the increase in the difference between the global mean land-ocean surface temperature delta and the 5 year average temperature delta from 1880-2013 [1]. From Figure 1.1, the increase in average temperature delta is observed to be 0.45 ^{o}C between 1980 and 2005, which influenced the occurrence of various natural calamities around the world. The major greenhouse gases (GHGs) are: sulfur hexafluoride (SF_6), polyfluorocarbons (PFCs), hydrofluorocarbons (HFCs), nitrous oxide (N_2O), methane (CH_4), and carbon dioxide (CO_2), [2] in the descending order of global warming potential (GWP) in the Earth's atmosphere. Of these GHGs, although SF_6 and other PFCs have the significant GWP, but their contribution towards global warming is less due to lower generation rate. On the other hand, CO_2 is generated in large quantity due to rapid industrialization, exhibiting the highest contribution of 76% towards global warming. Table 1.1 shows the contribution to global warming by various GHGs [2]. International Energy Agency [3] predicts 57% increase of energy demand from 2004 to 2030. In current stage, over 85% of world energy demand is supplied by fossil fuels which are responsible for roughly 40% of global CO_2 emissions. Global energy-related CO_2 emissions increased by 3.2% in 2010, reaching a record high of 31.2 gigatonnes (GT) in 2011 [4].

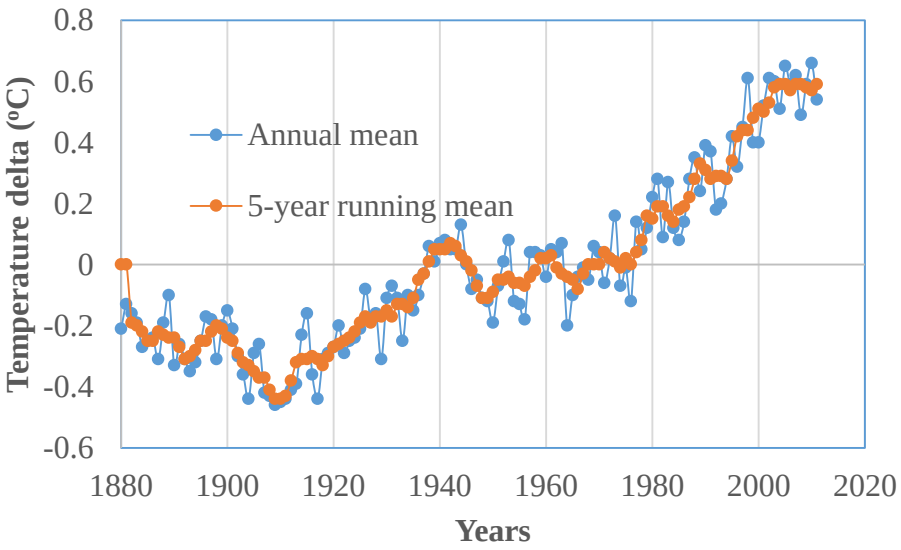

Figure 1.1 Global annual mean surface air temperature change [1]

Among the greenhouse gases (GHGs), CO_2 is the largest contributor in regard of its amount present in the atmosphere contributing to 76% of global warming effects, although methane and chlorofluorocarbons have much higher greenhouse potential as per mass of gases. Due to the greenhouse effect of CO_2, the enormous emission increased levels is a major cause of concern to the global warming. Hence, there is an urgent need to close the sizable gap between intentions and actions to reduce greenhouse gas emissions and its utilization in a sustainable method is a major concern around the world [6].

Table 1.1 GHGs: contribution to global warming [5]

GHGs	**Descriptions**	**GWP**	**Contribution to Global Warming**
CO_2	Produced by living organisms and human/ industrial activities, especially fossil fuel combustion	**1**	**76%**
CH_4	Produced by plant and animal material decay; the main constituent in natural gas	21	12%
N_2O	Produced during fossil fuel combustion, production/ application of nitrogen fertilisers, and from natural sources	310	11%
HFCs	Developed to replace CFCs; used in refrigeration as well as the manufacture of semi-conductors	140-11700	<1%
PFCs	Released during the aluminium refining process	7400	<1%
SF_6	Used in heavy industry to insulate high-voltage equipment and released in the production of magnesium	25000	<1%

The atmospheric concentration of the CO_2 was 390 ppm in 2000, a full 100 ppm above its pre-industrial level and further exceeded recently to 400 ppm and is growing rapidly about 1.5-2 ppm per year. Intergovernmental Panel on Climate Change (IPCC) predicts that, by the end of 21^{st} century, the atmosphere may contain up to 570 ppm CO_2 if no mitigation and emissions reduction options are applied. To have a reasonable chance of avoiding such dire consequences of global warming, the IPCC has recommended a 50-85% reduction of global GHG emissions from 2000 to 2050 and a peak in emissions no later than 2015. IEA recommends to cut down the CO_2 emissions by 50-65% of their 2005 levels by 2030 [4] – the target necessary to limit the global warming between 2-3 ^oC that would require a reduction of 43 GT of CO_2 per year.

Energy can be generated from renewable sources and used more efficiently; fossil power can be de-carbonized by CO_2 capture and storage. Efforts to limit CO_2 emissions will need to be strengthened massively if they are to keep concentrations from reaching dangerous levels.

The challenges are not unbeatable, but will require a steadfast, coordinated approach -one that is orders of magnitude larger and faster than current progress. There are three options to minimize total CO_2 emission into the atmosphere, (a) to reduce energy intensity, (b) to reduce carbon intensity, and (c) to enhance the sequestration of CO_2. The first option involves efficient use of energy, while the second option needs alternative use of non-fossil fuels such as hydrogen and renewable energy. The third option requires the development of technologies to capture and sequester more CO_2.

1.2 Trends in CO_2 capture development

Currently, there are two general trends in CO_2 capture development: (i) to address the inefficiencies of amine absorption process and identify ways to improve it and (ii) to develop alternative capture technologies that have the potential for dramatic operating and capital cost reduction. The first pathway is expected to provide reductions of 20% to 30% of cost in the near-term and 40% to 50% in the mid-term. Improvements in cost in the near-term could come from using promoted chemicals, improved reactor design, and better stripping conditions.

Other improvements may include the use of high-quality steam in the stripper to regenerate solvents, which could impact the operation and output of the steam turbine significantly. Further, improved solvents with faster kinetics, lower oxidation losses, and improved absorbers (i.e., geometry, packing, staging, and lower-cost construction materials) may also contribute towards improvement. Another trend is to find altogether new chemistries or processes that will reduce the cost of capture by a factor of two to four. The chance of success is lower for this research route and the research timescale extends further into the future. Examples of technologies in this area are adsorption with metal organic frameworks, bio-fixation, and membrane facilitated separation. Several research groups are working on capture cost assessment and retrofit for specific existing plants to achieve optimum capture plant thermodynamics and economic performance.

Although several CO_2 capture systems have operated commercially for nearly two decades on a portion of power plant flue gases, no capture units have yet been applied to the full flue gas

stream of a modern coal-fired or gas-fired power plant. Thus, one or more demonstrations of CO_2 capture at full scale are widely regarded as crucial for gaining the acceptance of this technology by power and process plant. One reason is the high cost of each project, estimated at roughly $1 billion for CO_2 capture at a 400 MW unit operating for five years. Most of the announced demonstration of full scale power plant CO_2 capture have been cancelled or delayed due to construction price escalation. Nevertheless, it appears reasonable to assume that at least some of the large scale projects for CO_2 capture will materialize over next few years with costs shared between the public and private sectors [7].

In general, the more efficient the power plant, the smaller are the energy penalty impacts. For this reason, replacing or repowering an old, inefficient plant with a new, more efficient facility with CO_2 capture can still yield a net efficiency gain that decreases all plant emissions and resource consumption. Thus, the net impact of the energy penalty is best appreciated in the context of strategies for reducing emissions across a fleet of plants, including existing facilities as well as planned new units. Innovations in power generation, refineries and development of new carbon capture technologies are expected to further reduce future energy penalties and their impacts.

1.3 Technology options for CO_2 capture

A wide range of technologies currently exist for separation and capture of CO_2 from gas streams, although these might have not been designed specifically for single point source emission from power plant, refinery or any other process plants. These are based on different physical and chemical processes including absorption, adsorption, membranes and cryogenics in accordance to technology options as shown in Figure 1.2.

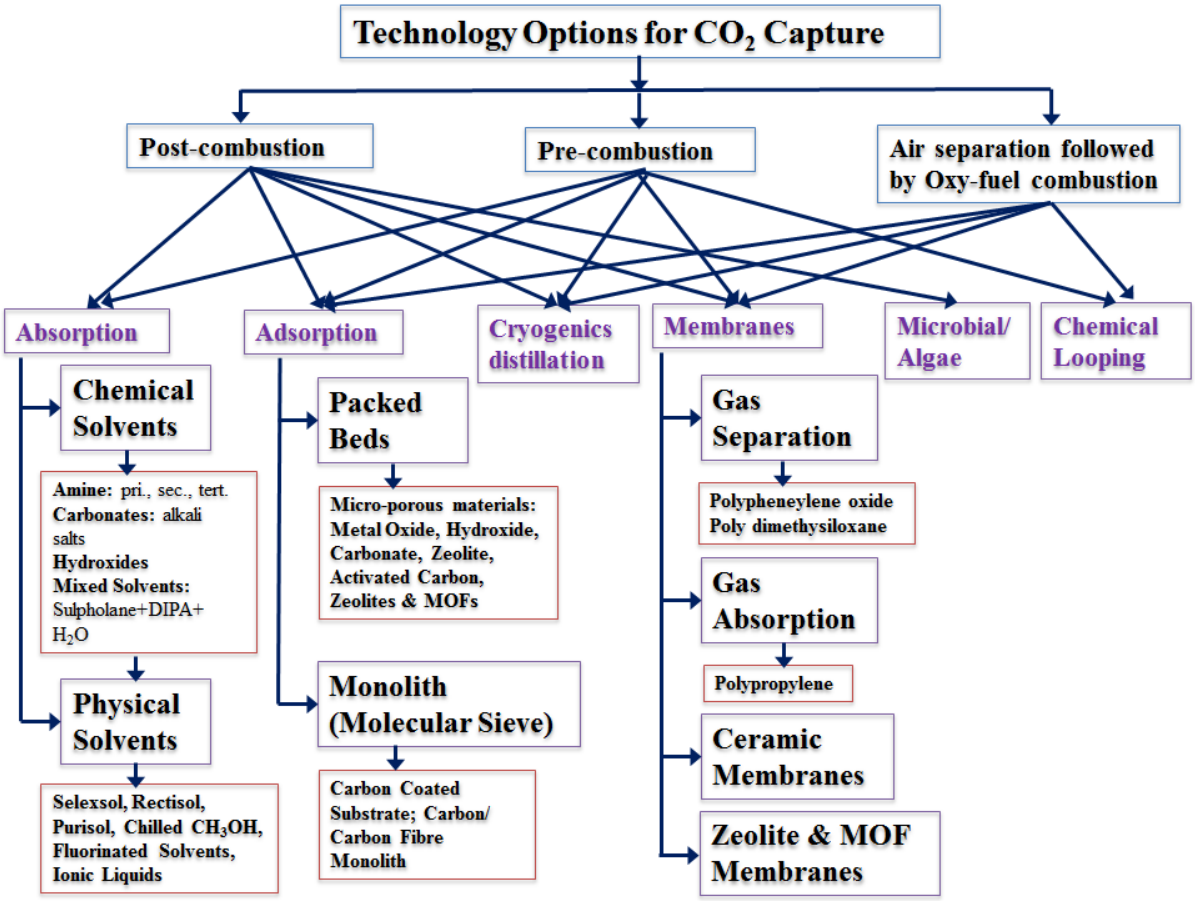

Figure 1.2 Technology options for CO_2 separation and capture [8]

Three approaches namely, pre-combustion, post-combustion and oxy-fuel combustion are generally adopted to reduce CO_2 emissions from large stationery sources. Among these three approaches, post-combustion capture route is preferred due to its low cost of capture, capable to handle dilute flue gas and easy retrofitting. The choice of a suitable technology depends upon the characteristics of the flue gas stream from which CO_2 needs to be separated. It is sure that capture process which would recover 80-90% of the CO_2 from a given source will attract considerable attention even though it may incur 60-80% of the overall CCS cost, both in terms of capital (CAPEX) and operating (OPEX) expenditure. The greater attention is primarily focussed on energy efficiency and volumetric capture capacity of the process. Various post-combustion CO_2 capture processes including absorption, membrane separation, cryogenic techniques etc. are well-known for capturing CO_2 from flue gas streams. But these processes have some demerits like higher regeneration energy, operational and reliability issues and high cost for CO_2 capture [9-10]. Classically on thermal basis, an energy expense of 3.5-4.2 GJ/ton CO_2 is incurred by the conventional absorption amine (MEA) solvents. A 1.25-2 GJ/ton CO_2

is often considered as a major target in order to achieve acceptable CO_2 capture costs. Hence, the demand for more sustainable and effective CO_2 capture process has driven renewed interest in adsorption route. The solid adsorption process offers potential for selective uptake and release of CO_2. The unique features that make adsorption process more receptive to CO_2 capture are: (i) high sorption capacity; (ii) excellent tunable physical properties; (iii) lower regeneration energy and temperature; (iv) tolerance to impurities; (v) low cost; (vi) minimal reliability issues, e.g. no corrosion/ degradation etc. Although the adsorption route possess alternative to conventional capture processes, it also invite improvements for its applicability. Various solid adsorbents including zeolites 13X, activated carbon, alkali metal carbonates, metal organic framework (MOF), etc. are reported in literature for effective separation of CO_2. Among these, MOFs have presented significant CO_2 adsorption capacity (3-33 mmol/g at 25 ^oC, 40 bar) [11]. These materials are promising candidates for adsorptive separation of CO_2 using pressure swing adsorption (PSA) technique. On the other hand, alkali metal carbonate based solid adsorbents are widely investigated as a capture media for CO_2 from dilute flue gas streams [12-20] by temperature swing adsorption. Previous studies on K_2CO_3 based adsorbents have shown better CO_2 adsorption capacity than Na_2CO_3 [13].

In this research work, efforts have been focused on the development of novel adsorbents and energy-efficient process for post-combustion CO_2 capture that could lead to effective cost reduction in terms of CAPEX (capital expenditure) and OPEX (operating expenditure). This work is aimed at producing potassium carbonate-based adsorbents supported on alumina and an energy-integrated process for CO_2 removal from simulated refinery flue gas for application on post-combustion carbon capture. This research has focussed on the effect of adsorbent preparation method, improvement in adsorbent regeneration properties and a process for continuous CO_2 removal at low regeneration temperature.

1.4 The scope and objectives of thesis

It has been observed, in general, that CO_2 adsorption-regeneration studies have been carried out on different types adsorbents based on alkali metal carbonates as active precursor. So far, a great amount of work has been progressed with K_2CO_3-based adsorbents, still there is huge scope to improve the adsorption-regeneration characteristics of CO_2 adsorbents; particularly in increase in capture capacity, effective dispersion of active phase (like K_2CO_3) inside the porous structure and stability after multiple tests [12-22]. Moreover, activity of these K-based adsorbents in continuous CO_2 removal is merely reported so far.

The present work intends to bridge the gaps related with the improvement in both adsorbent and process development. The present work particularly emphasizes on the effect of the adsorbent preparation method by single- and multi-step wet impregnation of K_2CO_3/Al_2O_3 adsorbents and their adsorption/ regeneration characteristics in a down-flow fixed-bed reactor. The physico-chemical properties of the adsorbents prepared by both the methods are well correlated with on adsorption and regeneration characteristics.

Another objective of this study is to improve regeneration properties of K_2CO_3-based adsorbents with stable adsorption capacity during multiple cycle testing. The total acidity of alumina support is supposed to be responsible for the formation of deactivating species $KAl(CO_3)_2(OH)_2$, which requires higher regeneration temperature (> 300 ^oC) as reported in literatures [21-22]. In respect of this, the alumina support materials have been modified/ stabilized by (i) applying heat treatment, (ii) treatment with alkali hydroxide followed by heat treatment, etc. so as to reduce the concentration of surface hydroxyl group/acid sites. The adsorption-regeneration studies were conducted with modified adsorbents in a fixed bed reactor system at 55-75 ^oC with 8 vol% of CO_2 in a simulated flue gas stream. The results of various physico-chemical properties of the support and adsorbents were explained the adsorption as well as regeneration of prepared adsorbents.

This study also focused on carbonation-regeneration characteristics of K_2CO_3/Al_2O_3 adsorbents in both non-circulating fluidization and continuous circulation between two inter-connected fluidized-bed reactor systems. The key interest of this study is to highlight the effect of process parameters such as adsorption temperature, water content in inlet flue gas, GHSV and nature of sweep gas used for desorption. The work attempts to bring out the important results of Pilot scale trials using an existing FCC pilot unit. In particular, it presents results which are critical for transitioning from Lab scale to the most efficient industrial scale in the development of low cost CO_2 capture process with lower regeneration temperature and multi-cycle stability.

Another objective of this study is to develop a low cost, energy-integrated process for CO_2 capture from flue gas stream. Since, conventional amine absorption technique is only available to capture CO_2 from flue gas streams, which is involved with high capture cost and wasting of heat energy. Therefore, in this study, an approach for developing low cost energy-integrated adsorptive CO_2 capture process is undertaken. A base case study with conventional MEA absorption process is performed using ProMax software. The key interest of this study is to

develop a low CO_2 capture cost process and compared with the conventional amine absorption route.

The overall objective of the research is to develop effective adsorption process, stable under the acidic conditions of flue gas, for the continuous removal of CO_2.

The specific objectives are:

- Preparation and characterization of adsorbent(s).
- Kinetic study of CO_2 removal from simulated refinery flue gas streams using different adsorbent(s).
- Regeneration study of selected adsorbent(s).

1.5 Thesis overview

This thesis is divided into eight chapters. Various experimental methods were applied to measure and analyze the support materials, K_2CO_3-based adsorbents, and characteristic products of the CO_2 adsorption-regeneration. These methods include BET surface area and pore volume analysis, average particle size, X-ray diffraction (XRD), scanning electron microscopy (SEM) with energy dispersion X-ray spectroscopy (EDX), transmission electron spectroscopy (TEM), Fourier transmission infrared spectroscopy (FTIR), temperature programme desorption (TPD), total acidity, thermo-gravimetric analysis (TGA), attrition index (AI).

Chapter 1 covers the various greenhouse gases and their potential to global warming. This chapter introduces trends in CO_2 capture development and emerging technology options for CO_2 capture. This chapter also presents aims and objectives of this research work.

Chapter 2 discusses the literature review, wherein a detailed literature study on CO_2 capture processes including their merits and demerits, various post-combustion capture routes including absorption, solid adsorption, membrane process, etc. Much attentions have been given on adsorption route for CO_2 capture using various commercial adsorbents, metal-impregnated adsorbents.

Chapter 3 covers the experimental methods, which includes fundamental techniques used in characterizing and analyzing different supports and adsorbents for obtaining results. The

modification of support materials, method of adsorbents preparation have been discussed in this chapter. It also presents the experimental set up for carrying out the entire experimental work in both fixed-bed (laboratory scale) and fluidized-bed (pilot scale). Various adsorption isotherms and kinetic models are discussed to obtain the adsorption kinetic parameters.

Chapter 4 presents the results obtained by preparing adsorbents of Na_2CO_3 supported on alumina-clay based composite materials. In this work, experiments were carried out to evaluate CO_2 adsorption performance with different carbonate loading and at different adsorption temperature.

Chapter 5 presents the results obtained by preparing adsorbents in different approaches and their efficacy in terms of CO_2 adsorption capacity, metal carbonate dispersion. In this work, K_2CO_3/Al_2O_3 adsorbents were prepared using single- and multi-step incipient wet impregnation method. The activity of these various adsorbents were evaluated in a fixed-bed adsorber system. In this chapter, various physico-chemical properties have been discussed to explain how multi-step impregnation method is superior to single-step method with similar active phase loading. Isosteric heat of adsorption for K_2CO_3/Al_2O_3 adsorbents has been first discussed in this chapter.

Chapter 6 discusses the results obtained from the surface modification of the support materials and adsorbents. In this chapter, the preparation methods of support material, specifically gamma alumina and their textural and chemical properties have been discussed. In this work, the support material was modified using heat treatment at higher temperatures and also with alkali treatment followed by calcination to reduce total acidity. Various textural and chemical characteristics have been studied to explain reduction of formation of deactivating species $KAl(CO_3)_2(OH)_2$ with calcination temperatures. This chapter presents a detailed investigation on how acidity of gamma alumina significantly affect adsorbent regeneration properties.

Chapter 7 discusses the results obtained from continuous CO_2 adsorption-regeneration in circulating fluid-bed reactors at pilot scale level. In this chapter, effects of several operating parameters have been widely discussed in both batch fluidization and circulating fluidization mode. In this work, effects of water in simulated flue gas, mode of water injection into the adsorber, gas velocity, regeneration temperature, mode of sweep gas, etc. in circulating fluidized bed reactors have been given. This chapter presents how partial regeneration of

adsorbent helps to achieve more than 80% CO_2 removal efficiency in a circulating fluidized bed reactors with low temperature differential between adsorption and desorption.

Chapter 8 presents an approach for developing low-cost, energy-intensive adsorptive process for CO_2 capture from flue gas. In this chapter, a base case performance evaluation is performed for conventional monoethanol amine (MEA) absorption process for CO_2 capture using ProMax equilibrium model. An energy-integrated process for CO_2 capture is also developed based on circulating fluidized bed reactors system to minimize cost of CO_2 capture using heat integration concept.

Finally, **Chapter 9** presents the conclusions and further work.

Chapter 2

Literature Review

2.1 Introduction

The control of anthropogenic carbon dioxide emissions is one of the most challenging environmental issues facing industrialized countries, because of the implications to atmospheric carbon dioxide levels and climate change [23]. Specifically, the Energy Information Administration (EIA) within the U.S. Department of Energy (DOE) estimates that the combined CO_2 emissions from China and India in 2030 from coal use will be three times that of the Unites States (China, 8286 million tonnes of CO_2; India, 1371 million tonnes of CO_2; U.S., 3226 million tonnes of CO_2) [24-25]. This illustrates that no single nation can sufficiently reduce GHGs to stabilize their atmospheric concentrations. The effort must be unified and cost effective to sustain global economic growth while reducing GHG emissions.

Carbon dioxide (CO_2) capture and storage (CCS) is a process consisting of the separation of CO_2 from industrial and energy-related sources, transport to a storage location and long-term isolation from the atmosphere. Under this concept, CO_2 would be captured from large point sources, such as power plants, and injected into geologic formations, such as depleted oil and gas fields, saline formations, and unmineable coal seams [26-27]. This approach would lock up (sequester) the CO_2 for thousands of years.

None of the currently available CO_2 capture processes are economically feasible on an implementation scale to capture CO_2 for sequestration, since they consume large amounts of parasitic power and significantly increase the cost of electricity. Thus, improved CO_2 capture technologies are vital if the promise of geologic sequestration, enhance oil recovery (EOR), and enhanced coal bed methane (ECBM) production is to be realized. The most likely options for CO_2 separation and capture include chemical absorption, physical and chemical adsorption, cryogenic separation, gas-separation using membranes, mineralization/bio-mineralization, and vegetation. The most commonly used method today is absorption of carbon dioxide by chemical or physical solvents. For low CO_2 concentrations the chemical solvents such as alkanolamines are used. For higher partial pressures physical absorbents like cold methanol, propylene carbonate, etc. are preferred. But these processes have many disadvantage like energy intensive, low capacity (CO_2 absorbed per unit mass), amine solution also has a limited lifetime due to degradation through oxidation of the amine. In addition, corrosion problems are usually observed for the aqueous amine process.

Recently, adsorption technique has been referred as a promising technique for effective separation of components in purification process namely, waste water treatment, contaminants removal from gaseous mixture, etc [10, 28-29]. Several solid sorbents (both physical and chemical adsorbents) have been utilized to remove carbon dioxide from industrial flue gas streams. Porous materials, like activated carbons and zeolites, are suitable candidates for CO_2 capture by physical adsorption, due to their highly developed porous structure. The other adsorbents which can be considered are hydrotalcites, carbon fiber composite molecular sieves, metal oxides, and metal organic frameworks (MOFs). Chemical adsorption on porous solid material has shown a significant role for CO_2 removal from dilute flue gas system. The dry regenerable solid adsorbents showed a significant cost reduction for CO_2 capture by lowering heat requirement for regeneration of capture media than that of the cost associated with conventional amine-based absorption process. On the other side, the solid adsorbents have lower heat capacity than that aqueous amine-based solvent [30-33]. Moreover, the heat capacity of solid sorbent is comparatively lower than that of an aqueous amine solvent. The success of such an approach is also dependent on the development of new materials with high adsorption capacity, high CO_2 selectivity, durability, and relatively fast kinetics of sorption and desorption. In view of the above, in the past few years, several research groups worldwide have initiated work on the development of new solid sorbents for CO_2 capture from flue gas with superior performance and desired economics.

2.2 CO_2 capture processes

Capture of CO_2 can be applied to large point sources. Large point sources of CO_2 include large fossil fuel or biomass energy facilities, major CO_2-emitting industries, natural gas production, synthetic fuel plants, oil refineries and fossil fuel-based hydrogen production plants. Capturing CO_2 directly from small and mobile sources in the transportation and residential & commercial building sectors is expected to be more difficult and expensive than from large point sources [34]. CO_2 capture from a power plant is the most expensive step, accounting for approximately 75% of the total cost. Therefore, the development of an efficient and cost-effective CO_2 capture technique is considered to be one of the highest priorities in the field of CCS [35].

There are different types of CO_2 capture systems: post-combustion, pre-combustion and oxyfuel combustion as illustrated in Figure 2.1 In post-combustion capture, the CO_2 is separated from other flue gas constituents either originally present in the air or produced by combustion. In pre-combustion capture, it is removed from the fuel before combustion, and in

oxy-combustion, the fuel is burned in an oxygen stream that contains little or no nitrogen. Table 2.1 provides a summary of the inherent advantages and disadvantages of each of these pathways. Post-combustion capture applies primarily to coal-fueled power generators that are air fired. Pre-combustion capture applies to gasification plants. Oxy-combustion can be applied to new plants or retrofitted to existing plants. Post-combustion carbon capture has the greatest near-term potential for reducing CO_2 emissions, because it can be retrofitted to existing units that generate two-thirds of the CO_2 emissions in the power sector. Typical flue gas compositions from refinery gas-fired furnaces/ heaters contain 8-12 vol% CO_2, 2-3 vol% O_2, rest N_2, along with SO_x, NO_x as impurities.

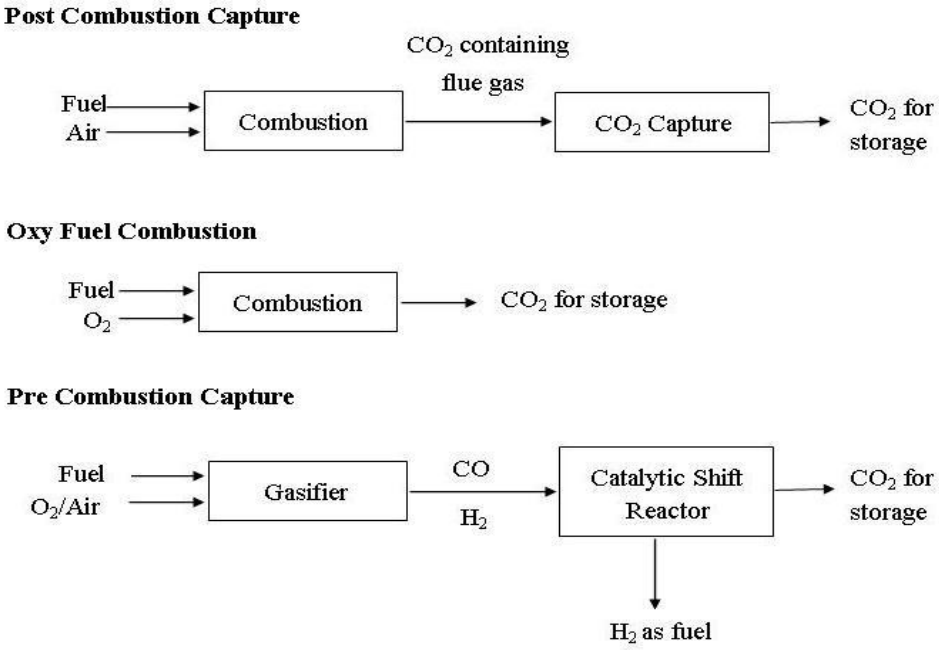

Figure 2.1 Schematic representation of CO_2 capture systems

Table 2.1 Advantages and disadvantages of different CO_2 capture approaches [23]

Capture processes	**Advantages**	**Barriers to implementation**
Post-combustion	◦ Applicable to the majority of existing coal-fired power plants ◦ Retrofit technology option	◦ Flue gas is ➢ Dilute in CO_2 ➢ At ambient pressure resulting in - Low CO_2 partial pressure - Significantly higher performance or circulation volume required for high capture levels

		- CO_2 produced at low pressure compared to sequestration requirement
Pre-combustion	◦ Synthesis gas is ➢ concentrated in CO_2 ➢ High pressure resulting in - High CO_2 partial pressure - Increased driving force for separation - More technologies available for separation - Potential for reduction in compression costs/loads	◦ Applicable mainly to new plants, as few gasification plants are currently in operation ◦ Barriers to commercial application of gasification are common to pre-combustion capture ◦ Availability ◦ Cost of equipment ◦ Extensive supporting systems requirements
Oxy-combustion	◦ Very high CO_2 concentration in flue gas ◦ Retrofit and repowering technology option	◦ Large cryogenic O_2 production requirement may be cost prohibitive ◦ Cooled CO_2 cycle required to maintain temperatures within limits of combustion materials ◦ Decreased process efficiency ◦ Added auxiliary load

2.3 Post combustion CO_2 separation and capture processes

There are several post combustion gas separation and capture technologies being investigated [35], namely; (a) absorption, (b) cryogenic separation, (c) membrane separation and (d) micro algal bio-fixation (e) adsorption. As discussed in Section 1.3, Figure 1.2 summarizes various technology options for post combustion CO_2 capture. The advantages and challenges of major CO_2 capture routes are described in Table 2.2 [36].

Table 2.2 Brief comparisons of processes for CO_2 separation and capture [36]

Processes	Advantages	Challenges
Absorption (Chemical)	- Operates at dilute CO_2 (3-20 vol%) streams and lower temperature (40-60 ^oC) with fast kinetics. - Allows good heat integration and ease of heat management.	- Solvent degradation due to impurities (SO_x, NO_x) in the gas stream amounts to solvent consumption (1.5-3.0 kg/ton CO_2). - Reclaimer stage is energy intensive. - Significant amount of steam (~2 ton/ton CO_2) required during stripping which de-rates power plant. - Significant energy required to heat, cool, and pump non-reactive carrier liquid (usually water). - Vacuum stripping can reduce regeneration energy requirement by 5-20% but is expensive; bad economy of scale.
Adsorption	- Active sites provide high adsorption capacity with fast kinetics, enabling capture from streams with low CO_2 partial pressure. - Higher capacities on per mass or volume (0.088-0.18 g CO_2/g adsorbent) basis than similar absorbents. - Lower energy requirement than absorption.	- Heat required for regeneration should be brought down. - Heat management is difficult which can limit capacity and/or create operational issues. - Pressure drop can be large in flue gas applications. - Sorbent attrition may be high.
Membrane	- Simplicity: No steam load and chemicals losses. - Membranes tend to be more suitable for high-pressure processes such as IGCC. - Simple, compact and modular designs - Lower capital costs. - Avoidance of operational problems associated with absorption such as foaming, flooding, entrainment etc.	- Gas streams must be compressed to 15-20 bar for efficient separation. - Trade-off between recovery rate and product purity (difficult to meet both at same time). - May require multiple units and recycling due to lower product purity. - Requires high selectivity (due to low CO_2 content and low pressure ratio). - Poor economies of scale. - Multiple stages and recycle streams to attain high CO_2 capture efficiency. - Membrane to handle high temperature flue gas.

Cryogenic distillation	- Physical separation of CO_2 from other gases on the basis of dew and sublimation point. - Achieves 93% CO_2 removal efficiency from a 15% CO_2 containing gas stream of $CO_2/H_2O/N_2$. - Flue gas must contain greater than 10% CO_2, as lower concentration of CO_2 will lead to higher cooling requirement per mass of CO_2 captured.	- Requires high cost of refrigerant used to cool the system. - High capital cost of equipment. - Buildup of solid CO_2 reduces the efficiency of the evaporator over time. - Water content in the feed stream must be removed to prevent equipment from formation of ice.

Although mature, absorption technology suffers from inherently high regeneration cost, equipment corrosion, and amine oxidative degradation. As a result, there is a strong tendency to develop recyclable solid sorbents to achieve competitive, less energy intensive acid gas removal alternatives [39]. Adsorption has received much attention for its low energy consumption, low equipment cost, and ease of application [40]. It has recently been reported that the cost of the capture or separation step in post combustion CO_2 capture can be reduced by using this technology [41]. Hence it appears to be a promising technology if effective and selective CO_2 adsorbents are developed [42].

2.4 Adsorption technologies

Adsorption is the process where a molecule becomes selectively attached (adsorbed) onto a surface of another phase [43]. Thus, by using special solids (called adsorbents), substances from gaseous (or liquid) mixtures can be selectively removed. The separation of a substance, the adsorbate, is achieved by its accumulation at the surface of the adsorbent. Adsorption is effective in purification of gas streams and for bulk separations. There are two principal mechanisms of adsorption of molecules on surfaces: physical adsorption (physisorption) and chemical adsorption (chemisorption). The difference lies in the nature of the bonding between the captured molecule and the surface. In physical adsorption bonding is by weak Van der Waals - type forces [44]. In chemisorption bonding is chemical, involving substantial rearrangement of electron density; the nature of this bond may lie anywhere between the extremes of virtually complete ionic or complete covalent character. From a practical point of view, chemisorption from a gas generally takes place only at temperatures above 200 °C and may be slow and irreversible. For this reason, most commercial applications rely on physical adsorption [45]. However, chemical adsorption provides higher selectivity and removal efficiency because of higher chemical affinity between adsorbate and adsorbent. This is why, chemical adsorption at lower temperatures could be a possible route after heat exchanging or direct cooling of flue gas from high temperature to low temperature.

2.4.1 Basic types of industrial adsorbents

Several commercial adsorbents, their characteristics and applications are given in Table 2.3. The major types of adsorbents used are activated alumina, silica gel, activated carbons, zeolites and polymeric adsorbents. In selecting the appropriate adsorbent for a specific application the

following criteria should be met: The adsorbent should demonstrate high selectivity to the gas species to be separated (CO_2 in this case), high capacity to minimize the amount of adsorbent needed, fast adsorption kinetics, chemical and thermal stability, capacity of being easily regenerable and being of relatively low cost [46].

Table 2.3 Commercially important adsorbents and their characteristics [47]

Adsorbent	**Characteristics**	**Commercial uses**	**Strengths**	**Weaknesses**
Activated carbon	Hydrophobic surface, favours organic over air or water	Removal of organic pollutants from aqueous or gaseous effluents	Cheapest hydrophobic adsorbent, workhorse of pollution control	Difficult to regenerate if fouling occurs, may catch fire during air regeneration
Carbon molecular sieve (CMS)	Separates on the basis of difference in intraparticle diffusivity	Production of N_2 from air	The only practical adsorbent for selective adsorption of O_2 over N_2	The only commercial application is in air separation
Silica gel	High capacity, hydrophilic adsorbent	Drying of air and other gases	Higher capacity than zeolite molecular sieves (ZMS)	Not very effective if the moisture level has to be reduced to very low
Activated alumina	High capacity, hydrophilic adsorbent	Drying of gas streams	Higher capacity than ZMS	Not as effective as ZMS for the removal of moisture in traces
Zeolite molecular sieve (ZMS)	Hydrophilic surface, polar regular channels	Dehydration, air separation, separation of molecules based on size and shape	Separation of molecules based on both polarity and geometry	Lower adsorption capacity than many other adsorbents
Silicalite	Hydrophobic surface	Removal of organics from gas streams	Can be regenerated by burning more easily	Quite expensive
Polymer adsorbents	Styrene/divinyl benzene copolymer is most common	Removal of organics from gas streams	Less prone to fouling than activated carbon	Much more costly than activated carbon

The commercial adsorption processes for separating gas and liquid mixtures are accomplished due to selective adsorption of certain substances from their mixtures. The same idea is true for purification of gas and liquid mixtures and drying of some industrial gases. For those purposes, the pore system of adsorbents used is sufficiently wide to enable fast diffusion; separation is caused mainly by selective adsorption that depends upon the van der Waals forces between the adsorbent and the constituents of the gas or liquid mixtures. Adsorptive separation and purification are also realized in terms of both steric and kinetic mechanisms. Both of them are usually treated as equilibrium separation processes [48]. The major typical industrial gas adsorption separations are displayed in Table 2.4.

Table 2.4 Few commercial gas-adsorption separations [37]

Separation*	**Adsorbent**
I. Gas separation	
Normal paraffins/iso-paraffins, aromatics, olefins	Zeolites
N_2/O_2	Zeolites
O_2/N_2	Carbon molecular sieve
CO, CH_4, CO_2, N_2, NH_3/H_2	Zeolites, activated carbon
Acetone/vent streams	Activated carbon
C_2H_4/vent streams	Activated carbon
II. Gas purification	
H_2O/olefin-containing cracked gas, natural gas, air, synthesis gas, etc.	Silica, alumina, zeolite
CO_2/C_2H_4, natural gas, etc.	Zeolite
Organics/vent streams	Activated carbon, others
Sulfur compounds/natural gas, hydrogen, liquefied petroleum gas (LPG), etc.	Zeolite
Solvents/air	Activated carbon, zeolites
Odors/air	Activated carbon
NO_x/N_2	Zeolites, carbons
SO_2/vent streams	Zeolites, carbons
Hg/chlor-alkali cell gas effluent, other off gases	Zeolites, carbons

**Adsorbates are listed first*

Research has demonstrated that only activated carbon and zeolites can find applications in CO_2 separation. In general, molecular sieves have the higher capacity to adsorb CO_2 in terms of per unit weight compared with active carbons. Most physical CO_2 adsorbents such as 13X zeolite, [49] activated carbons, [28, 50] unmodified periodic meso-porous silicas, [51] and metal-organic frameworks (MOFs) [52] require large pressure and/ or temperature gradient between the adsorption and desorption stages to enable both efficient adsorption performances and near complete desorption of CO_2. Moreover, they exhibit relatively low selectivity toward CO_2 and generally low tolerance to water vapor in the gas feed, and their CO_2 separation performance decreases drastically at increasing temperature. Liu et al. [91] and Wang et al. [92] investigated on CO_2 adsorption using zeolites (5A, 13XAPG) at the temperatures between 30 ^oC and 120 ^oC under vacuum (8-20 kPa) using dry, impurities free flue gas and achieved higher CO_2 adsorption capacity (1.5-4.2 mmol/g).

Essentially, adsorption of CO_2 using basic adsorbents requires high pressure operation, hence modified adsorption routes need to be developed with higher adsorption capacity, less energy and cost intensive. This can be achieved by two ways, namely (i) modification of adsorbents and (ii) development of nano-structured adsorbents.

2.4.2 Modification of adsorbents

Most of the conventional adsorbents have low selectivity and capacity for CO_2 adsorption. Moreover, they require high energy in adsorption–desorption cycle. Therefore, there is a need to improve capacity and selectivity of these adsorbents. Some efforts have been made in this direction as summarized in Table 2.5. A promising approach for CO_2 adsorbents that has been developed in recent years is the incorporation of amines into a high surface area support [54-57], combining good capacity and selectivity at moderate temperature. The presence of the surface-bound amine groups is thought to provide such materials with a selective affinity for CO_2 via the formation of ammonium carbamate species under anhydrous conditions and, in addition, via transformation to ammonium bicarbonate and carbonate species in the presence of water.

Table 2.5 Modification of adsorbents

Adsorbents (types)	Modifier	Characteristic of adsorbents	Reference
Amine as precursors			
Zeolites (Zeolite 13X, β-Zeolite)	Monoethanol amine (MEA), Ethylene Diamine (ED), Isopropanolamine (IPA)	- BET surface area and total pore volume decrease with amine loading - High CO_2 adsorption capacity at higher temperature as compared to bare zeolite - High selectivity for CO_2 over N_2 - Retained adsorption capacity over various adsorption-desorption cycles - Amine leaching in presence of moisture in flue gas	[56-58]
Activated Carbon	Diethylenetriamine (DETA), Pentaethylenehexamine (PEHA), Polyethyleneimine (PEI), Aqueous suspension of metal oxides like Cr_2O_3 and Fe_2O_3	- Drastic decrease in BET surface area - Low CO_2 adsorption capacity at room temperature - 80% regeneration after various adsorption-desorption cycles at room temperature	[59-60]
Silica (Monolithic Silica)	Polyethyleneimine (PEI), Tetraethylenepentaamine (TEPA)	- BET surface area and total pore volume decrease with amine loading - High CO_2 adsorption capacity at higher temperature (75 ^oC) - Retained adsorption capacity over various adsorption-desorption cycles	[61]

Alkali metal carbonates as precursors			
Activated carbon	Sodium carbonate (Na_2CO_3) Potassium carbonate (K_2CO_3)	- Lower CO_2 adsorption capacity (0.4-2 mmol/g of adsorbent) over 10-30 wt% alkali metal loading - Higher adsorbent regeneration temperature (>200 ^oC) - Limited to fixed bed application for CO_2 removal	[62]
Alumina	Sodium carbonate (Na_2CO_3) Potassium carbonate (K_2CO_3)	- Lower CO_2 adsorption capacity (0.86-2.9 mmol/g of adsorbent) over 18-50 wt% alkali metal loading - Higher adsorbent regeneration temperature (>300 ^oC) - Limited to fixed bed application for CO_2 removal - Losing multi-cycle adsorption capacity at low temperature regeneration (120-200 ^oC) - Not easy to prepare adsorbent	[17-20], [21-22], [63-68]
RTI's adsorbent	Sodium carbonate (Na_2CO_3) Potassium carbonate (K_2CO_3)	- Very low CO_2 adsorption capacity (0.09-1.45 mmol/g of adsorbent) over 10-40 wt% alkali metal loading - Higher adsorbent regeneration temperature (>200 ^oC) - Limited to fixed bed application for CO_2 removal - Performance in entrained-bed and down-flow reactor promises some challenges for continuous CO_2 removal	[15]
KEPRI's adsorbents	Sorb NX, Sorb KX	- Adsorbents have stable multi-cycle CO_2 adsorption capacity at 35 wt% of alkali metal carbonates loading - Higher temperature for regeneration (>200 ^oC)	[69-72]

The most promising MCM-41 sample in terms of CO_2 adsorption capacity, i.e., MCM-41-100 prepared at 100 °C, was compared to a number of typical CO_2 adsorbents. At high pressure (e.g., 45 bar), MCM-41-100 exhibited higher volumetric capacity than activated carbons and 13X zeolite. Moreover adsorption of pure CO_2 on MCM-41 at ambient temperature was completely reversible and exceedingly fast [51].

Zeolite 13X had been modified with monoethanol amine (MEA) using methanol as the solvent. The adsorbent had been characterized for crystallinity, surface area, pore volume, and pore size. The CO_2 adsorption capacity of adsorbents was evaluated using the breakthrough adsorption method in the temperature range of 30–120 °C. The adsorbents showed improvement in CO_2 adsorption capacity over the unmodified zeolite by a factor of ca. 1.6 at 30 °C, whereas at 120 °C the efficiency improved by a factor of 3.5. The adsorbent was also studied for CO_2 selectivity over N_2 at 75 °C. The MEA modified adsorbent had selectivity for CO_2 over N_2 1.4 times more compared to bare zeolite 13X. The performance of the adsorbent was also satisfactory in repeated cycles of adsorption [56].

Li et al. [76] developed a novel adsorbent by coating polyethyleneimine (PEI) on glass fiber matrix and using epichlorohydrin as cross-linking agent. The physicochemical properties of the fibrous adsorbent were characterized. The experimental results showed that this fibrous PEI adsorbent exhibited much higher adsorption capacity of 3.98 mmol CO_2/g at 30 °C. Factors that affect the adsorption capacity of the fibrous adsorbent were studied. The adsorbent can be completely regenerated at 120 °C. This PEI-modified fibrous adsorbent had high thermal stability (about 250 °C) and is stable in the presence of moisture [76].

Xu et al. [58] synthesized a new type of composite adsorbents by incorporating monoethanol amine into β-zeolite. The adsorption behavior of carbon dioxide (CO_2), methane (CH_4), and nitrogen (N_2) on these adsorbents was investigated at 30 ºC. The results showed that the structure of zeolite did not deteoriate after MEA modification. In comparison with CH_4 and N_2, CO_2 was preferentially adsorbed on the adsorbents investigated. The introduction of MEA significantly improved the selectivity of both CO_2/CH_4 and CO_2/N_2. Very high selectivity of CO_2/N_2 of 25.67 was obtained on 40 wt% of MEA-functionalized β-zeolite (MEA(40)-β) at 1 atm and 30 °C. Steric effect and chemical adsorbate-adsorbent interaction were responsible for such high adsorption selectivity of CO_2. The adsorption capacity was constant after 6 cycles of adsorption and desorption [58]. Still, leaching of amine from the adsorbent could be a major reliability issue in moisture-containing flue gas.

Chen et al. [61] prepared monolith silica with a hierarchical pore structure. It was impregnated with polyethyleneimine (PEI) and tetraethylenepentaamine (TEPA). Amine-impregnated monolith silica exhibited significantly higher CO_2 adsorption capacity than other silica-supported amine sorbents, and produced a reversible and durable sorption performance. In particular, the PEI/monolith exhibited very reversible and durable CO_2 capturing performance (4.77 mmol/g of CO_2 at 75 °C), and also showed excellent performances in both diluted and moisture-containing CO_2 conditions [61].

Different alkylamines were evaluated as a potential source of basic sites for CO_2 capture, and a commercial activated carbon was used as a preliminary support in order to study the effect of the impregnation [59]. Diethylentriamine (DETA), pentaethylenehexamine (PEHA), and polyethyleneimine (PEI) were used for impregnation. The amine coating increased the basicity and nitrogen content of the carbon. However, it drastically reduced the microporous volume of the activated carbon, which was chiefly responsible for CO_2 physisorption, thus decreasing the capacity of raw carbon at room temperature. Vacuum swing adsorption was applied to the prepared impregnated carbons. They do not achieve complete regeneration because of the chemisorptions character of these adsorbents [59].

Low cost carbon materials derived from fly ash were studied by Arenillas et al. [78] for CO_2 adsorption through impregnation with organic bases like polyethyleneimine aided by polyethylene glycol, tetraethylene-pentaamineacrylonitrile (TEPAN) and diethanolamine (DEA). The results showed that for same substrate, impregnated with different amines, the CO_2 adsorption capacities were relatively high (from 0.91 to 1.36 mmol/g of CO_2) especially at high temperatures (75 °C), where commercial active carbons relying on physi-sorption had low capacities. The addition of PEG into the PEI-loaded adsorbents not only increased the CO_2 adsorption capacity but also decreased the time taken for the sample to reach equilibrium, i.e. become saturated with CO_2. Adsorbent retained the capacity after an adsorption-desorption cycle [78].

Impregnation of activated carbons by metal oxides can be an efficient way to improve the surface adsorption characteristics of activated carbons. The effect of impregnation of activated carbon with Cr_2O_3 and Fe_2O_3 and promotion by Zn^{2+} on its adsorptive properties of CO_2 was studied by Somy et al. [60]. Slurry and solution impregnation methods were used to compare CO_2 capture capacity of the impregnated activated carbon promoted by zinc. The results showed that the amount of CO_2 adsorbed on the samples impregnated by Cr_2O_3 was increased

about 20% at 20 °C as compared to raw activated carbon. It was found that Fe_2O_3 was not an effective impregnating species for activated carbon modification. Also slurry impregnation method showed higher CO_2 adsorption capacity in comparison with solution impregnation method. Samples prepared by co-impregnation of two metal species showed higher adsorption capacity than samples impregnated by just one metal species individually. Washing the samples with distilled water after impregnation caused an increase in adsorption capacity attributed to removal of metal oxides covering the surface physically and increasing the surface area. Also, decreasing impregnation temperature from 95 to 25 °C in solution method showed a significant increase in CO_2 adsorption capacity [60].

Adsorption of pure CO_2 on SBA-15 impregnated with branched polyethyleneimine (PEI) has been studied by Sanz et al. [81]. Pure CO_2 adsorption isotherms on modified SBA-15 materials were obtained at 45 °C, showing high adsorption efficiency for CO_2 removal at 1 bar. Chemisorption of CO_2 on amino sites of the modified SBA-15 seemed to be the main adsorption mechanism. CO_2 adsorption strongly depends on the PEI content of the silica material and the adsorption temperature of adsorption process, being possible to obtain a maximum adsorption value close to 2.04 mmol/g of CO_2 at 75 °C and 1 bar. Adsorption capacity was also tested after regeneration of the PEI-impregnated SBA-15 materials. Results show that these branched PEI-impregnated materials are very efficient even at low pressure and after several adsorption–regeneration cycles [81].

Two approaches, thermal swing adsorption (TSA) cycles over a range of temperatures and time in an atmosphere of CO_2 and thermally assisted pressure swing desorption, are explored for the regeneration of the polyethyleneimine (PEI) based adsorbents. Thermal swing regeneration was demonstrated to give good cyclic regeneration capacities (2 mmol/g). The reactions occurring during the TSA regeneration of PEI based adsorbents in an atmosphere of CO_2, especially the formation of a thermostable complex between PEI and CO_2 above 130 °C are described. However, further reaction of the regenerable carbamate ion to form urea linkages, significantly reduces cyclic capacity and therefore the lifetime of the adsorbent. Regeneration of this secondary reaction product at elevated temperatures was attempted in a nitrogen atmosphere, and whilst recovering some of the original capacity did not fully regenerate the adsorbent. Adsorbent regeneration with nitrogen as a stripping gas was used as an alternative regeneration method, the results of which suggest that steam stripping may be a potential method for adsorbent regeneration [47-48].

From the above scientific investigations, amines-impregnated supported adsorbents provide high CO_2 adsorption capacity from dry flue gas streams under vacuum swing adsorption (VSA) or temperature swing adsorption (TSA) at low temperatures (30-75 ^oC). But the foremost issues are related with the amine leaching under moisture environment in flue gas. Even, degradation of amines in O_2 environment in flue gas could be a major reliability issue during operation. That is why, surface interaction between amines, particularly high molecular weight polymeric amines and support materials is the major concern for stabilizing the adsorbents under moist conditions both in fixed and fluidized bed applications.

Among solid adsorbents, dry alkali metal carbonate based adsorbents are widely studied as a capture media for CO_2 from dilute flue gas streams [12-22]. The adsorbents e.g. Na_2CO_3 and K_2CO_3 react with CO_2 and H_2O to form alkali hydrogen carbonate [15, 82]. The carbonate-bicarbonate reaction chemistry for K_2CO_3 is given below:

$$K_2CO_3(s) + CO_2(g) + H_2O(g) \Leftrightarrow 2KHCO_3(s) \quad (\Delta H_r = -141kJ/mol) \qquad (2.1)$$

Previous studies evaluated K_2CO_3 based adsorbents that have shown better CO_2 adsorption capacity than Na_2CO_3 [12-13]. The CO_2 adsorption capacity for K_2CO_3 based adsorbents falls in the range of 0.23 to 2.70 mmol CO_2/g of adsorbent. MgO-promoted K_2CO_3 supported on Al_2O_3 showed high adsorption capacity but requires much higher temperature (400 ^oC) for complete regeneration [16-18]. Lee et al. [19] reported improvement in sorbent regeneration using modified alumina and α-Al_2O_3. It was found that K_2CO_3 based sorbents can be regenerated between 130-200 ^oC depending upon the type of alumina used [19-20]. In the series of work published by Zhao et al. [21, 22, 62-68], the focus was on the carbonation and regeneration behaviors of supported K_2CO_3. The K_2CO_3 supported on γ-Al_2O_3 adsorbent showed higher adsorption capacity among other sorbents. Zhao et al. [62-68] reported that $K_2CO_3 \cdot 1.5H_2O$ is the main active precursor for adsorption and higher regeneration temperature was required due to the formation of intermediate stable species such as $K_4H_2(CO_3)_3 \cdot 1.5H_2O$ and $KAl(CO_3)_2(OH)_2$. The CO_2 capture process performance using different alkali-metal based adsorbents were investigated with respect to effect of water pretreatment, reaction kinetics, carbonate loadings, multi-cycle stability etc [14, 68]. Lei et al. [83] reported multi-step impregnation method for Al_2O_3 supported K_2CO_3/MgO adsorbent and achieved improved adsorption capacity (2.4 mmol CO_2/g) with composite adsorbent of 30 wt% K_2CO_3 and 20 wt% MgO at 60 ^oC and regeneration at 300 ^oC. Wei and Mo [84] investigated incorporation of high amount of titania into SBA-15 for the removal of estrogen using multi-step impregnation

method and showed its superiority over single-step impregnation. It is worthy to mention that the effect of adsorbent preparation method on the physico-chemical properties and performance of the K_2CO_3/Al_2O_3 adsorbents have not been reported in literature. It would be interesting to examine the influence of multi-step impregnation and single-step impregnation technique on the pore structure and pore size distribution which greatly affect CO_2 adsorption capacity.

Extensive research studies have been reported on CO_2 adsorption and regeneration of the solid adsorbents. These mainly include sorbent with alkali carbonate impregnated on various inorganic supports such as activated carbon, silica gel, TiO_2, MgO, Al_2O_3, etc [12-22]. To enhance CO_2 capture capacity from flue gases, K_2CO_3-based alumina supported adsorbents have been widely studied in fixed bed and fluidized bed adsorption systems [62-68, 70]. The K_2CO_3-based adsorbents have good adsorption capacity but showed disadvantages as its cyclic capacity decreased over multiple adsorption-regeneration [20, 62-67]. This is mainly due to some deactivating stable compounds such as $KAl(CO_3)_2(OH)_2$ [13, 21] or $KAl(CO_3)_2$, $1.5H_2O$ [85] $K_4H_2(CO_3)_3 \cdot 1.5\ H_2O$ [13], which are formed during adsorption of CO_2 and require higher regeneration temperature (> 300 ^oC) [13, 21]. However, very few relevancies so far are available addressing this problem. Lee et al. investigated on improvement in regeneration of sorbents using modified alumina and α-Al_2O_3 [20] and their results showed that K_2CO_3 based sorbents can be regenerated between 130-200 ^oC. They claim that the fabrication of alumina support in the preparation stage in presence of CO_2 forms stable $KAl(CO_3)_2(OH)_2$ phase and allows regeneration of adsorbent at lower temperature (<200 ^oC) retaining its identity throughout the process [19-20]. Sharma et al. [30-31] suggested that the modification of adsorbent materials is needed to remove major gaseous pollutants such as SO_x, NO_x, CO, etc., which influence the characteristics of the support materials.

Many scientific literatures have described the performance of various solid-based adsorbents for CO_2 capture in fixed-bed mode including CaO-based chemical looping combustion for CO_2 capture [53]. These adsorbents showed excellent CO_2 adsorption capacities at various operating conditions but their regeneration properties invite lowering of regeneration temperature. To increase the efficiency of adsorptive capture route, many researchers have investigated the potassium-based adsorbent in continuous fluidization system under atmospheric pressure, where adsorption takes place in one fluidized-bed reactor at 50-80 ^oC and regeneration takes place in another fluidized-bed reactor at 120-300 ^oC. It is interesting to note that fluidized bed reactors are preferred due to the following reasons: (i) high heat and mass transfer rates between

gas and solid particles, (ii) quick heat removal during exothermic reaction, (iii) maintains isothermal conditions throughout the reactor due to rapid mixing etc. This facilitates its usage for large-scale operations.

A simplified model was developed to investigate effect of important operating parameters for entrained bed adsorption and bubbling bed regeneration [86]. It was concluded that increase of static bed height or moisture content in the adsorber leads to higher CO_2 capture efficiency, while higher adsorption temperature and gas velocity adversely affect the capture efficiency. The efficacy of water pretreatment during carbonation in a non-circulating bubbling fluidized bed was investigated to achieve 100% CO_2 removal [69]. The water pretreatment before carbonation was found to be more effective and important than water supply during carbonation to achieve higher CO_2 removal due to complete conversion of K_2CO_3 to $K_2CO_3 \cdot 1.5\ H_2O$. The performance of Na-based adsorbents was reported using a down-flow fluidized bed reactor with multi-cycle tests. A high attrition-resistant Na-based adsorbent was capable to achieve 90% CO_2 removal after 96 h of continuous operation using screw-conveyor as solid transport [15]. CO_2 capture capacity and regeneration property for K_2CO_3/Al_2O_3 as a function of the cycle number was studied in a bubbling fluidized bed reactor [65]. The CO_2-capture conversion for K_2CO_3/Al_2O_3 was above 90% during the 10 cycles, while the microstructure character of K_2CO_3/Al_2O_3 was relatively stable. The work indicated that K_2CO_3/Al_2O_3 has potential to be used as a sorbent for a large-scale CO_2 capture process. The carbonation behavior of K_2CO_3/Al_2O_3 adsorbent was systematically investigated in a bubbling fluidized bed reactor [22]. The total carbonation conversion increases with the increase in CO_2 and H_2O contents, but decreases with the increase in temperature and pressure. The surface area and pore volume of the adsorbent remains stable, and the pore size distribution behavior was not changed even after 80 cycles. The potassium-based solid adsorbent was studied to see the effect of bed-height in carbonation/ regeneration in a non-circulating bubbling fluidized bed reactor and found that at each cyclic run, CO_2 adsorption capacity decreased as L/D (length *vs.* diameter) ratio was increased [70]. Yi et al. [71, 87] investigated the performance of the dry adsorbent process in the continuous solid circulation mode between a fast fluidized carbonator and a bubbling bed regenerator. The author examined the effects on CO_2 removal (50-73%) by several variables like carbonation temperature (70-90 ^oC), gas velocity (1.7-3.0 m/s), H_2O concentration (7-30%), and solid circulation (7-35 $kg/m^2.s$). Further, the authors concluded that the concept of the dry sorbent CO_2 capture process to be one of viable methods for capturing CO_2 from dilute flue gas of fossil fuel-fired power plants.

Wu et al. [73] performed continuous sorption-desorption in three bubbling fluidized-bed reactors (two carbonation reactor and one regeneration reactor) with screw-conveyor for solid transport to study influence factors such as bed height, solid circulation rate, carbonation/regeneration temperature, water content, etc. The 20 h continuous operation demonstrated 96% CO_2 removal efficiency with excellent adsorbent stability. Kim et al. [72] studied effect of CO_2 or steam partial pressure on the performance of supported K_2CO_3 based adsorbent in two-interconnected bubbling fluidized beds system. The CO_2 removal increased (83% to 97%) as the mole fraction of steam in the fluidization increased, while it decreased (83% to 55%) as that of CO_2 increased. Recently, Jaiboon et al. [74-75] concluded that the CO_2 capture capacity of the sorbent changed dramatically depending on the flow patterns/regimes in fluidized bed/circulating fluidized bed. The turbulent regime provided best CO_2 capture capacity at about 90% of the stoichiometric theoretical value. The CO_2 capture capacity in bubbling and fast fluidization was reported as 66-72% of theoretical CO_2 capture capacity and 53-60% in fixed and slugging bed regimes. They also investigated the effect of regeneration temperatures on CO_2 adsorption capacity over multiple cycles. From the literature reported so far, it is realized that continuous dry solid adsorbent circulation in integrated adsorber-desorber fluidized-bed system needs to be studied to understand the various factors, such as effect of adsorption temperature, water content in inlet flue gas, gas hourly space velocity (GHSV) and solid circulation rate (SCR). It would be a significant achievement if temperature difference between adsorption and regeneration is further narrowed down during continuous operation, which would help in easier heating and cooling of adsorbent with lower energy needs.

This study focused on carbonation-regeneration characteristics in both non-circulating fluidization and continuous circulation between two inter-connected fluidized-bed reactor systems. The key interest of this study is to highlight the effect of process parameters such as adsorption temperature, water content in inlet flue gas, GHSV and nature of sweep gas used for desorption. The work attempts to bring out the important results of pilot scale trials using an existing FCC pilot unit. In particular, it presents results which are critical for transitioning from Lab scale to the most efficient industrial scale in the development of low cost CO_2 capture process with lower regeneration temperature and multi-cycle stability.

2.5 Future trends and prospects

Research has demonstrated that silica, zeolites and activated carbon have application in the field of CO_2 capture but at room temperature. Zeolites have been modified by various research groups. Still these adsorbents need modification for better adsorption capacity, selectivity and regenerability at higher temperatures, to efficiently capture CO_2 from flue gases. These support materials need modifications on the stability of the adsorbents at flue gas conditions with impurities like, H_2O, O_2, etc. Alumina has not been used for CO_2 adsorption and research can be carried out in this direction. It can be synthesized in order to have controlled pore size and other characteristics to achieve high adsorption capacity. Moreover, alkali metal carbonate based (Na_2CO_3, K_2CO_3) adsorbent systems have shown high CO_2 adsorption capacity at the temperatures between 50-70 ^oC with flue gases containing impurities. Still, there is a huge scope of research on capacity improvement of the K_2CO_3-based adsorbents. Moreover, minimizing regeneration temperature and multi-cycle stability of supported adsorbents needs to be addressed. The future research should primarily be focused on that why CO_2 adsorption capacity decreases with multiple cycle testing. It is also worthwhile to investigate the process for continuous removal of CO_2 from dilute flue gases in a fluidized bed process to present an energy-efficient process.

This research work is intended to bridge the above-mentioned gaps on K_2CO_3/Al_2O_3 systems. This work is primarily focused on the effect of adsorbent preparation method to enhance the CO_2 adsorption capacity of the prepared adsorbents by improving dispersion of active phase (K_2CO_3) inside the support material (Al_2O_3) with higher loading of K_2CO_3. The work is also carried out to improve the regeneration properties of K_2CO_3/Al_2O_3 adsorbents and their multi-cycle stability under simulated flue gas conditions by introducing methods of stabilization of the support material. This research work is also directed to evaluate the modified adsorbent performance in a continuous circulating fluidized bed system with varying performance process parameters. And lastly, an energy-integrated CO_2 capture process is developed with the objective of minimizing CO_2 capture cost.

Chapter 3

Experimental

3.1 Introduction

This chapter presents the experimental techniques and methods utilized in obtaining results in this research work. Various physico-chemical characterization techniques, such as Brunauer-Emmett-Teller (BET) surface area analysis, particle size analysis, scanning electron microscopy (SEM), transmission electron microscopy (TEM), X-Ray diffraction (XRD), Fourier transform infrared (FTIR) spectroscopy, temperature programmed desorption (TPD), thermo-gravimetric analysis, etc. were used to characterize the adsorbent properties and adsorption-regeneration characteristics. A fixed bed reactor set up was used to evaluate the adsorption-regeneration characteristics. A circulating fluidized bed reactor set up at pilot scale was also used to assess continuous removal of CO_2 from simulated flue gas.

3.2 Adsorbent preparation method

3.2.1 Reagents and materials

The following raw materials were taken for CO_2 adsorbent preparation:

(i) Alumina-clay composite (Intercat, USA)
(ii) Gamma alumina (Saint Gobain, Norpro, USA)
(iii) Alpha alumina (Saint Gobain, Norpro, USA)
(iv) Sodium carbonate (Na_2CO_3) (LR grade, Merck)
(v) Potassium carbonate (K_2CO_3) (LR grade, Merck)
(vi) De-ionized water

3.2.2 Calcination of support materials

In this research work, three inorganic materials were chosen as support materials namely, alumina-clay composite, gamma alumina and alpha alumina. First, alumina-clay composite (ALC) was used to prepare Na_2CO_3-based adsorbents. The support material was first calcined at 350 ^oC for removal of water and volatile organic materials at a temperature ramp 10 ^oC/min. The ALC was procured from Intercat, USA as a bottom cracking additive (BCA), which is used to improve yield of high boiling components in commercial fluid catalytic cracking (FCC) unit. The surface area and total pore volume of this ALC material are 131 m^2/g and 0.345 cm^3/g respectively.

The adsorbents were prepared using gamma alumina (γ-Al_2O_3) as a support material. The spray-dried γ-Al_2O_3 was procured from Saint Gobain, Norpro, USA with specific surface area of 172 m^2/g and total pore volume of 0.482 cm^3/g. Before adsorbent preparation, the support material was calcined at 550 ^oC for 4 h to remove free water and volatile organic materials. The calcination was performed in a muffle furnace (make: Cole Parmar) at a temperature scanning rate of 10 ^oC/min under N_2 atmosphere. The alpha alumina (α-Al_2O_3) procured from Saint Gobain, USA was used as received.

3.2.3 Impregnation on support material

The adsorbents were prepared by incipient wetness impregnation method. This preparation method includes the incorporation of impregnation solution (Na_2CO_3, K_2CO_3 solution) into the pores of the support materials by capillary action. The adsorbents were prepared by single-step and multi-step incipient wetness impregnation method. For example, in case of K_2CO_3-based adsorbents, which were prepared by single step impregnation method, wherein K_2CO_3 was dissolved in required volume of water such that it corresponds to water pore volume of the support. The support was poured into the solution and mixed thoroughly for 30 min so that the K_2CO_3 solution was allowed to enter into the pores of the support materials by capillary action. On the other hand, multi-step impregnations were followed for higher loading of metal carbonates (10-60 wt%). For example, 10 wt% of K_2CO_3 was impregnated at successive stages to attain higher loading. After every impregnation stage, adsorbent was dried at 120 ^oC for 24 h and the water pore volume was then measured and accordingly, subsequent stages were performed to complete the desired K_2CO_3 loading. A flow sheet for the adsorbent preparation method is shown in Figure 3.1. During adsorbent preparation, one should be careful about measurement of water pore volume (WPV) of the support materials. The excess de-ionized water as well as excess impregnation solution may exhibit inhomogeneous dispersion of K_2CO_3 onto the support resulting poor CO_2 adsorption capacity.

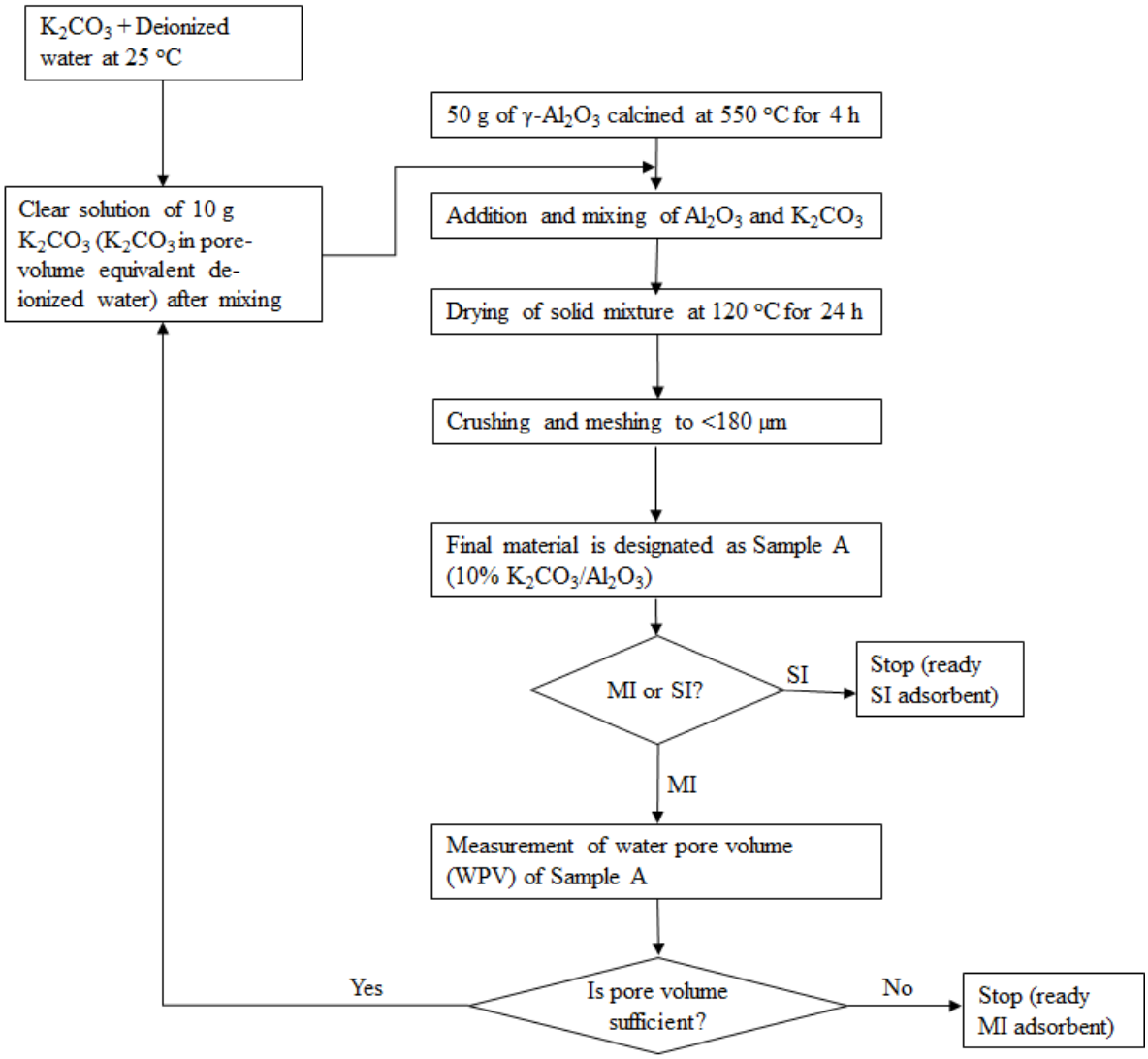

Figure 3.1 Flow sheet of adsorbent preparation method

3.2.4 Modification of support material

The support material (γ-Al_2O_3) was modified in this research to improve the regeneration properties of the adsorbents. The γ-Al_2O_3 has been modified by (i) applying heat treatment, (ii) treatment with alkali hydroxide followed by calcination, etc. so as to reduce the surface hydroxyl concentration/ acid sites. Prior to the impregnation of K_2CO_3, the γ-Al_2O_3 was pretreated by calcining between 700-950 ^oC for 6 hours. As discussed in Section 3.2.3, the K_2CO_3 was dissolved in de-mineralized water equivalent to water pore volume of the support. The support was poured into the solution and mixed thoroughly, held up for 1 h at room temperature for equilibration and followed by drying at 120 ^oC for 24 h. Another method was adopted to pretreat the support material with 1 wt% NaOH solution and dried at 120 ^oC for 24

h. The dried support was then calcined at 700 ^{o}C/ other temperatures as specified for 6 h. The K_2CO_3/α-Al_2O_3 was prepared following the same method, wherein the α-Al_2O_3 was taken as such.

3.2.5 Higher loading of K_2CO_3

The loading of K_2CO_3 in the γ-Al_2O_3 is mainly governed by the water pore volume of support material. For higher loading, K_2CO_3 was dissolved into water at higher temperature (70 ^{o}C). Herein, the amount of K_2CO_3 is dissolved at 70 ^{o}C based on the solubility of K_2CO_3 at high temperature under continuous stirring. The γ-Al_2O_3 was then added in the impregnation solution.

3.3 Characterization methods

The important physico-chemical characteristics of the support material and prepared adsorbents were systematically determined to correlate the adsorption-desorption characteristics under various operating conditions. The various characterization methods utilized in this research are briefly described below.

3.3.1 Surface area and pore volume measurement

The textural properties like BET surface area, total pore volume of the adsorbents were determined using nitrogen adsorption–desorption experiments (Micromeritics ASAP 2020). The samples were evacuated at 90 °C for 1 h and 300 °C for 3 h prior to analysis. The total pore volume was calculated from the amount of N_2 adsorbed at relative pressure (p/p_o) of 0.99. The total surface area was calculated using multi-point Brunauer-Emmett-Teller (BET) surface area method. More details are described in Section 3.8.2. This characterization of prepared adsorbents was employed to achieve deeper insight of the adsorbents, specifically, the change in BET surface area, total pore volume and average pore diameter after active component loading and application of thermal treatment for support material modification. These data are well-correlated with CO_2 adsorption performance as described in subsequent chapters.

3.3.2 Scanning electron microscopy (SEM)

The morphology of the adsorbent particles was measured by field emission scanning electron microscopy (SEM: JEOL JSM-6100). The selected adsorbent samples were examined by the SEM with freshly prepared adsorbents. The samples were coated with gold on carbon

templates. The images were taken at suitable magnifications using voltages of 5-15 kV. These imagery data are used to establish the morphological characteristics of the support and adsorbents, specifically, how active phase is distributed onto the support material adopting different method of adsorbent preparation.

3.3.3 Transmission electron microscopy (TEM)

The structure of the alumina support and adsorbents was investigated by transmission electron microscopy (TEM: Technai-20, Phillips) operated at 200 kV. Before analyzing, the samples were sonicated using sonicator to make the samples into nanoparticles. The nanoparticles were deposited on copper grids for capturing images at different magnifications. The micrographs obtained from the TEM analysis are carefully correlated to understand the dispersion of active phase on the support material. This analysis is very useful to establish the superiority of multi-step impregnation method over single-step method for adsorbent preparation. This analysis also provides insight on porous structure of the support material after thermal treatment on support material.

3.3.4 X-Ray diffraction (XRD)

XRD is used for the identification of phases in a crystalline material and determination of unit cell dimension. In XRD, diffraction occurs when each object in a periodic array scatters radiation coherently, producing concerted constructive interference at specific angles. Bragg's law is a simplistic model to understand what conditions are required for diffraction. The Bragg's law is expressed as:

$$\lambda = 2d_{hkl}sin\theta$$

where, λ= wavelength of X-ray, d = space between diffracting planes, θ = Bragg's angle

The x-axis, 2-theta, corresponds to the angular position of the detector that rotates around the sample and y-axis, intensity corresponds to peak intensity of the atoms in the diffracting plane. The phase characteristics of the adsorbent materials were performed by X-ray diffraction (XRD, X'Pert Pro, PANalytical) using CuKα radiation at room temperature. The analysis was performed at a scanning rate of 0.02^o/min between 5^o and 90^o. The XRD data provides the information on the presence of phases in the adsorbed and regenerated adsorbents. This information helps to describe the adsorption-regeneration characteristics of CO_2 adsorption

using K_2CO_3/Al_2O_3 system. This technique is also helpful in analyzing the crystalline phases of γ-Al_2O_3 on thermal treatment.

3.3.5 Fourier transform infrared (FTIR) spectroscopy

FTIR is an analytical technique, which provides information on molecular structure and chemical bonding of materials. In FTIR, IR radiation is passed through a sample specimen of material. Some of the radiation is absorbed and some transmitted through the material. The resulting spectrum analysis provides the information on chemical bonding structure of the material. The presence of chemical bonding of the prepared adsorbents was examined using Fourier transformed infrared spectroscopy (FTIR: Nicolet 6700 FTIR spectrometer) over the range 4000–400 cm^{-1} at a scanning resolution of 2 cm^{-1}.

3.3.6 Average particle size measurement

The average particle size was measured using Malvern Mastersizer 2000 and was found between 75 and 90 μm for various adsorbents. The average particle size of the adsorbent particles is measured to study the adsorbent performance in bubbling fluidized regime in continuous fluidization system.

3.3.7 Temperature programmed desorption (TPD)

A temperature programmed desorption (TPD) study was carried out using a gas chromatography (GC: Perkin-Elmer) with thermal conductivity detector (TCD). The temperature programme was set for 40 min with initial temperature 30 ^oC and the ramp of 10^oC/min in N_2 atmosphere. Using this technique, the adsorbed adsorbents undergo desorption from room temperature to 400 ^oC to identify the peaks for decomposition of chemical components. These data were purely used to describe the presence of deactivating species formed during CO_2 adsorption.

3.3.8 Total acidity measurement

Total acidity of γ-Al_2O_3, modified γ-Al_2O_3, and α-Al_2O_3 were measured in Micromeritics AutoChem II 2920 by TPD-NH_3 method. The sample is pre-activated at 600 ^oC under helium flow. The number of acidic sites was calculated from experimental TPD-profiles. The determination of acidic sites of the support materials as well as the modified supports provides the support-active phase interaction during adsorbent preparation and carbonation reaction.

How the calcination temperature affect support characteristics is explained by the total acidity of the support materials.

3.3.9 Thermo gravimetric analysis (TGA)

The thermal stability of selected adsorbents was determined using thermo-gravimetric analyzer (TGA: Universal V4.5A TA Instruments) using N_2 as carrier gas at the heating rate of 10 ^oC/min. TG analyses provided the thermal stability as well as decomposition species formed during adsorption-regeneration, which helped to explain adsorption-regeneration characteristics of the adsorbents. TGA data is also useful to determine CO_2 adsorption capacity, which is comparable with the fixed-bed CO_2 adsorption study.

3.3.10 Attrition index (AI)

Attrition resistance of the selected adsorbents was measured as Attrition Index (AI) by ASTM D5757 method. This property of the adsorbent is determined to know the loss of material during circulating fluidized bed CO_2 removal process.

3.4 Calibration

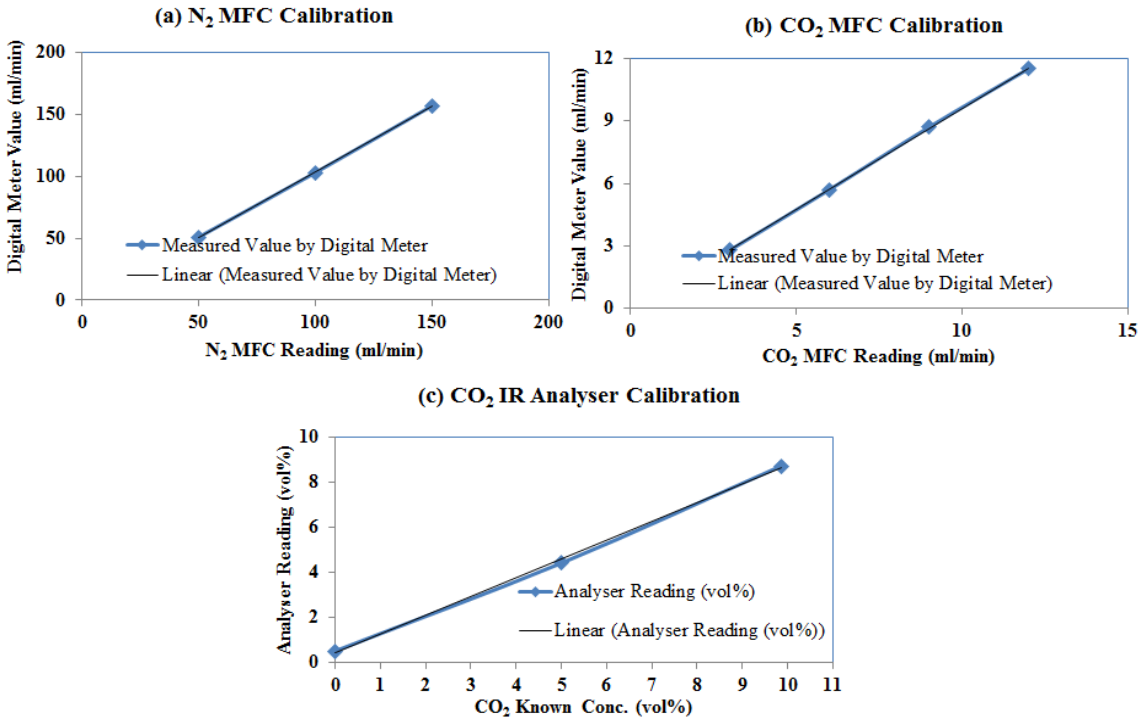

Figure 3.2 Calibration of (a-b) MFCs for N_2 and CO_2 and (c) CO_2 IR analyzer

The external mass flow controllers (MFCs) for the permanent gases such as N_2, CO_2 and the IR analyzer were calibrated for the experiments carried out in the fixed-bed reactor. The calibration graphs for MFCs for both the gases and CO_2 IR analyzer are shown in Figure 3.2 (a-c).

3.5 Fixed-bed reactor system

A fixed-bed reactor was used to perform the CO_2 adsorption-regeneration studies using a simulated refinery flue gas stream. The experimental set-up mainly consists of three sections: the gas injection, fixed-bed adsorption, and CO_2 analysis in effluent stream. The reactor is made of 316 stainless steel with height of 42 cm and shell internal diameter of 3.5 cm. The diameter and height of the adsorbent zone are 1.7 cm and 8.3 cm respectively. The temperatures along the reactor were measured by thermocouples at three different positions: 4, 8, and 12 cm from the bottom.

Figure 3.3 represents the schematic diagram of the fixed-bed reactor system. A simulated flue gas composition of 3-9 vol% CO_2, 5-15 vol% H_2O and rest N_2 was used in all the adsorption study. The N_2 and CO_2 were supplied from high-purity gas cylinders with flow rates controlled using Brooks mass flow controllers. The simulated gas mixture of N_2 and CO_2 was passed through a temperature-controlled water saturator to saturate the stream at a given temperature. The feed lines and the line between the reactor and dryer were heated and insulated to ensure complete vaporization. The total flow rate of the feed gas stream was 150±2 ml/min. Then the simulated gas mixture was passed through the adsorbent bed. The adsorbent was pretreated with water vapor for 30 minutes to achieve higher adsorption capacity. The treated effluent stream was passed through a dryer to remove the water and the outlet concentration of CO_2 was measured continuously by on-line IR analyzer (Servomex 1440 series, measurement limit 0-10 vol%). After adsorption was completed, the regeneration was carried out at 120-300 ^oC under N_2 atmosphere. The temperature was decreased again to the adsorption temperature and the multi-cycle testing was carried out. Feed lines and the line between the reactor and condenser were heated and insulated to insure complete vaporization. About 8 gm of solid adsorbent was used for each experimental run. A layer of glass wool of 3 mm thick was inserted in the reactor to support the adsorbents during loading.

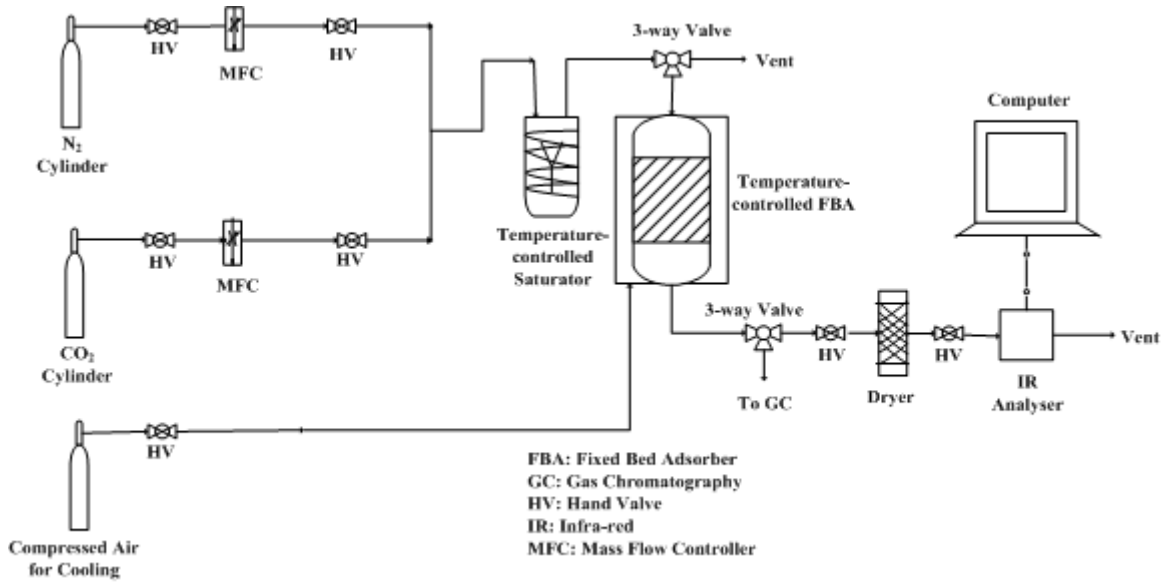

(a)

(b)

Figure 3.3 (a) Schematic of experimental setup and (b) fixed bed reactor system

3.6 Fluidized-bed reactor system

Figure 3.4 shows a picture of existing pilot plant for fluid catalytic cracking unit (FCC) at Reliance Industries Limited (RIL), used for CO_2 capture experiments. As such, this unit consists of (i) riser, (ii) stripper, (iii) combustor, (iv) regenerator, (v) cyclone separators, (vi) two-interconnected stand-pipes with slide valves for controlling catalyst circulation, (vii) CO_2 infra-red analyzer, (viii) filters for collecting fines (abraded adsorbent particle). In this unit, regenerator and riser-stripper assembly were used as adsorber and desorber respectively. In the subsequent sections, the adsorber and desorber terms imply their respective meaning. Both

adsorber and desorber are operated in bubbling fluidization flow regime. The bubbling fluidized mode operation is expected to provide efficient adsorption of CO_2 in the adsorber and efficient desorption in the regenerator.

All the dimensions of this pilot plant unit is the property right of RIL. The Adsorber is connected to the Desorber through the riser via standpipes. All reactors and inter-connected lines are surrounded by electric heating elements, which are controlled remotely by PLC-based control system. The simulated flue gas composition: 8-10 vol% CO_2, 10-23 vol% H_2O and balance N_2 was fed through pre-calibrated mass flow controllers (MFCs) into the adsorber. The detailed experimental procedure is described in Section 7.2.3 of Chapter 7. In the adsorber, CO_2 in presence of H_2O reacts with supported K_2CO_3 adsorbent coming from the desorber, at temperature between 50 and 80 ^oC according to forward reaction shown in equation (3.1). The potassium bicarbonate ($KHCO_3$) formed in the adsorber is regenerated at 130-200 ^oC with N_2/ CO_2 as sweep gas as shown by backward reaction in equation (3.1).

$$M_2CO_3 + CO_2 + H_2O = 2MHCO_3\ (where, M = Na, K) \qquad (3.1)$$

Figure 3.4 Picture of circulating fluidized bed system

The post-combustion adsorptive CO_2 capture processes using K_2CO_3/Al_2O_3 adsorbents were assessed to present an experimental set of data to design a low cost energy efficient process.

The experiments were carried out both in fixed bed and fluidized bed systems to evaluate adsorbent performance at different operating and process conditions. Table 3.1 shows a comparison between fixed bed reactor and circulating fluidized bed reactor.

Table 3.1 Comparison between fixed bed and circulating fluidized bed reactor

Features	**Fixed bed**	**Circulating fluid bed**
Adsorbent capacity	Sorbent capacity decides cycle length, hence larger sorbent bed required	Not critical since sorbent circulation as well as recycle rate enhance adsorbent capacity
Operation	Unsteady state operation adsorption and regeneration: swing mode for regeneration	Steady state: closer to optimum
Temperature distribution	Highly non-uniform axial/radial temp gradient	Close to uniform
Heat integration	Requires external stream for heating/ cooling	Energy efficient process due to exchange of heat with circulating adsorbent
Pressure drop (ΔP)	Higher ΔP	Lower ΔP
Effect of impurities	Permanent replacement only after shutdown	Can be overcome with fresh sorbent make up on regular basis

3.7 Calculation of CO_2 adsorption capacity

As discussed in Section 3.5, the outlet CO_2 concentration in treated simulated gas was measured using IR analyzer. The response time of this analyzer was recorded as 1-2 seconds. The net CO_2 adsorption capacity was calculated per minute basis excluding the dead time of the analyzer (4 minutes). A calculation procedure for CO_2 capture capacity is shown in Figure 3.5.

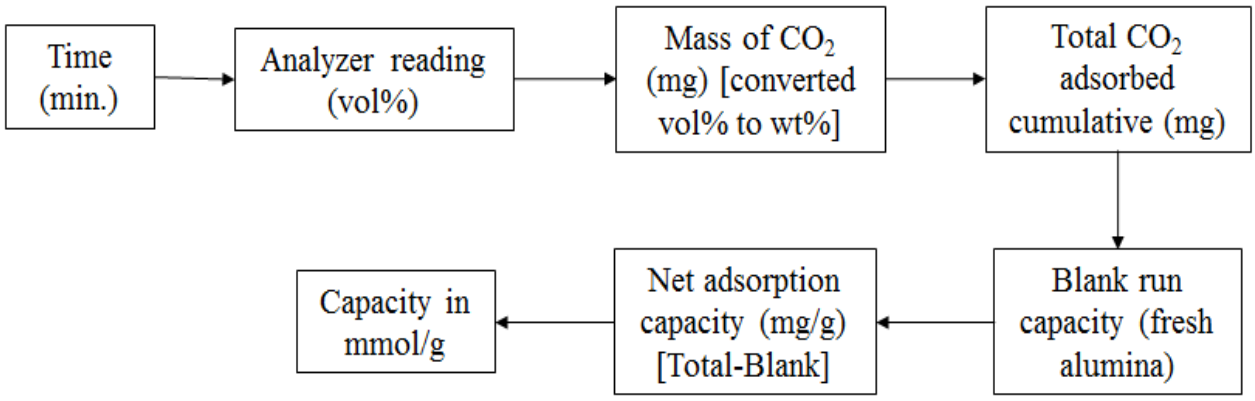

Figure 3.5 Calculation procedure for CO_2 capture capacity in mmol/g

The CO_2 adsorption capacity was determined using the following equation:

$$Net\ CO_2\ adsorption\ capacity, mmol/g = \frac{Total\ mass\ of\ CO_2\ adsorbed - Blank}{gm\ of\ adsorbent \times 44} \quad (3.2)$$

Similarly, the percent regeneration is calculated as

$$\%\ regeneration = \frac{adsorption\ capacity\ at\ each\ cycle}{adsorption\ capacity\ at\ fresh\ cycle} \times 100 \quad (3.3)$$

3.8 Adsorption isotherm models

Adsorption is a separation process in which some materials, (called as adsorbate) is concentrated from a bulk vapor or liquid phase on the surface of a porous solid (called as adsorbent). The amount adsorbed is measured as a function of the partial pressure or concentration at a given temperature and the results expressed as an adsorption isotherm. The amount adsorbed (V) is only a fraction of a monolayer (V_m), but this layer may be of multi-layer due to surface heterogeneity. The various physical properties of the adsorbents, such as surface area, pore volume, pore size or energy distributions are determined from the adsorption isotherms. The isotherm curve helps to calculate CO_2 uptake capacity at equilibrium condition in determining the economics of the separation process. There are various adsorption isotherm models based on some model assumptions, such as Langmuir isotherm, BET isotherm, Freundlich isotherm, etc. A brief description of these isotherm models are described in the subsequent sub-sections.

3.8.1 Langmuir adsorption isotherm

The amount adsorbed is measured as a function of the partial pressure or concentration at a given temperature and the results expressed as an adsorption isotherm. Among various adsorption models, the Langmuir adsorption isotherm model is the most common. The Langmuir adsorption isotherm model [88] is applied universally for physisorption and chemisorption. This model envisaged the dynamic equilibrium between adsorbate in the gas phase at pressure p, and the amount of adsorbed species on the surface as fraction of sites coverage (θ). This model was based on the following assumptions:

- Each active site can accommodate one adsorbate molecule
- The adsorbent surface is completely uniform so that there is the same probability of adsorption on all sites
- No interaction between adsorbate molecules

- Maximum adsorbed molecules corresponds to monolayer phase.

At equilibrium, the rate of adsorption is equal to rate of desorption, mathematically,

$$k_a p(1-\theta) = k_d \theta \qquad (3.4)$$

Where, k_a and k_d are the adsorption and desorption rate constants respectively. By arranging the above equation,

$$\theta = \frac{bp}{(1+bp)} \qquad (3.5)$$

Where, b = adsorption equilibrium constant = k_a/k_d

3.8.2 BET adsorption isotherm

Brunauer et al. [89] modified some of the assumptions of Langmuir model and proposed an extended Langmuir model popularly known as the Brunauer-Emmett-Teller (BET) model. They attempted to generalize the Langmuir equation by considering the lateral interaction among adsorbed molecules, their mobility and the energetic surface homogeneity of the solid surface. The Langmuir model assumes monolayer adsorption while the BET model represents multi-layer adsorption. The BET equation is derived by balancing the rates of evaporation and condensation for the various adsorbed molecular layers. At saturated vapor pressure, the adsorbate molecules condense to liquid on the surface of the solid leading to infinite layers. The BET isotherm equation is given as:

$$\frac{p}{V(p_o - p)} = \frac{1}{V_m C} + \frac{(C-1)}{V_m C}\frac{p}{p_o} \qquad (3.6)$$

Where, p and p_o are the equilibrium and saturation pressure of adsorbates at adsorption temperature and V and V_m are the adsorbed gas quantity and monolayer capacity respectively. C is the BET constant.

3.8.3 Freundlich adsorption isotherm

Freundlich [90] proposed an empirical relation between the amounts of gas adsorbed by the solid adsorbent with pressure. The Freundlich isotherm is applicable to both monolayer adsorption (chemisorption) and multilayer adsorption (van der Walls adsorption). The Freundlich adsorption equation is given by the following equation:

$$\frac{x}{m} = q_e = K p^{1/n} \qquad (3.7)$$

Where, x = mass of adsorbate

m = mass of adsorbent

p = equilibrium pressure of adsorbate

K and n are constants for a given adsorbate and adsorbent at a particular temperature.

3.9 Types of adsorption isotherms

Adsorption isotherms are characteristics representation of the amount of adsorbate adsorbed at equilibrium gas pressure. The adsorption isotherms provide the adsorbate-adsorbent interaction in the adsorption system and the amount of adsorbate adsorbed including the estimation of surface area, pore volume and pore size distribution. The experimental procedure includes the use of relative pressure, which is expressed as a ratio of the partial pressure of gas (P) and the saturation vapour pressure (P_o) at a constant adsorption temperature. Adsorption isotherms are classified in six types according to Brunauer, Deming, Deming and Teller (BDDT) classification as discussed below:

Type I isotherm

Type I isotherm exhibits completion of adsorption in a single mono-layer filling at P/P_o of 0.1. Type I isotherm is observed in adsorbents whose pore sizes are in narrow micro-porous exhibiting a complete micro-pore filling of gases. Zeolites, activated carbon, MOFs, show this type of isotherm.

Type II isotherm

Type II isotherms exhibit mono-layer adsorption of gases followed by multi-layer adsorption on the non-porous materials. In Figure 3.6, at the point B of Type II isotherm, there is a complete formation of mono-layer, after that multi-layer is formed. The adsorption of nitrogen on carbon at -196 ^oC exhibits this type of isotherm.

Type III isotherm

This isotherm is associated with non-porous and micro-porous solids. It occurs when there is weak interaction between adsorbate and adsorbent, resulting in a low uptake of gases at low relative pressure [43-44]. When the interaction is stronger, it leads to higher uptakes at higher relative pressure. This type of isotherm includes the adsorption of water on carbon.

Type IV isotherm

This isotherm is similar to the Type II isotherm except that adsorption ends near to P/P_o of 1. This isotherm exhibits mono-layer and multi-layer coverage onto the meso-porous materials. This isotherm also contains hysteresis loops due to capillary condensation of gases at $P<P_o$.

Type V isotherm

This isotherm is similar to the Type III isotherm, exhibits a weak interaction between adsorbate-adsorbent. This type of isotherm is associated with micro- and meso-porous materials and exhibits hysteresis loop due to capillary condensation. Adsorption of water shows this type of isotherm.

Type VI isotherm

This type of isotherm is introduced as a hypothetical isotherm for uniform non-porous materials [44]. The first bend in Figure 3.6 of Type VI isotherm represents a complete mono-layer before progression of subsequent layers.

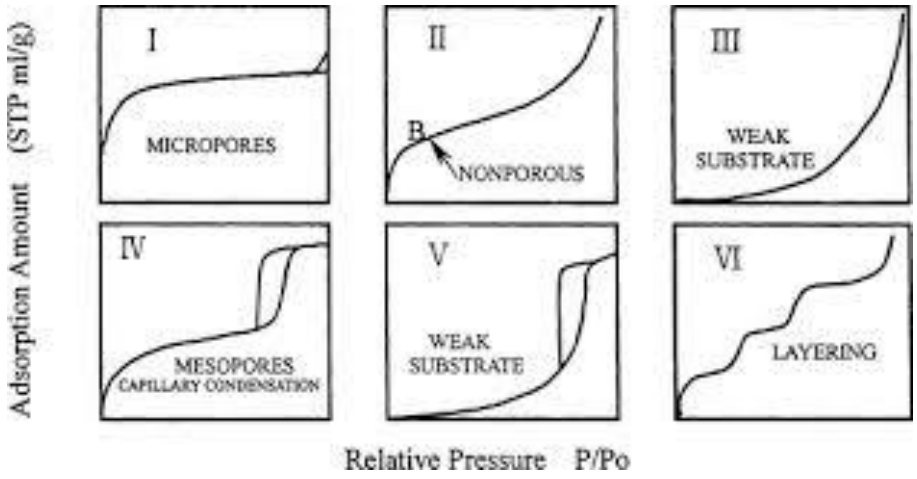

Figure 3.6 Adsorption isotherms according to the IUPAC classification

3.10 Isosteric heat of adsorption for CO_2

Isosteric heat of adsorption is defined as the ratio of the infinitesimal change in the adsorbate enthalpy to the infinitesimal change in the amount adsorbed. The estimation of the heat released is important in the kinetic studies because the heat released due to adsorption is partly absorbed by the adsorbent and partly released to the surroundings. The released heat portion absorbed

by the adsorbent increases the particle temperature and that slows down the adsorption kinetics because the mass uptake is controlled by the rate of cooling of the particle in the later course of adsorption. The isosteric heat also indicates the temperature sensitivity of equilibrium constant and thereby provides insight to the variation of adsorption and desorption kinetics with temperature. Hence, it is a critical design variable in estimating the performance of CO_2 adsorption process. It also gives some indication about the surface energetic homogeneity and heterogeneity in accordance to variation with surface coverage. The dependence of isosteric heat of adsorption with surface coverage signifies the strength of interaction between adsorbent–adsorbate followed by the adsorbate–adsorbate interaction [93].

Using Langmuir isotherm which shows dependence of the adsorbed amount q from the pressure p is shown by equation (3.8):

$$q = q_m \frac{Kp}{1 + Kp} \tag{3.8}$$

where q_m is the maximum adsorption capacity, and K is the affinity constant. The temperature dependency of affinity constant and maximum adsorption capacity can be expressed as:

$$K = K_o exp\left[\frac{Q}{RT_o}\left(\frac{T_o}{T} - 1\right)\right] \tag{3.9}$$

$$q_m = q_{m,o}\ exp\left[\varphi\left(1 - \frac{T_o}{T}\right)\right] \tag{3.10}$$

where, Q= heat of adsorption, $q_{m,o} = q_m$ at T_o (=298K), φ = dimensionless parameter which may be ~0 or < 0. Substituting equation (3.9) and (3.10) in (3.8), the relationship between adsorbed quantity and pressure is given by equation (3.11):

$$q = q_{m,o}\ exp\left[\varphi\left(1 - \frac{T_o}{T}\right)\right]\left[\frac{K_o\left[\frac{Q}{RT_o}\left(\frac{T_o}{T} - 1\right)\right]p}{1 + K_o\left[\frac{Q}{RT_o}\left(\frac{T_o}{T} - 1\right)\right]p}\right] \tag{3.11}$$

The experimental data 'q *vs* p' for CO_2 adsorption on K_2CO_3 supported on MI adsorbent were non-linearly regressed using Matlab® surface fitting tool box to calculate simultaneously the optimal values of K_o, $q_{m,o}$, φ and Q.

From sets of isotherms, the coverage-dependent isosteric heat of adsorption was deduced using the van't Hoff equation [93]:

$$\frac{\Delta H}{RT^2} = -\left(\frac{\partial lnp}{\partial T}\right)_q \qquad (3.12)$$

Also the isosteric heat of adsorption from equations (3.8-3.10 and 3.12) can be expressed in term of surface coverage as [90].

$$-\Delta H = Q - \varphi RT_o \frac{1}{1-\theta} \qquad (3.13)$$

where, $\theta = q/q_m$ = fractional coverage of the adsorbent.

Chapter 4

Development of Low Temperature Regenerable Sorbent for Carbon Dioxide Adsorption from Flue Gases

4.1 Introduction

In this work, CO_2 adsorption studies were performed using a series of adsorbents prepared by incipient wet impregnation method. Several adsorbents using alumina-clay (ALC) as support and sodium carbonate (Na_2CO_3) as active component were prepared and characterized for textural properties with the objective to correlate with CO_2 adsorption and desorption. The effects of adsorption temperature, Na_2CO_3 loading on the support material and feed CO_2 concentration were evaluated using simulated flue gas with 3 – 9 vol% CO_2, 2.5 vol% H_2O and balance N_2 at 55 °C in a fixed bed reactor. The experimental data for CO_2 adsorption were described by the Langmuir isotherm to determine adsorption isotherm parameters.

4.2 Experimental

4.2.1 Materials

Alumina-clay composite as BCA (bottom cracking additive) and sodium carbonate were supplied by Intercat, USA and Merck India Ltd., respectively. All reagents and solvents were supplied by S. D. Fine-Chem Limited, India.

4.2.2 Preparation of adsorbents

As mentioned in Section 3.2.1, a composite of alumina (68 wt %) and clay (32 wt %) was chosen as a support for the study and it has good surface area of 131 m^2/g, pore volume of 0.345 cm^3/g and attrition index of 5%. The ALC was procured from Intercat, USA as a bottom cracking additive (BCA), which is used to improve yield by cracking heavy bottoms components in commercial fluid catalytic cracking (FCC) unit. Before undertaking the preparation, the above alumina-clay composite (ALC) was conditioned by drying and calcinations at 350 ^oC. The modification of the surface chemistry of ALC was carried out by impregnation with sodium carbonate (SC). Various loadings of Na_2CO_3 have been carried out using wet impregnation technique, where in the solution quantity equivalent to pore volume and solubility of solute would govern the loading of active component, in this case it is Na_2CO_3. Higher loading of active component is achieved through successive impregnation stages. Impregnated samples are dried at 110 ^oC overnight and labeled the sample as given in Table 4.1.

Table 4.1 Labeling details and physical characterization of prepared samples

Sample name	Support	Na_2CO_3 Loading (wt %)	Surface Area (m^2/g)	Total Pore Volume (cm^3/g)
ALC-SC-0	ALC	0	130	0.34
ALC-SC-1	ALC	5	112	0.32
ALC-SC-2	ALC	10	96	0.31
ALC-SC-3	ALC	15	82	0.30
ALC-SC-4	ALC	20	81	0.27
ALC-SC-5	ALC	25	71	0.25

4.2.3 CO_2 adsorption measurements

The adsorption studies have been performed in a fixed bed, continuous adsorption system with precise control over flow rates of various gases, temperature of adsorbent and continuous CO_2 analyzer at the outlet. The schematic diagram of this study set up is given in Figure 4.1.

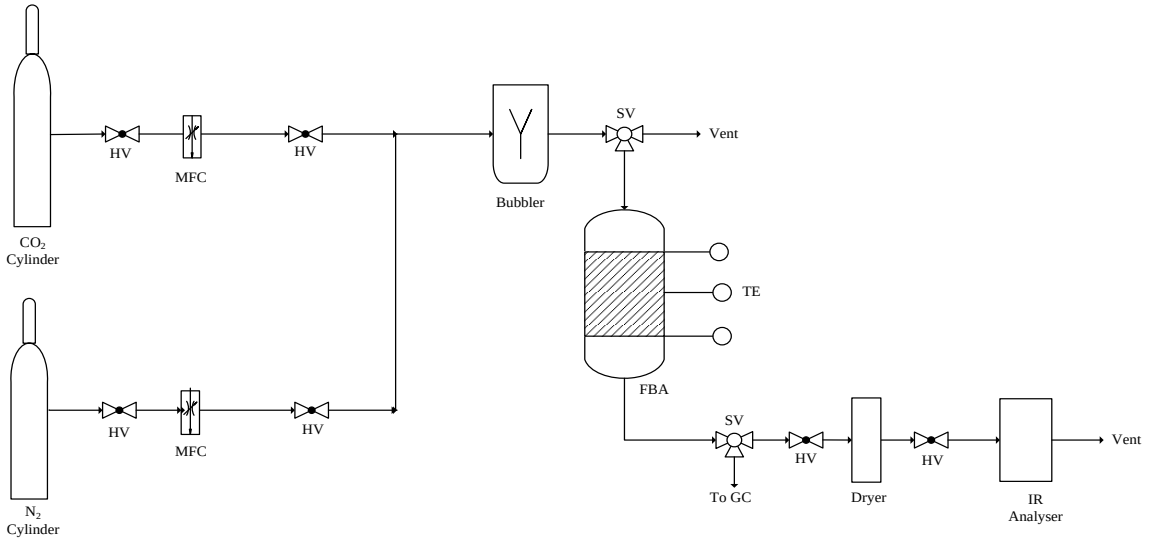

Figure 4.1 Fixed-bed adsorption study set-up

The total system was calibrated and tested for leak proof condition. A simulated flue gas composition of 3-9 vol% CO_2, 2.5 vol% H_2O and rest N_2 was used in all the adsorption study. The N_2 and CO_2 were supplied from high-purity gas cylinders with flow rates controlled using pre-calibrated mass flow controllers. The simulated gas mixture of N_2 and CO_2 was passed

through the water saturator to saturate the stream at room temperature. The total flow rate of the feed gas stream was 150±2 ml/min. Then the simulated gas mixture was passed through the adsorbent bed. The adsorbent was pretreated with water vapor for 30 minutes to achieve higher adsorption capacity. The treated effluent stream was passed through a dryer to remove the water and the outlet concentration of CO_2 was measured continuously by on-line IR analyzer (Servomex 1440 series, measurement limit 0-10 vol%).

4.3 Results and discussion

4.3.1 Adsorbent properties

4.3.1.1 Textural properties

The BET surface area of ALC-SC-0 and ALC-SC-4 were estimated to be 131 m^2/g and 81 m^2/g and the total pore volume were 0.345 cm^3/g and 0.271 cm^3/g respectively. The average particle size of the adsorbent was 85 μm. As expected, the impregnation of Na_2CO_3 has resulted in the reduction of pore volume and surface area. The pore size distribution is shown in Figure 4.2. The support system shows bimodal distribution with presence of both narrower and broader meso-pores in the range of 30 Å and 90 Å respectively.

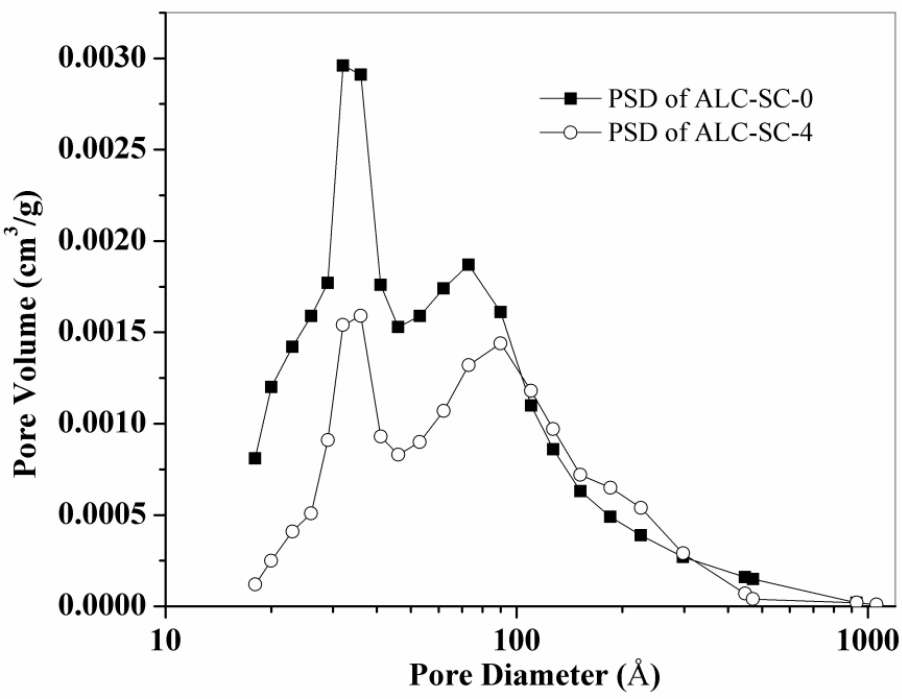

Figure 4.2 Pore size distribution plot of ALC-SC-0 (support) and ALC-SC-4 (20% Na_2CO_3 loading)

4.3.1.2 SEM analysis

The particle morphology images for Na_2CO_3 based adsorbents were evaluated by SEM (Figure 4.3). Figure 4.3a shows the particle image of fresh ALC support, which are spherical in shape. Figure 4.3 b and c show that Na_2CO_3 is distributed on ALC support. As the loading amount was increased, the Na_2CO_3 on ALC support was deposited on the surface of the support. At 20-wt% Na_2CO_3 loading, Na_2CO_3 was found to be deposited on the support surfaces, while at 25-wt% Na_2CO_3 loading, the support materials become agglomerated due to excessive growth of Na_2CO_3 on the support, which decreased the active sites for CO_2 adsorption. This may be due to the inhomogeneous dispersion of Na_2CO_3 into the narrower meso-porous structure of this ALC material. Therefore, the role of support materials for effective dispersion of active phase needs to be investigated.

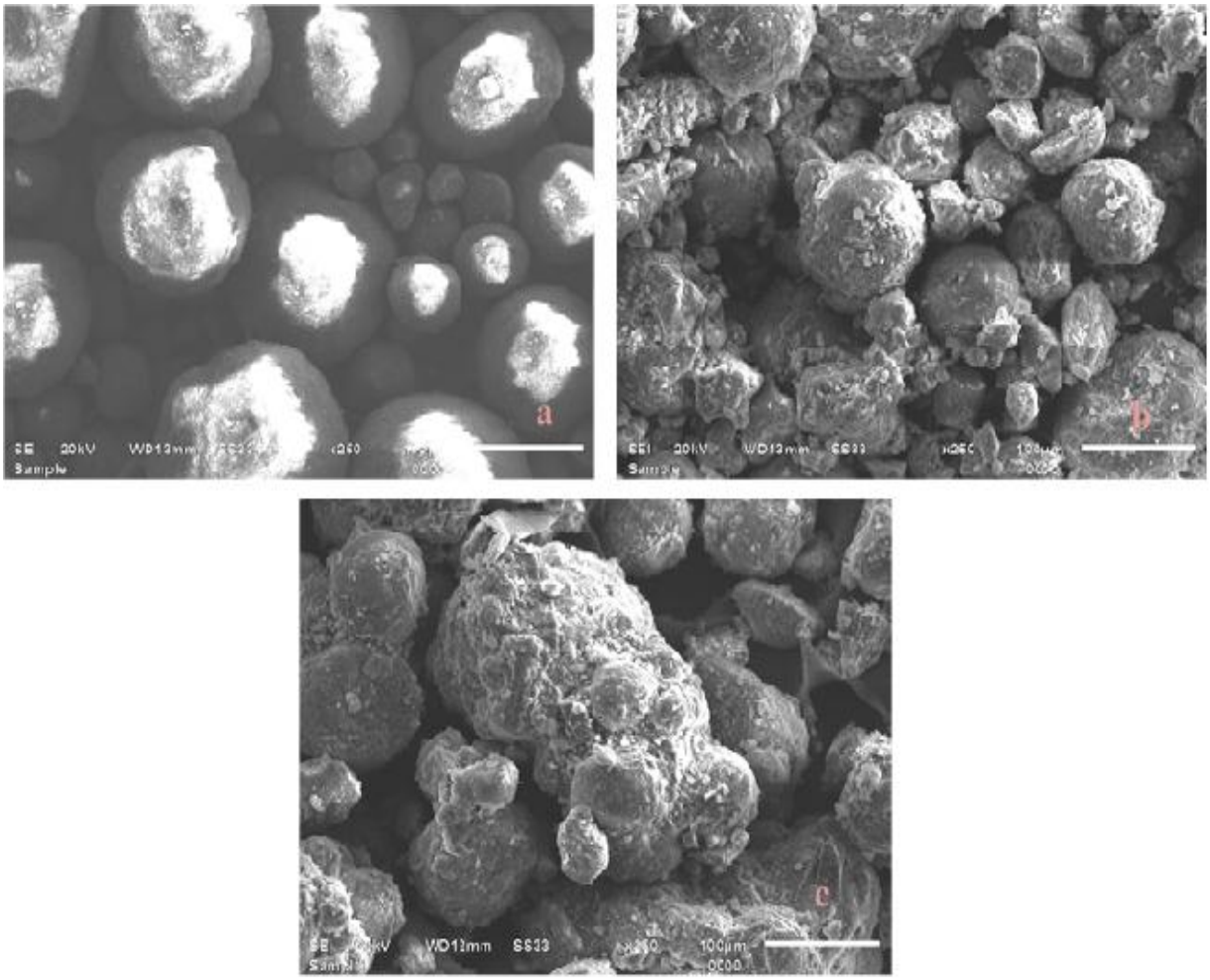

Figure 4.3 SEM images taken at the magnification 250X for (a) ALC-SC-0, (b) ALC-SC-4, (c) ALC-SC-5

4.3.2 CO_2 adsorption studies

CO_2 adsorption has been used for screening and selecting the adsorbent for detailed parametric study. The adsorption of CO_2 at close to atmospheric pressure requires chemical adsorbents with sodium carbonate impregnated over inorganic supports to increase the affinity towards CO_2 capture from flue gases. The results are given in Figure 4.4 and Table 4.2. Overall, ALC-SC-4, i.e. with 20% Na_2CO_3 on ALC is having the highest CO_2 adsorption at 55 °C (Table 4.2).

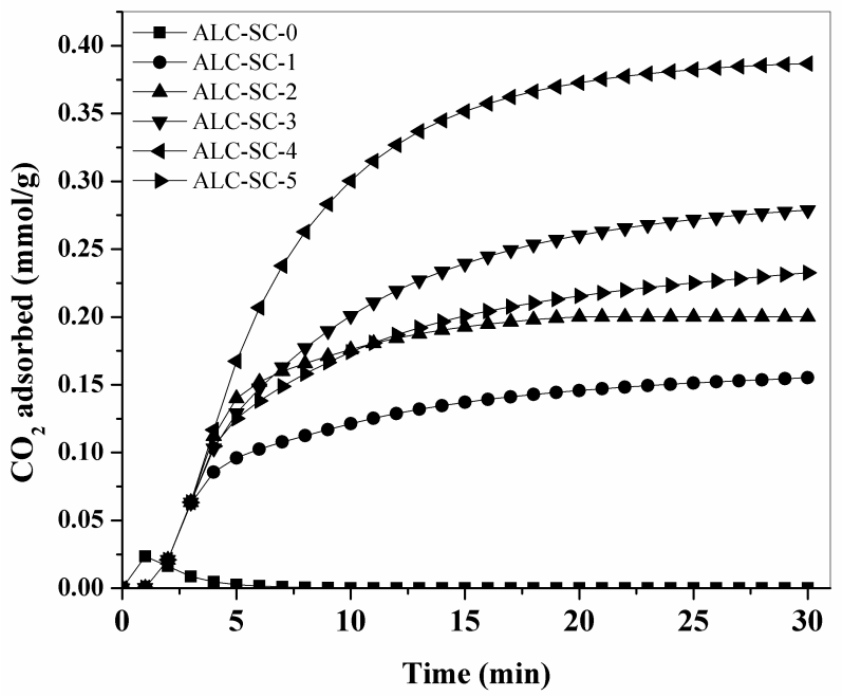

Figure 4.4 Comparison of CO_2 adsorption capacity of different adsorbents as a function of Na_2CO_3 loading at 8 vol% CO_2 concentration

Table 4.2 Adsorption capacities of selected samples alkali-impregnated ALC with 8 vol% CO_2 in simulated flue gas

Sample ID	Na_2CO_3 Loading (wt %)	CO_2 Adsorbed in (m mol/g-Adsorbent) at 55°C
ALC-SC-0	0	0.0
ALC-SC-1	5	0.16
ALC-SC-2	10	0.20
ALC-SC-3	15	0.28
ALC-SC-4	20	0.39
ALC-SC-5	25	0.23

Table 4.2 shows that CO_2 adsorption capacity increases with increase in carbonate loading up to 20 wt% and it drastically decreases at 25 wt% carbonate loading. This may be due to the lower accessibility of carbonate into the pores of the adsorbent. To check the reproducibility of the above results, the experiments were performed three times under identical conditions. The results are quite reproducible with standard deviation of 5%. It is also seen from Table 4.2 that the CO_2 adsorption capacity of this Na_2CO_3-based is quite less as we observed in our further study using 20-wt% K_2CO_3/Al_2O_3 system. The specific reason of this lower adsorption capacity using this ALC-SC-4 adsorbent is the use of water content in simulated flue gas. This adsorption study was carried out using lower water content (2.5 vol%), while further experiments were conducted with higher water content (up to 15 vol%). Higher the water content in simulated flue gas, higher is the active phase formation, such as $Na_2CO_3 \cdot 1.5\ H_2O$, $K_2CO_3 \cdot 1.5\ H_2O$ during adsorption [66-68]. This active species formation in the adsorbent is responsible for higher CO_2 adsorption capacity, which has been discussed in detail in chapters 5 and 6. These studies show the role of water content in flue gas streams on CO_2 adsorption capacity.

4.3.3 Breakthrough curves

The breakthrough adsorption experiments for virgin ALC and adsorbent of 20-wt% Na_2CO_3 impregnated on ALC were carried out at different CO_2 concentrations of 3–9 vol% in simulated flue gas and at constant adsorption temperature of 55 ^oC and atmospheric pressure. The progress of the effluent concentration of CO_2 from the bed when subjected to a concentration input variation was recorded, i.e., its breakthrough curve which are shown in Figure 4.5.The equilibrium CO_2 adsorption capacity and the breakthrough time were calculated to study the adsorption kinetics. In this case, experiments were carried out until adsorbent saturation was reached, in order to assess the maximum dynamic adsorption capacity of the adsorbents.

The breakthrough curves were measured for the adsorbents and CO_2 concentration in the exit simulated flue gas was plotted versus time (Figure 4.5). It shows that there is an instrumental time lag of around 4 minutes after which CO_2 response was observed. The mass transfer rate was high near the bed inlet where CO_2 first contacts with the adsorbent. When the time proceeds, the bed inlet becomes saturated and the mass-transfer zone shifted further which is S-shaped.

At a given adsorption temperature and different CO_2 concentrations in the feed (Figure 4.5) a lower CO_2 concentration leads to higher breakthrough times because the CO_2 concentration per site was not sufficient at the bed. In this case, at 55 ^oC, the CO_2 adsorption front of 3 vol% CO_2 containing feed reached the bed outlet after 13 min. The breakthrough time then decreased for higher CO_2 concentrations (Figure 4.5). A narrow mass-transfer zone is desirable to make efficient use of the adsorbent and to reduce regeneration energy consumption. The narrower the mass-transfer zone, the greater the degree of utilization of the bed.

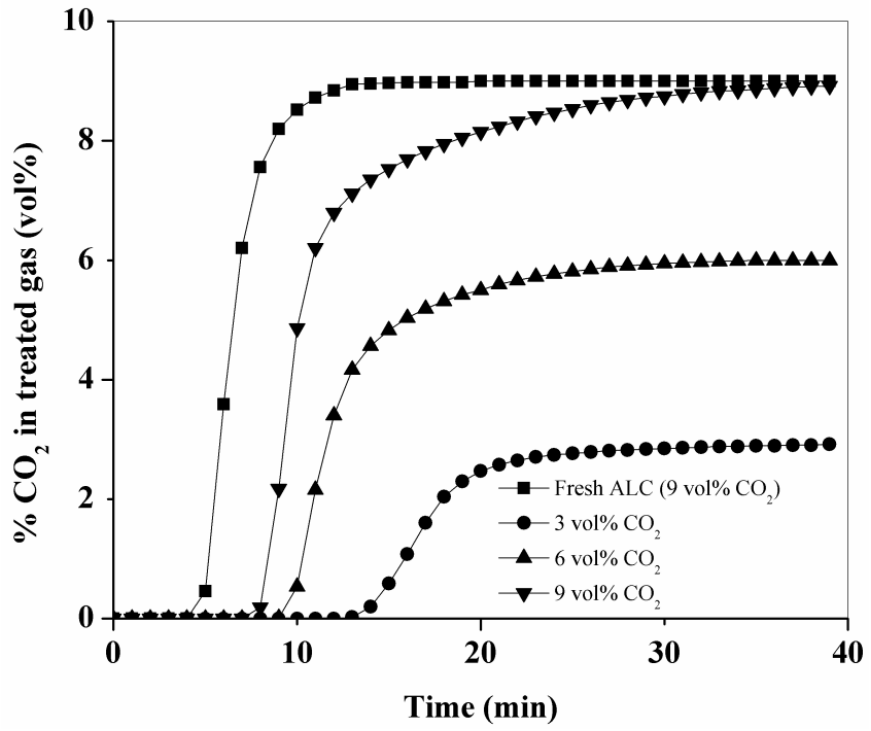

Figure 4.5 Breakthrough curves of adsorbent as a function of CO_2 concentration at 20 wt% Na_2CO_3 loading at 55 °C

4.3.4 Effect of adsorption temperature and CO_2 content in simulated flue gas

The effects of adsorption temperature have been studied at total flow rate of 150 cm^3/min (Table 4.3). On increasing the temperature from 55 ^oC to 65 ^oC, the CO_2 adsorption capacity is decreasing. This may be due to desorption of CO_2 at temperatures above 55 °C. It has been observed that there was no significant change in adsorption capacity with change in adsorption temperature in low concentration of CO_2 (3 vol%) as compared to higher CO_2 concentrations in simulated flue gas stream, which may be due to the limitation of CO_2 availability per site of adsorbent.

Table 4.3 Adsorption capacity (mmol/g) of ALC-SC-4 at different temperatures and CO_2 concentrations in simulated flue gas

Temperature (^oC)	3 vol% CO_2	6 vol% CO_2	9 vol% CO_2
55	0.184	0.287	0.386
60	0.151	0.184	0.252
65	0.133	0.135	0.227

4.3.5 Adsorption isotherms

The adsorption isotherm at 55 °C obtained from this experimental study is presented in Figure 4.6. The adsorption capacity appears to level off at 8.7 cm^3/g when the CO_2 pressure is beyond 0.08 bar. A typical Langmuir adsorption isotherm [88] was selected to describe the relationship between the volume adsorbed and CO_2 partial pressure governed by the following equation:

$$\frac{1}{V_{ads}} = \left(\frac{1}{K_e V_m}\right) \times \frac{1}{p_{CO_2}} + \frac{1}{V_m} \qquad (4.1)$$

Where,

V_{ads} = CO_2 adsorption capacity (mmol CO_2/g-adsorbent)

V_m = Maximum capacity of CO_2 adsorption (mmol CO_2/g-adsorbent)

K_e = Equilibrium constant (bar^{-1})

p_{CO2} = Partial pressure of CO_2 at inlet (bar)

The best fitted parameters using the Langmuir equation are presented in Figure 4.6. We also performed the linear curve fitting of $1/V_{ads}$ vs. $1/p_{CO2}$ to obtain V_m (0.875 mmol/g) and k (0.148 bar^{-1}) as shown in Figure 4.7. This value of V_m is much higher as compared to observed CO_2 adsorption capacity. This is due to the lower water content in the simulated flue gas and also insufficient active sites available for CO_2 adsorption due to narrower meso-pores in the support material (Figure 4.3 b). The estimated activation energy (E) using Arrhenius equation was found to be 42 kJ/mol (from Figure 4.8).

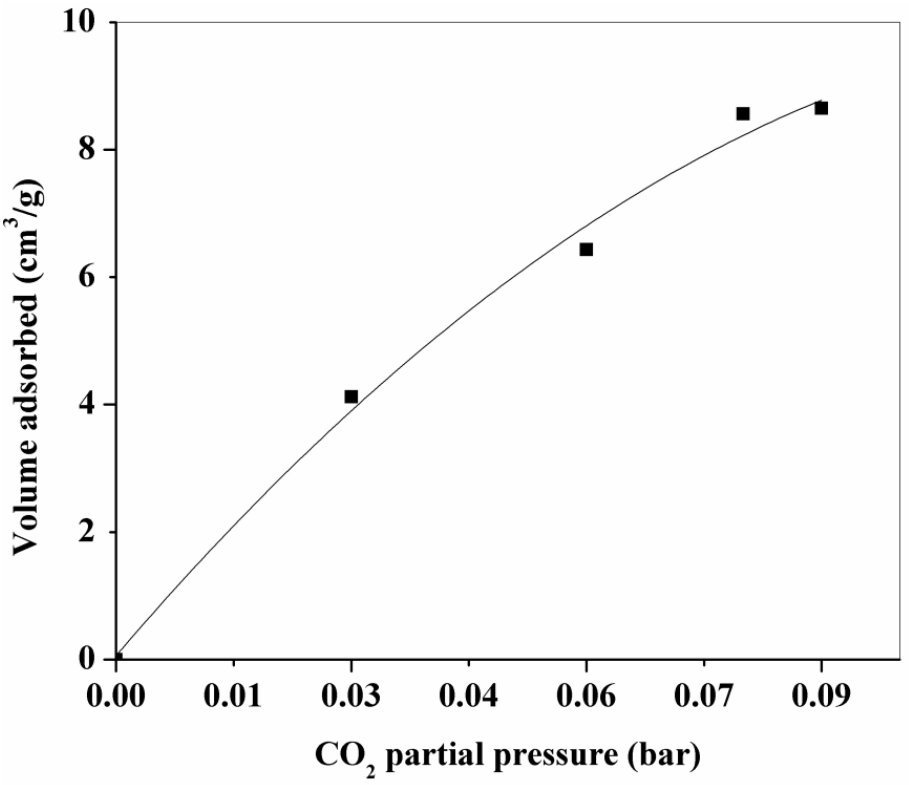

Figure 4.6 Adsorbent capacity and the best fitted Langmuir isotherm at 55 °C

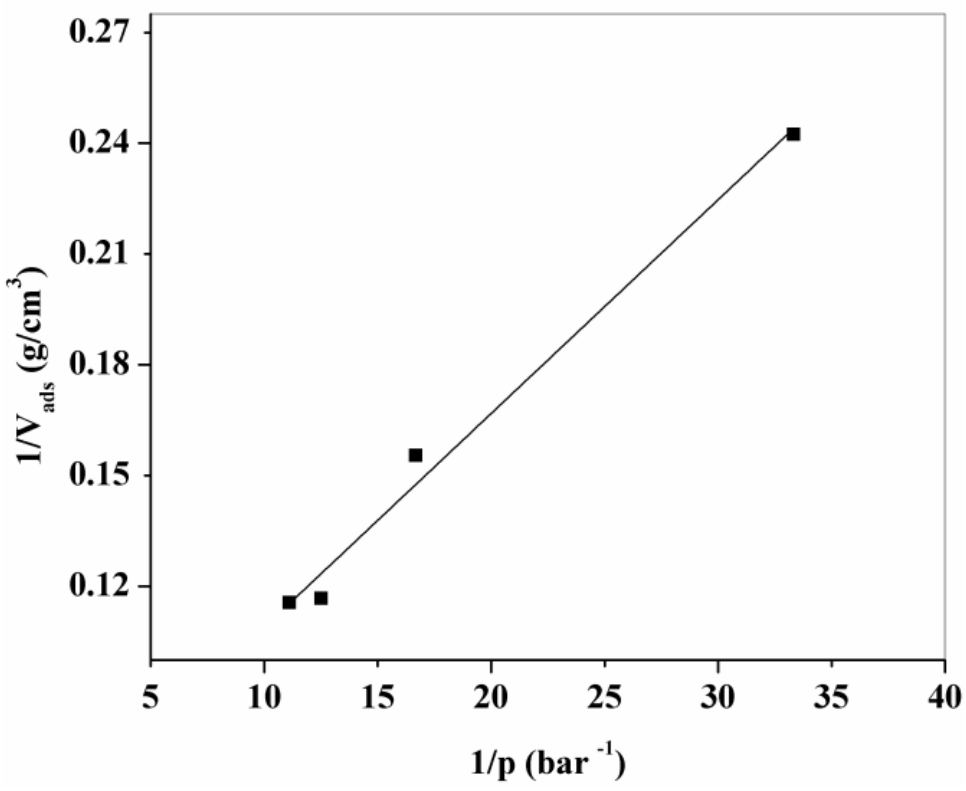

Figure 4.7 Plot of $1/V_{ads}$ vs. $1/p_{CO2}$ at 55 °C

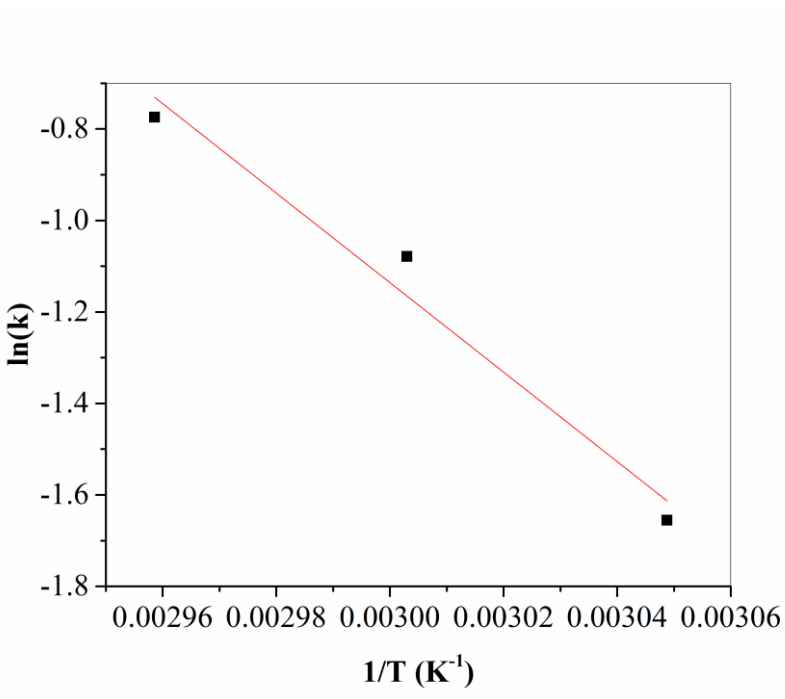

Figure 4.8 ln(k) vs. 1/T plot

4.4 Conclusions

Among various alumina-clay based adsorbents with different Na_2CO_3 loading, 20-wt% Na_2CO_3 based adsorbent shows maximum CO_2 adsorption capacity of 0.39 mmol/g of adsorbent at flue gas temperature of 55 °C and CO_2 content of about 8 vol%. At increased adsorption temperature, CO_2 adsorption capacity of this adsorbent decreases. The best fitted parameters, V_m of 0.875 mmol/g and k of 0.148 bar^{-1} using the Langmuir equation are estimated. The estimated activation energy of this adsorbent system is 42 kJ/mol. The lower CO_2 adsorption capacity with these adsorbent systems is due to the effect of water content in flue gas streams. That is why the role of water content in feed simulated flue gas needs to be examined. Similarly, textural properties of the support material play an important role to achieve higher CO_2 adsorption capacity. Homogeneous dispersion of active phase needs to be assured to produce available active sites for CO_2 adsorption.

Chapter 5

Effects of Adsorbent Preparation Method for CO_2 Capture from Flue Gas using K_2CO_3/Al_2O_3 Adsorbents

5.1 Introduction

In this chapter, the effect of preparation method on CO_2 adsorption capacity of K_2CO_3/Al_2O_3 adsorbents is examined. A series of adsorbents were prepared using single- and multistep incipient wet impregnation method. The activity of these various adsorbents was evaluated in a fixed-bed adsorber system. Various physico-chemical properties have been discussed to explain how multi-step impregnation method is superior to single-step method with similar active phase loading. The multi-step impregnation (MI) method enables uniform dispersion of active species (K_2CO_3) in the broad macro-pores without blocking narrower meso-pores. This facilitates higher loading of accessible K_2CO_3 for CO_2 adsorption and hence, higher adsorption capacity. The single-step impregnation (SI) method suffers from blockage of narrower meso-pores by excessive growth of K_2CO_3. This limits the CO_2 accessibility towards active species in the porous structure due to the formation of larger aggregates of active species. The experimental data for CO_2 adsorption were described by the Langmuir isotherm, and the isosteric heat as a function of fractional coverage of the adsorbent was calculated using the van't Hoff equation. The isosteric heat of CO_2 adsorption showed decreasing trend with increase in surface coverage of the adsorbent. This work is very unique in terms of adsorbent capacity improvement using effective adsorbent preparation method.

5.2 Effect of K_2CO_3 loading on physico-chemical properties of adsorbents

5.2.1 Textural analysis

The structural properties of supported adsorbents prepared by 10-60 wt% K_2CO_3 impregnation using single and multi-step impregnation method is shown in Table 5.1. Both BET surface area and pore volume decrease with increase in K_2CO_3 loading. In impregnation method, the active component (i.e. K_2CO_3) and the support material are two separate phases and their interaction does not lead to any significant changes in the meso-porous structure of the support [95]. Therefore, the BET surface area (SA) and total pore volume (TPV) decrease with increasing K_2CO_3 loading as K_2CO_3 is contained within the pore walls and sequentially fills up the pores during multi-step impregnation method.

It is seen from Table 5.1 that for a given loading, SA and TPV are higher in multi-step than those in single-step impregnation (SI). For example, at 40-wt% K_2CO_3 loading, the SA and TPV of MI method are 55 m^2/g and 0.156 cm^3/g vs. 52 m^2/g and 0.142 cm^3/g respectively in SI method.

Table 5.1 Physical characteristic of prepared adsorbents

Adsorbents*	**Preparation method**	**Adsorbent name**	**K_2CO_3 loading (wt %)**	**BET surface area (m^2/g)**	**Total pore volume (cm^3/g)**	**Average pore diameter (Å)**
Fresh γ-Al_2O_3		γ-Al_2O_3	0	172	0.482	102
K_2CO_3/ γ-Al_2O_3	Multi-step impregnation	10MI	10	158	0.402	105
		20MI	20	127	0.350	107
		30MI	30	98	0.278	113
		40MI	40	55	0.156	103
		50MI	50	44	0.126	105
		60MI	60	23	0.063	108
		50MI†	50	29	0.074	103
	Single-step impregnation	10SI	10	151	0.393	107
		20SI	20	102	0.317	110
		30SI	30	75	0.239	109
		40SI	40	52	0.142	112
		50SI	50	42	0.117	114
		37SI	37	65	0.165	101
* Abbreviations used for designated adsorbent like 10MI 10 wt% K_2CO_3 impregnated on Al_2O_3 using multi-step impregnation method, MI: Multi-step impregnation (up to 5-step impregnation) SI: Single-step impregnation, †Two-step impregnation (25+25 wt%).						

The pore size distribution (PSD) was examined by the Barrett-Joyner-Halenda (BJH) method. Figure 5.1a shows uniform distribution of pores with maximum average meso-pore diameter of 100 Å for K_2CO_3-based adsorbents. It is seen that the adsorbents prepared by both methods exhibit broader maxima at slightly increasing meso-pore diameters (ranges from 103-113 Å), but the remaining total pore volume in the meso-pores were significantly decreasing at higher K_2CO_3 loading than those were in the fresh alumina. This indicates that K_2CO_3 residing into the pores attributed to the decrease in the meso-porosity. On the other hand, the average pore diameter of the various adsorbents is slightly increasing with the K_2CO_3 loading. In fact, during impregnation of γ-Al_2O_3, the smaller pores are completely filled during loading of K_2CO_3 solution. Therefore, in averaging the pore diameter, there is no contribution of very small pores. Thus, calculated average pore diameter gets increased but physically none of the pore gets

widened. All the adsorbents prepared by both MI and SI methods illustrate type IV isotherm and exhibit H2 hysteresis loops (Figure 5.1b), which are generally associated with the interconnected pores of meso-porous materials [96]. In all cases, the hysteresis loops results in complete filling of the meso-pores at $0.4 < P/P_o < 1$.

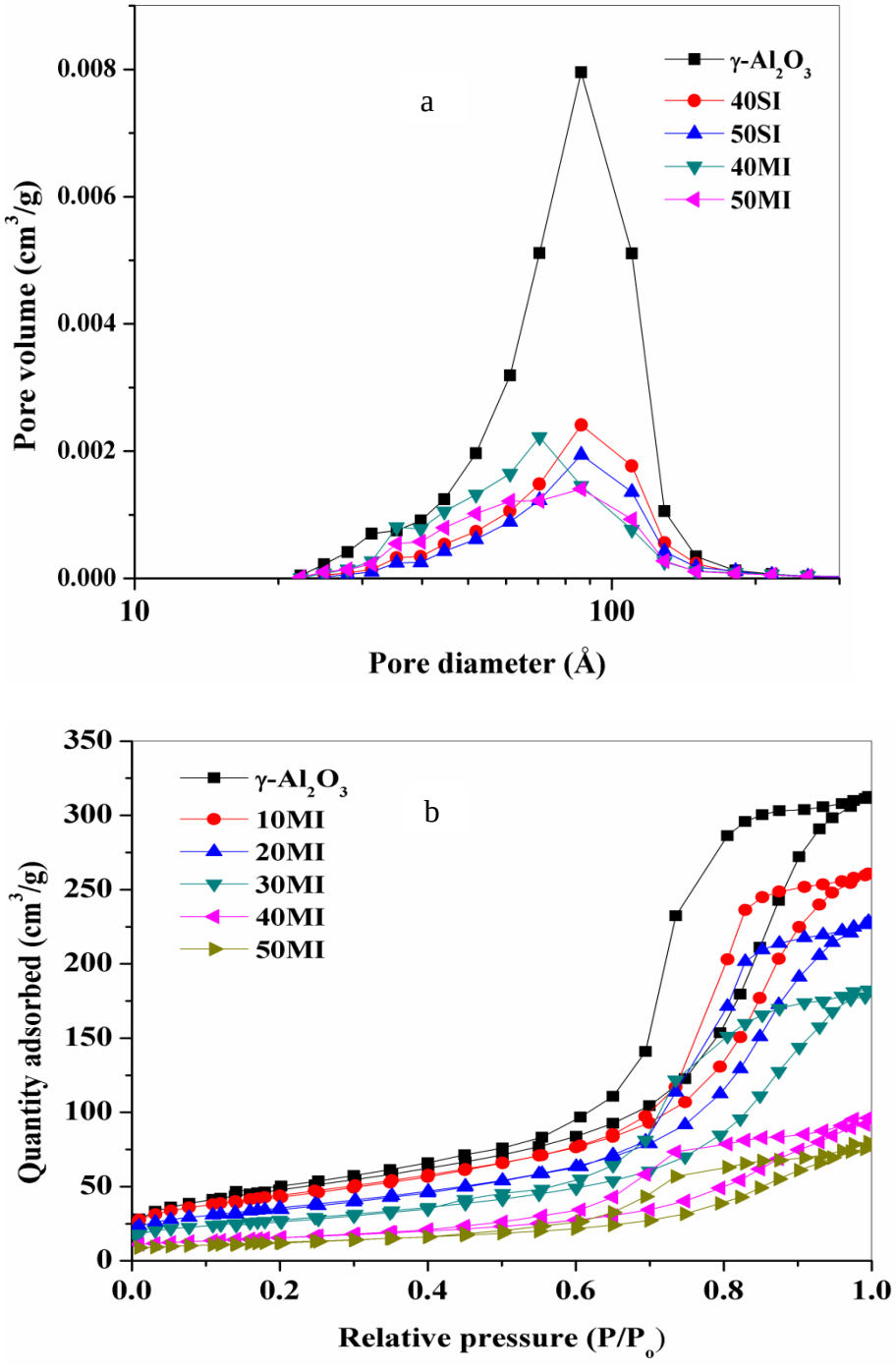

Figure 5.1 (a) PSD of γ-Al_2O_3 and supported K_2CO_3 based adsorbents and (b) adsorption isotherm of γ- Al_2O_3 and 10-50MI adsorbents with N_2 at -196 ^oC

Table 5.1 and Figure 5.1a shows a comparison of average pore diameter data of the prepared adsorbents. It is observed that for same carbonate loading, the MI method leads to lower average pore diameter but higher pore volume and surface area as compared to SI method. The homogeneous dispersion of K_2CO_3 in the longitudinal direction inside the broad meso-pores without blocking narrower meso-pores is expected in MI method, which is discussed in subsequent section [97].

On the other hand, the chance of blockage of narrower meso-pores by excessive growth of K_2CO_3 is highly expected in SI method. This limits the accessibility of CO_2 to K_2CO_3 in the porous structure due to the formation of larger aggregates of K_2CO_3. It is, therefore interesting to observe the attributes of MI method on the CO_2 adsorption capacity at similar loading as discussed in subsequent sections.

5.2.2 SEM analysis

The images on the particle morphology for K_2CO_3 based adsorbents were established by SEM (Figure 5.2). Figure 5.2a shows the uniform distribution of K_2CO_3 on γ-Al_2O_3 support prepared by multi-step impregnation method (MI). 50% K_2CO_3/Al_2O_3 samples prepared by MI method consisted of particles with regular spherical morphology and smooth surface. In MI method, the formation of K_2CO_3 layer is supposed to be increased with K_2CO_3 loading on the γ-Al_2O_3 support.

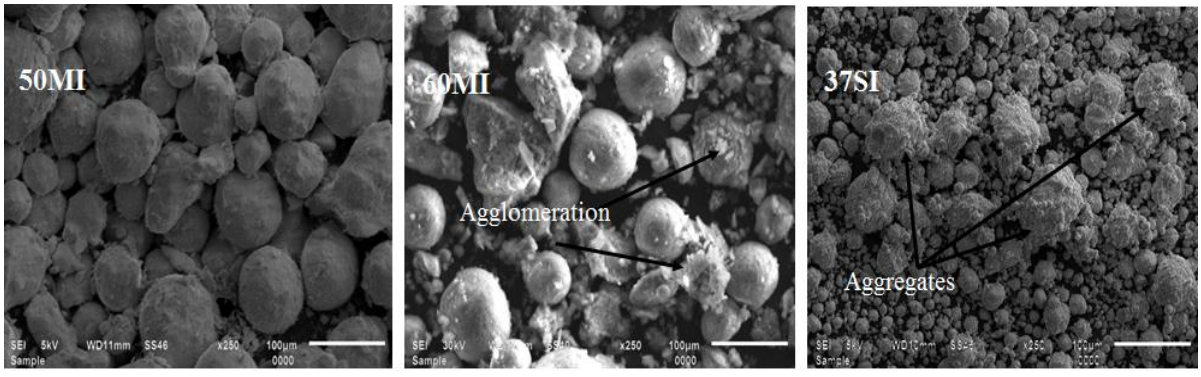

Figure 5.2 SEM images taken at the magnification 250X for (a) 50MI, (b) 60MI, (c) 37SI

Figure 5.2b shows the formation of large agglomeration of active component on the surface, which leads to decrease in active sites for adsorption for the higher loading (like 60-wt% K_2CO_3). Figure 5.2c shows some aggregates of support materials with K_2CO_3 (prepared by SI method), provide less active site for CO_2 adsorption. This may be due to the inhomogeneity of

metal salt dispersion in the support induced by capillary action. Similar observation was reported by Zhao et al. at higher K_2CO_3 loading (K_2CO_3: >45 wt%) [22]. Thus, the results showed that the preparation method strongly affected the morphology of the various K_2CO_3/Al_2O_3 adsorbents, as confirmed by XRD and BET results.

Figure 5.3a and 5.3b show the SEM with EDS (energy dispersive spectroscopy) cross-section images of 50MI and 50SI particles. It is observed that K_2CO_3 is uniformly distributed in 50MI as compared to 50SI. From the spectrum images, the EDS intensity line profiles were extracted along the green line drawn on the cross-section of adsorbents prepared by MI and SI method.

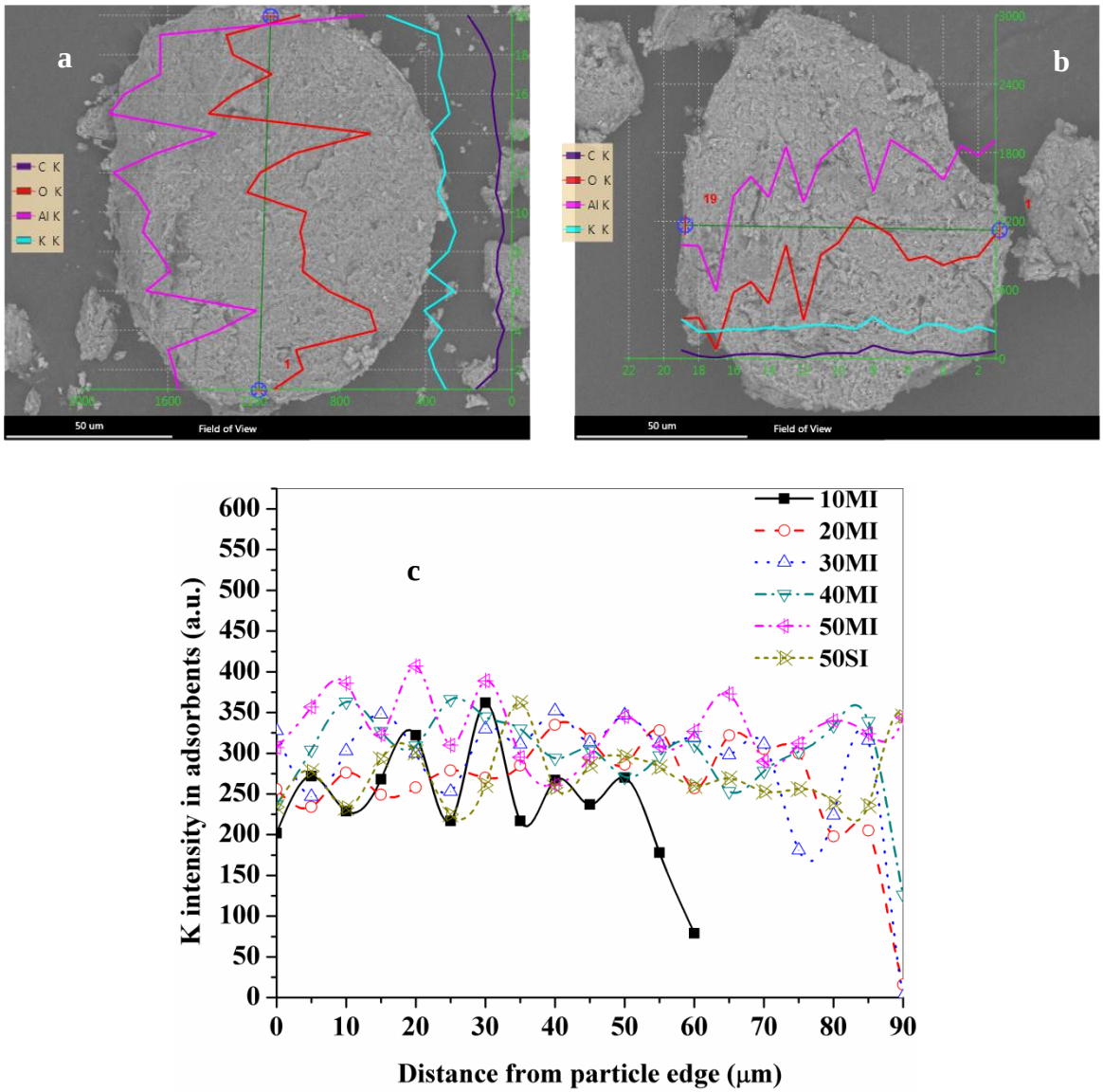

Figure 5.3 (a-b) Cross-section of 50MI and 50SI, (c) line scans across the cross-section of 10-50MI and 50SI showing distribution of K_2CO_3 inside the particle

Figure 5.3c also shows the distribution of K_2CO_3 active ingredient from the K (potassium) intensity line scans of cross-section for 10-50MI and 50SI adsorbents. For 10-50MI adsorbents, it can be noticed an increase in intensity of K inside the porous structure with increase in K_2CO_3 loading. This suggests a uniform distribution of K_2CO_3 as active phase during multi-step impregnation of active ingredient. From the comparison between the line scans for 50MI and 50SI, it indicates that K_2CO_3 is uniformly distributed inside the pores in case of 50 MI than 50SI as K intensity is higher for 50MI. It is also interesting to notice the K intensity near the particle surface for 50SI is high enough, which demonstrates the bulk deposition of K_2CO_3 at the surface during SI method. Hence, it is worthy to mention why CO_2 adsorption capacity is higher in the case of MI-adsorbents as compared to SI-adsorbents, which is discussed in the subsequent sections.

5.2.3 TEM analysis

The structure of the support material and arrangement of K_2CO_3 on the γ-Al_2O_3 was analyzed in order to determine the effect of adsorbent preparation method. In Figure 5.4a, the TEM image indicates the presence of about 0.5 µm size agglomerates of γ-Al_2O_3 particles in which the meso-pores of <100 Å are observed between the embedded particles of γ-Al_2O_3. The selected area electron diffraction (SAED) pattern of the support sample (see inset) shows concentric rings corresponding to (400) and (440) planes of γ-Al_2O_3, which are the reflections at 2θ of 46.3 and 67.2 respectively [99]. However, these concentric and diffused rings in the electron diffraction pattern emphasize the characteristic of polycrystalline structure and amorphous phase in γ-Al_2O_3.

Figure 5.4b shows that K_2CO_3 is quite uniform and distributed homogeneously in case of 50 MI as compared to 50SI and 60MI. It is observed from the TEM image that the K_2CO_3 is finely dispersed on γ-Al_2O_3 in MI method as indicated by considerably low concentration of rod like structures. Furthermore, the SAED image did not show dots pattern corresponding to crystalline K_2CO_3 phase. However, the K_2CO_3 present inside the meso-pores are not clearly visible due to low resolution of the TEM instrument.

TEM images of 50SI adsorbent depict a large amount of 0.4-0.5 µm long rod-like structures of uniform thickness of ~0.1 µm spread over the external surface of γ-Al_2O_3 particles (Figure 5.4c). These rod-like structures of K_2CO_3 on the γ-Al_2O_3 support surfaces are due to the

excessive growth of K_2CO_3 during SI method, which may block some of the meso-pores of γ-Al_2O_3.

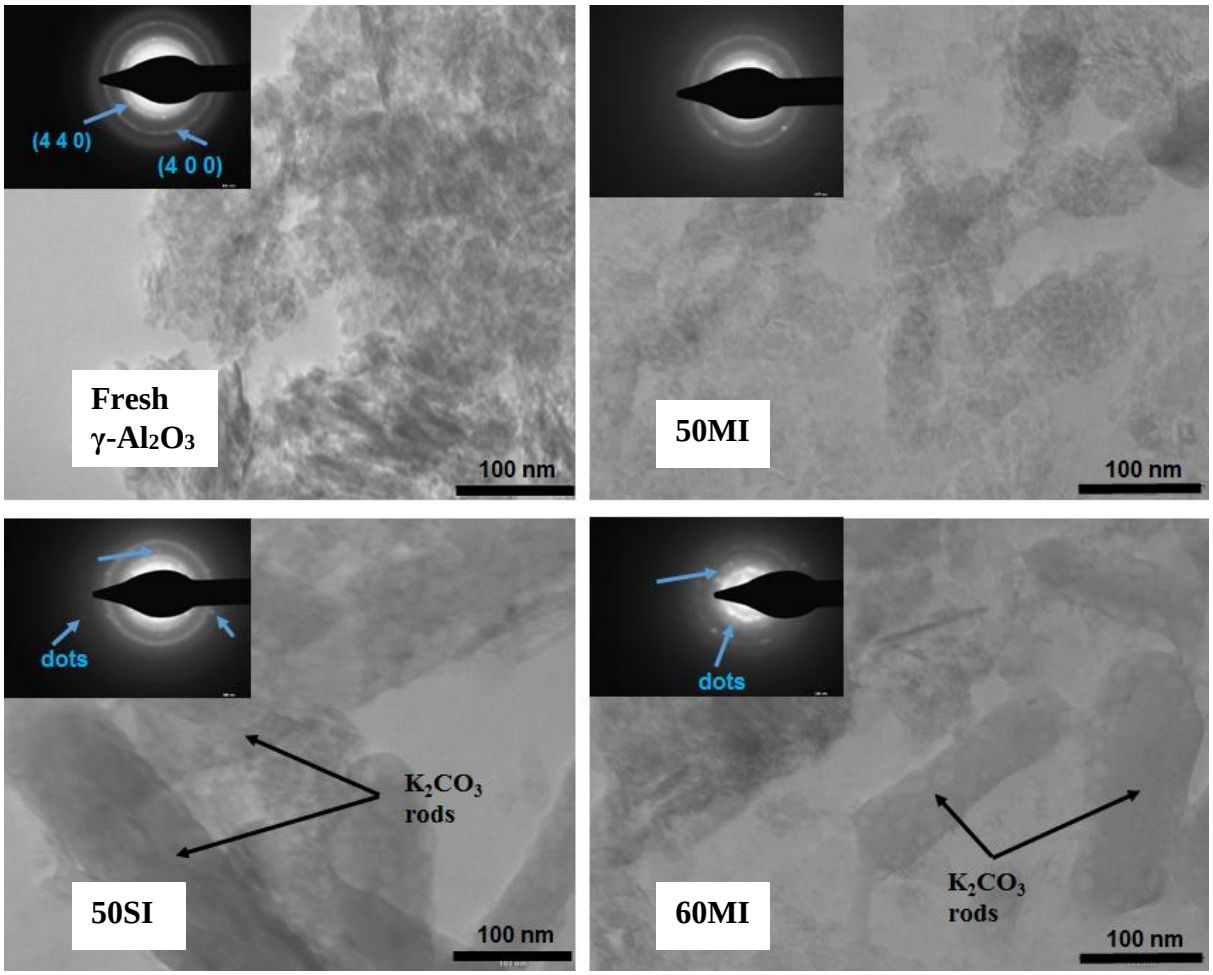

Figure 5.4 TEM images of (a) fresh γ-Al_2O_3, (b) 50MI, (c) 50SI, and (d) 60MI

Interestingly, K_2CO_3 rods displayed globular pores of varying size of 100-200 Å under high magnification. The globules inside the pores may be attributed to the removal of air entrapped inside the pores due to higher capillary pressure [100]. These kind of porous rods are more visible in 60% K_2CO_3/Al_2O_3 adsorbent (60MI). It suggests that the absence of these structures in fresh alumina sample clearly implies that this porous globular structure is originated due to K_2CO_3 phase. However, these kind of globular pores were not observed in 50MI indicating that K_2CO_3 is finely dispersed in the pores of γ-Al_2O_3. The SAED images taken at the rod like structures contained dotted pattern in between the concentric rings of γ-Al_2O_3. These dots can be correlated to diffraction from crystalline phases of K_2CO_3 (SAED image inset in Figure 5.4c). In case of 60MI, significant amounts of K_2CO_3 were found on the external surface (Figure 5.4d). Herein, K_2CO_3 beyond 50-wt% occupies the remaining pores of the adsorbent (remaining pore volume is 0.063 cm^3/g) and deposited on the external surfaces as excess metal

carbonate (Figure 5.2b). Hence, the reduced pore volume may exhibit a decrease in CO_2 adsorption capacity due to reduced accessibility to CO_2 diffusion as discussed in subsequent section.

5.2.4 XRD analysis

The XRD results as shown in Figure 5.5(a) reveals the presence of γ-phase in γ-Al_2O_3, K_2CO_3 in pure K_2CO_3 and different phases in fresh K_2CO_3/γ-Al_2O_3 adsorbents. As shown in Figure 5.5(a), there are mainly four peaks of γ-Al_2O_3 at 2θ of 37.2, 40.4, 46.3, and 67.2 (JCPDS 10-0425). All these peaks can be assigned to a cubic crystalline structure. XRD of pure γ-Al_2O_3 support exhibits a mix of broad and sharp peaks, which indicate the presence of amorphous and crystalline phases of Al_2O_3. The same observations are confirmed from TEM image of γ-Al_2O_3 (Figure 5.4a). It is also clear that γ-Al_2O_3 particles show the sharp peaks due to the presence of larger crystallites. The diffraction peaks present in pure K_2CO_3 and fresh K_2CO_3 based adsorbents with 2θ of 15.8, 26.2, 31.7, 32.1, 34.1, 42.8 and 48.9 are assigned to monoclinic crystalline phase (JCPDS 71-1466) of K_2CO_3. The peak intensity of K_2CO_3 increased with successive loading of K_2CO_3, which imply high crystalline phases of bulk K_2CO_3 on the support material. The diffraction peaks of $K_2CO_3 \cdot 1.5\ H_2O$ and $KAl(CO_3)_2(OH)_2$ were also observed in these fresh adsorbents with 2θ of 26.9, 29.7, 32.3, 32.6, and 41.3, and 45.8, 67.5 (JCPDS 73-0470 and 21-0979). On the other hand, with increase in K_2CO_3 loading in multi-step impregnation method, the peak intensity of γ-Al_2O_3 in K_2CO_3/γ-Al_2O_3 decreases. It clearly shows that K_2CO_3 was homogeneously dispersed inside the porous support, which may help in achieving higher CO_2 adsorption capacity as discussed in subsequent section.

The XRD features of various impregnated adsorbents (40SI and 40MI) do not provide any distinguished information for comparison between SI and MI methods. This may be due to the fact that as the active component loading is equal in quantity, the formation of crystallites are expected during both impregnation methods. Due to the particle aggregation formed during SI method, it is expected to absorb lower X-ray radiation and hence the intensity of incident beam is increased.

Similarly, Figure 5.5b shows the XRD patterns of the hydration and carbonation behavior of 37SI. It is found that there is a strong peak intensity of both $KHCO_3$ and $KAl(CO_3)_2(OH)_2$ phases in the fresh and adsorbed material. The diffraction peaks of these two phases with 2θ of 24.2, 30.0, 31.4, 34.0, 39.2 and 40.6 are assigned to $KHCO_3$ (JCPDS 70-1168), while 2θ of

15.9, 26.7, 28.0, 33.8, 35.8 and 45.8 are $KAl(CO_3)_2(OH)_2$ (JCPDS 21-0979). As shown in Figure 5.5b, the XRD pattern of 37SI does not show any indicative phases (looking almost flat) when CO_2 was adsorbed without water as if CO_2 alone was making all the peaks. This may be due to the absence of one of the reactants during chemisorption of CO_2. The XRD results also show the presence of $KAl(CO_3)_2(OH)_2$ species after adsorption for 37SI and 50MI adsorbents resulted in high temperature regeneration (>300 ^oC). This is in agreement with the observation reported by Zhao et al. [21]. It is noted from Figure 5.5b that higher the γ-Al_2O_3 content in the adsorbents (e.g. 37SI), higher is the stable species formation due to the support-active phase interaction.

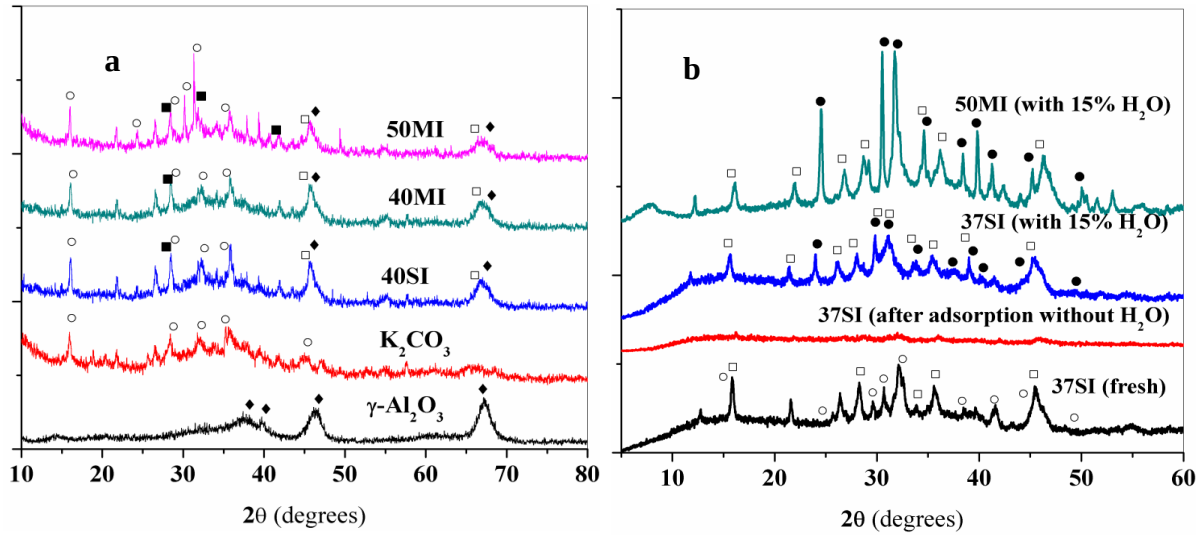

Figure 5.5 XRD patterns of (a) fresh adsorbents using multi-step impregnation (40 and 50 wt%) (b) 37SI (fresh / adsorption with and without water) (♦ γ-Al_2O_3, ○ K_2CO_3, ■ $K_2CO_3 \cdot 1.5$ H_2O, ● $KHCO_3$, □ $KAl(CO_3)_2(OH)_2$)

5.2.5 TG analysis

TG analyses for some selected adsorbent viz. γ-Al_2O_3, 40SI, 40MI, 50MI and 50MI after adsorption are shown in Figure 5.6. It is observed that there was a total loss of 12 wt% of pure γ-Al_2O_3 during thermo-gravimetric analyses, which are the losses due to removal of free and associated water at higher temperatures. It is also observed that with increase in K_2CO_3 loading from 10-60 wt% in fresh MI prepared adsorbents, the total weight loss increases from 13.3 to 28.2 wt%. In the first stage (~200 ^oC), there was a weight loss of $K_2CO_3 \cdot 1.5$ H_2O (decomposition temperature: 100-200 ^oC) [13] along with free residual surface water. In the subsequent stages-II (200-400 ^oC) and III (400-800 ^oC), there were weight losses due to

removal of stable deactivating components like, $KAl(CO_3)_2(OH)_2$ along with associated water [98].

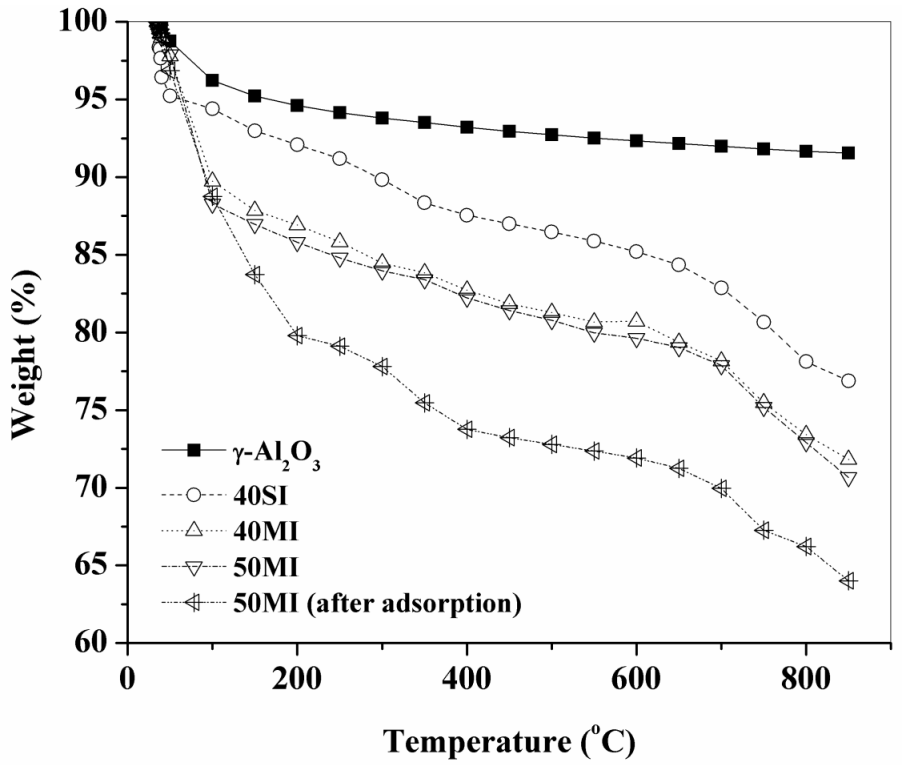

Figure 5.6 TG analyses for γ-Al_2O_3, 40SI, 40MI, 50MI (fresh) and 50MI (after adsorption/ regeneration step)

Figure 5.6 also shows that the total weight loss of 40MI was more as compared to 40SI. This is due to the method of stage wise impregnation, which leads to more associated water present in the form of $K_2CO_3 \cdot 1.5\ H_2O$, $KAl(CO_3)_2(OH)_2$. It should be noted that up to 200 ^oC, the total weight loss for 40MI is higher than 40SI. This suggests that dispersion of K_2CO_3 in Al_2O_3 during MI method is much better than SI method, which results higher active species ($K_2CO_3 \cdot 1.5\ H_2O$) formation for CO_2 adsorption (i.e. removal of more water of crystallization). In MI method, the dispersed phase is more uniform while in SI method, the aggregated phase of K_2CO_3 is expected on the γ-Al_2O_3. This observation is in good agreement with the SEM images shown in Figure 5.2 and 5.3c. This may facilitate higher CO_2 adsorption capacity in MI-prepared adsorbents as compared to those prepared by SI method.

It was also observed that there were more weight losses for adsorbed sample of 50MI in decomposition stages-I and II. These losses are primarily attributed to the decomposition of $KHCO_3$ in stage-I and $KAl(CO_3)_2(OH)_2$ in stage-II. The XRD results shown in Figure 5.5b also reveal the formation of $KHCO_3$ and $KAl(CO_3)_2(OH)_2$ phases during CO_2 adsorption [20, 98].

5.3 Effect of K_2CO_3 loading on CO_2 adsorption

The comparison of CO_2 adsorption capacity of various K_2CO_3 adsorbents prepared by both the methods and also with the reported in literature by SI method is shown in Figure 5.7. It is observed that in both SI and MI method, the CO_2 adsorption capacity increases gradually with increase in the metal carbonate loading. The CO_2 adsorption capacity was achieved as 3.12 mmol/g up to 50-wt% K_2CO_3 loading for MI prepared adsorbents. However, at higher loading (60 wt%), the CO_2 adsorption capacity abruptly drops. This is due to reduced pore volume of 60MI adsorbent at higher K_2CO_3 loading. It signifies the deposition of K_2CO_3 on the surface of particles instead of inside the pores, which exhibits the chance of blockage of some pores (Figure 5.2b). Therefore, accessibility of active K_2CO_3 sites for gas-solid contact is important for CO_2 adsorption. On the other hand, for 50SI, the adsorption capacity was limited to 1.93 mmol/g due to blockage of narrower meso-pores by excessive growth of K_2CO_3.

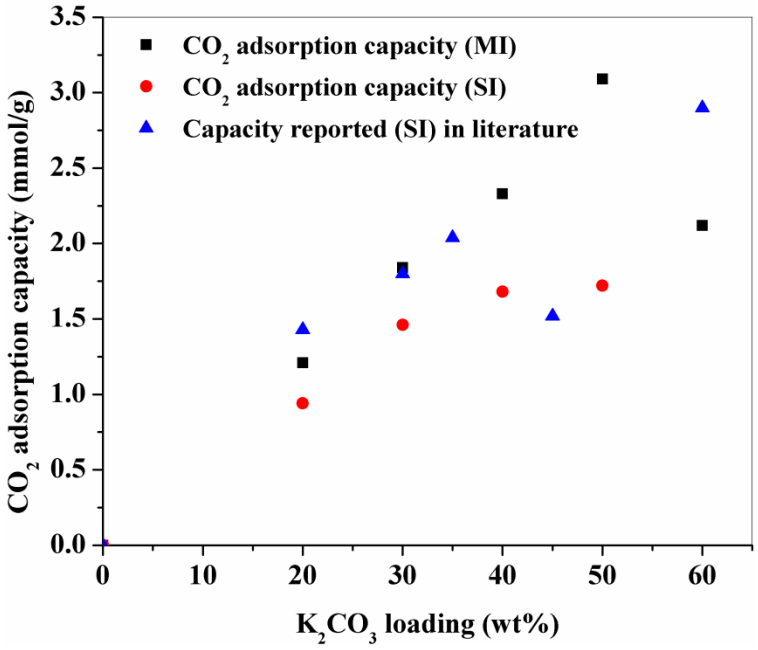

Figure 5.7 Comparison between CO_2 adsorption capacity reported in literature [19, 64] and the present study using SI and MI method (Conditions: 55 °C, atmospheric pressure with 8 vol% CO_2)

5.4 Effect of water on CO_2 adsorption capacity

The effects of water vapor on CO_2 adsorption capacity with varying concentration in simulated gas mixture were studied using 37SI and 40MI adsorbents. Figure 5.8 shows that the adsorption

capacity increases with increase in H_2O concentration. In absence of water, for 37SI adsorbent, the adsorption capacity was 0.30 mmol/g. The poor CO_2 adsorption capacity for 37SI is also validated by XRD analysis (Figure 5.5b). For 37SI, as the H_2O concentration in the simulated gas mixture is increased to 15 vol%, the adsorption capacity increased to 1.85 mmol/g. It is interesting to note that as the H_2O concentration in feed gas stream increases, the breakthrough time for CO_2 adsorption increases. This is due to the formation of active species K_2CO_3 1·5 H_2O with increase in H_2O concentration in simulated gas [14, 67], resulting in higher CO_2 adsorption capacity. The above observations are more pronounced for 40MI adsorbent (2.39 mmol/g) as compared to 37SI adsorbent (1.85 mmol/g).

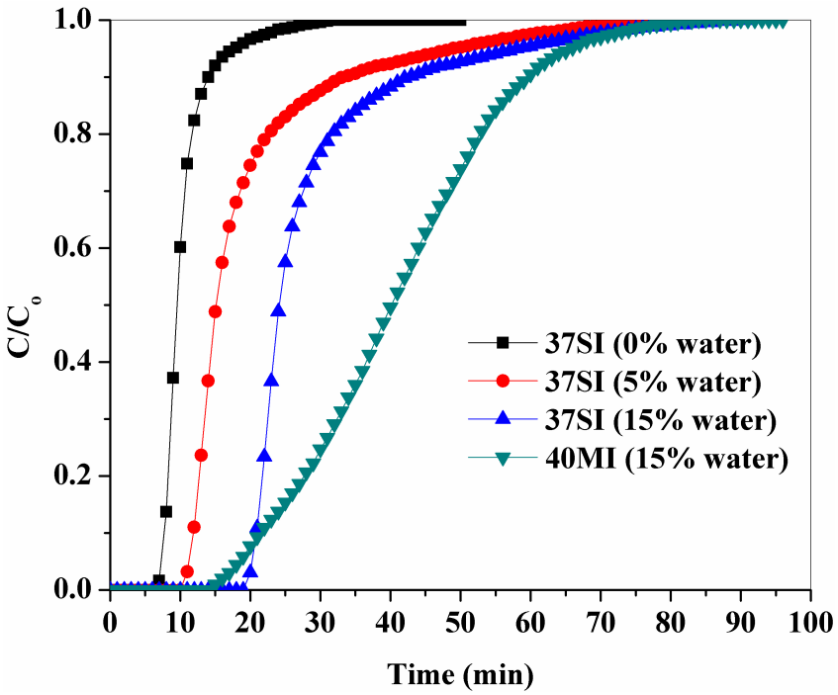

Figure 5.8 Effect of H_2O concentration on adsorbent performance at 55 °C using MI and SI-based adsorbents

5.5 Effect of adsorbent preparation method on adsorption breakthrough time

Figure 5.9a shows the effects of SI and MI method on the CO_2 adsorption at 55 ^oC. For a given adsorption temperature and CO_2 concentration in the feed simulated gas, 40 and 50MI adsorbents showed better adsorption characteristics than 40 and 50SI (as shown in Figure 5.3c). The possible explanation is as follows: in MI method, limited amount of K_2CO_3 (10 wt%) is impregnated sequentially followed by mixing and drying. During every step of impregnation followed by drying, the K_2CO_3 resided inside the pores provides porosity for exhibiting

accessibility to CO_2 diffusion due to expulsion of water of crystallization. While during SI method, excessive growth of K_2CO_3 limits the accessibility towards CO_2 diffusion inside the porous materials. Moreover, MI method allows uniform distribution of active K_2CO_3 ingredient into the pores of the support material as compared to single-step impregnation (formation of larger crystallites/ aggregates as shown in Figure 5.2 and Figure 5.4c). Therefore, MI method provides an adsorbent with higher loading of K_2CO_3 with more active sites for CO_2 adsorption, which exhibits longer breakthrough time (Figure 5.9a). In addition, TGA and XRD results also reveal the presence of active species ($K_2CO_3 \cdot 1.5\ H_2O$) in MI prepared adsorbents, which exhibits higher CO_2 adsorption than those prepared by SI method.

Figure 5.9b shows the CO_2 concentration profile with respect to time for a single adsorption-regeneration cycle of 50MI and 50SI adsorbents. It is seen that the total cycle time for single adsorption-regeneration is higher in case of 50MI as compared to 50SI. This is due to the active sites available for CO_2 adsorption as well as regeneration.

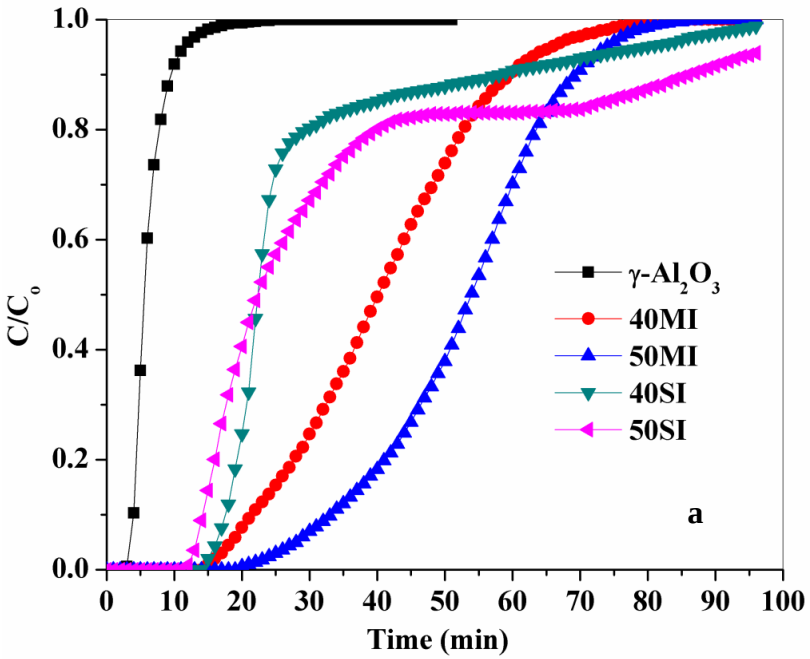

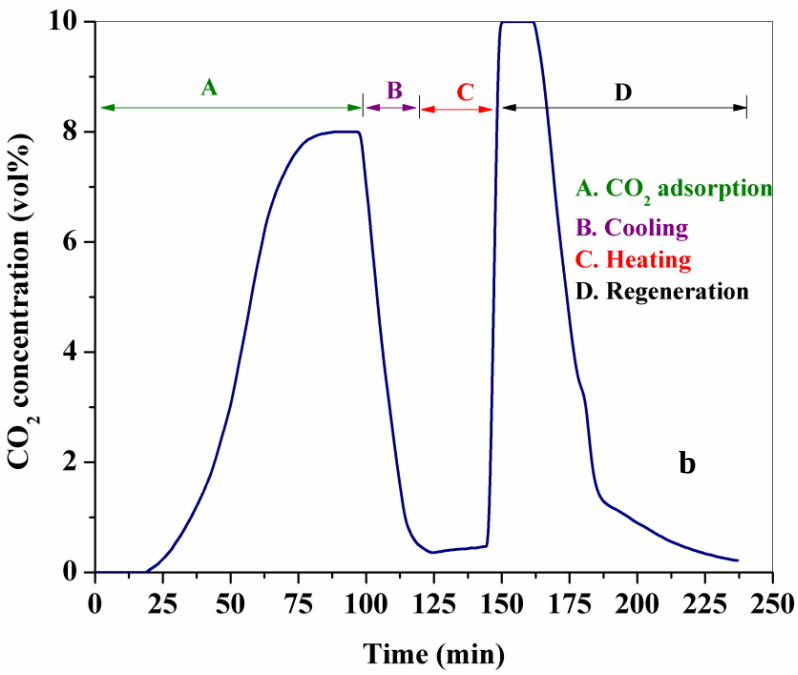

Figure 5.9 (a) Breakthrough curves for single and multi-step impregnated adsorbents at 55 °C and 1 atm (CO_2: 8 vol%, H_2O: 15 vol%), (b) cyclic study for 50MI adsorbent

5.6 Regeneration of adsorbents and their multi-cycle stability

The regeneration studies have been carried out for 50MI, 50SI and 37SI adsorbents in presence of N_2 as sweep gas. Figure 5.10 shows the effect of regeneration temperature and multi-cycle stability for 50MI, 50SI and 37SI adsorbents regenerated at 120 ^oC, 130 ^oC, and 300 ^oC. The regeneration characteristics of these K_2CO_3-based adsorbents are represented as percent regeneration, which is the ratio of cyclic capacity (i.e. capacity for regenerated adsorbent) with respect to fresh adsorption capacity. It was observed that nearly 65% and 56% regeneration were achieved for 50MI and 50SI respectively at 130 ^oC. As explained by XRD and TG analysis, after regeneration at 130 ^oC, the bicarbonate species is significantly converted back to carbonate species. For 37SI adsorbent, the regeneration achieved was 43% and 80% at 120 ^oC and 300 ^oC respectively. The decrease in regeneration efficiency at low temperature is due to the formation of stable component $KAl(CO_3)_2(OH)_2$, which only regenerates at high temperature (>300 ^oC) [13, 98]. The regeneration efficiency of the adsorbent prepared by MI method is higher than that of SI method which suggest that the regenerated MI adsorbent has more vacant site than SI adsorbent. It is due to the blockage of some mesopores during SI method, which contributes less active site for CO_2 adsorption as well as regeneration. This is

in good agreement as observed from TEM images. It is clear from Figure 5.10 that all MI and SI adsorbents exhibit stable multi-cycle stability.

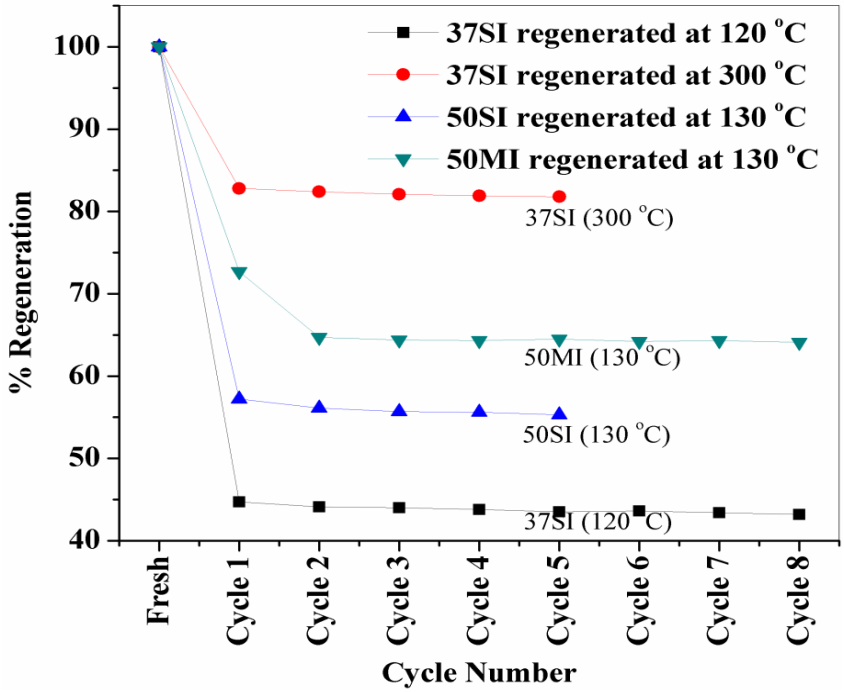

Figure 5.10 Effect of regeneration temperature and multi-cycle study for 37SI and 50MI. (sweep gas flow: 60 cm^3/min)

5.7 Isosteric heat of CO_2 adsorption

Isosteric heat of adsorption is defined as the ratio of the infinitesimal change in the adsorbate enthalpy to the infinitesimal change in the amount adsorbed. The detailed description for estimation of isosteric heat of CO_2 adsorption is explained in Section 3.10.

The experimental data '*q vs p*' for CO_2 adsorption on K_2CO_3 supported on MI adsorbent were non-linearly regressed (equation 3.11) using Matlab® surface fitting tool box to calculate simultaneously the optimal values of K_o, $q_{m,o}$, φ and Q. The calculated values of parameters K_o, and $q_{m,o}$ for best-fit Langmuir isotherm (Figure 5.11a) are 0.9343 and 3.243 respectively with regression coefficient $R^2 = 0.99$.

From sets of isotherms, the coverage-dependent isosteric heat of adsorption was deduced using the van't Hoff equation [93]:

$$\frac{\Delta H}{RT^2} = -\left(\frac{\partial lnp}{\partial T}\right)_q \qquad (3.12)$$

Also the isosteric heat of adsorption from equations (3.8-3.10 and 3.12) can be expressed in term of surface coverage as [94].

$$-\Delta H = Q - \varphi RT_o \frac{1}{1-\theta} \qquad (3.13)$$

where, $\theta = q/q_m$ = fractional coverage of the adsorbent.

The Figure 5.11b shows the plot of isosteric heat of adsorption with surface coverage. The isosteric heat of adsorption decreases and reaches zero at $\theta = 0.99$. This trend is similar to other isosteric heat profile obtained from other semi-empirical equilibrium adsorption model reported in literature for CO_2 adsorption on polyethyleneimine-functionalized TUD-1 mesoporous silica sorbent [93-94].

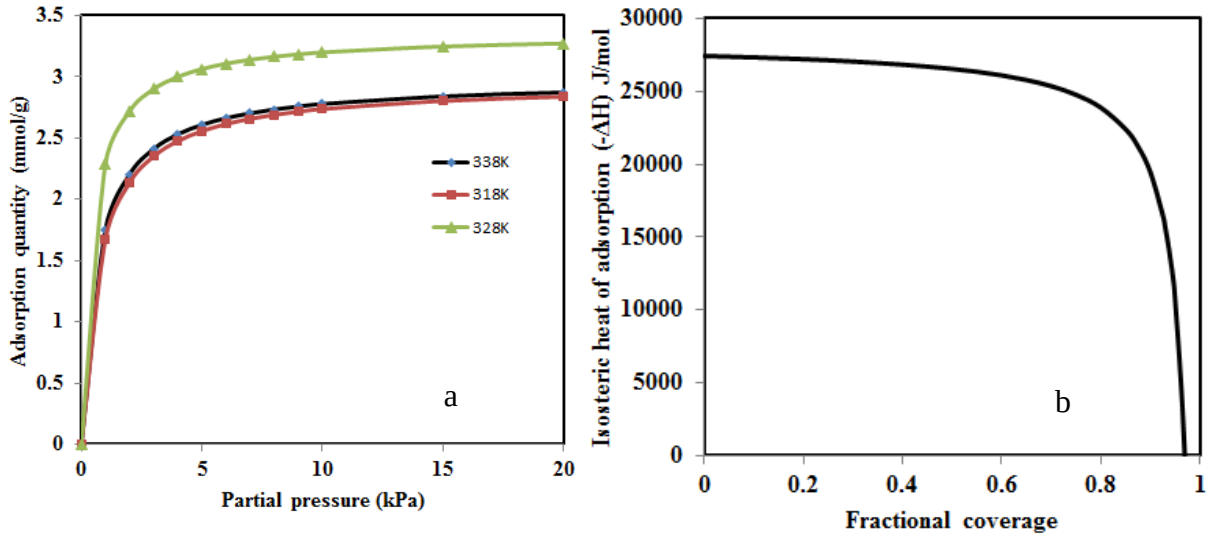

Figure 5.11 (a) CO_2 adsorption isotherms on 50 MI adsorbent at 318 K, 328 K and 338 with best fitting Langmuir theoretical isotherms, (b) Isosteric heat of CO_2 adsorption on 50 MI adsorbent as a function of the fractional coverage of the adsorbent

The carbonate-bicarbonate chemistry on K_2CO_3/Al_2O_3 adsorbent involving adsorbates *viz.* CO_2 and H_2O is altogether different reaction system with respect to its complex interaction among themselves and with the adsorbent. The isosteric heat of adsorption corresponding to zero coverage is 27.3 kJ/mol which is similar to the reported isosteric heat data of 27 kJ/mol for pure CO_2 in activated alumina [101]. Interestingly, in the reference study, the isosteric heat at zero coverage for CO_2 has been found to vary in the range between 16.6 and 27.0 kJ/mol depending on the concentration of water in the system. It appears that in the current sorbent, the effect of water on isosteric heat is balanced by the strong affinity of CO_2 towards the active sites provided by K_2CO_3. Hence, the isosteric heat at zero coverage in the present work is

matching with those reported for pure CO_2 without water and no K_2CO_3 in the sorbent. Further, it is also seen that the isosteric heat in the current sorbent decreases significantly with increase in surface coverage, which is quite similar to the trend reported by Gargiulo et al [94]. Thus, above surface coverage of 0.6, the isosteric heat decreases rapidly and reaches to zero value at coverage of 0.96. This could be due to the availability of lesser energetic surface of K_2CO_3 or due to restricted accessibility of active K_2CO_3 sites at higher surface coverage. Further, this may also be attributed to the dependency of sorbent capacity on temperature as reported by Gargiulo et al [94]. In any case, the variation of isosteric heat with surface coverage may be utilized quite effectively for enhancing the energy efficiency of large CO_2 capture plant. For example, by choosing the appropriate operating regime of surface coverage, it may be possible to minimize the temperature differential between the adsorption and desorption steps, which is a key objective to reduce the energy consumption for CO_2 capture.

5.8 Conclusions

The results presented in this work show that significant enhancement in CO_2 adsorption capacity by employing multi-step as compared to single-step wetness impregnation approach. The CO_2 adsorption studies were performed at 45 to 65 ^oC using 8 vol% of CO_2, 0-15 vol% of H_2O and rest N_2 in simulated flue gas mixture in a fixed bed system. Multi-step impregnation method increases the effective dispersion of active component on the alumina support resulting in higher specific surface area and pore volume of adsorbents, and significant improvement in the adsorption breakthrough time. The adsorbents prepared using multi-step impregnation method shows higher adsorption capacity (>85% of theoretical capacity) as compared to single-step impregnation method due to uniform dispersion of K_2CO_3 in the pores. The adsorbents with higher loading requires higher temperature (>300 ^oC) for regeneration due to the formation of stable deactivating component $KAl(CO_3)_2(OH)_2$ on the adsorbed species. The regeneration efficiency was also improved for MI prepared adsorbents due to the limited chance of blockage of meso-pores. Therefore, the multi-step impregnation method is effective to impregnate high amount of K_2CO_3 in porous alumina support to achieve higher CO_2 adsorption capacity. The derived isosteric heat of adsorption as a function of the fractional coverage showed that the heat was reduced with increase in surface coverage of the adsorbent.

Chapter 6

Improvement in Regeneration Properties and Multi-cycle Stability for K_2CO_3/Al_2O_3 Adsorbents for CO_2 Removal from Flue Gas

6.1 Introduction

This chapter discusses the results obtained from the surface modification of the support materials and adsorbents. The preparation methods of support material, specifically gamma alumina and their textural and chemical properties have been discussed. The support material was modified using heat treatment at higher temperatures and also with alkali treatment followed by calcination to reduce total acidity. Various textural and chemical characteristics have been studied to explain reduction of formation of deactivating species $KAl(CO_3)_2(OH)_2$ with calcination temperatures. This chapter presents a detailed investigation on how acidity of gamma alumina significantly affects the adsorbent regeneration properties. The performance of the adsorbents and their multi-cycle stability with adsorption and regeneration at 55 ^oC and 130 ^oC respectively were studied. The support (γ-Al_2O_3) is stabilized by thermal treatment and, alkali treatment with metal hydroxide followed by calcination. It is the first time that the multi-cycle stability for CO_2 adsorption-regeneration for K_2CO_3/Al_2O_3 adsorbents was achieved through reduction of acidic sites of support materials. The effects of operating parameters such as adsorption temperature, thermal treatment of support material, gas-hourly space velocity (GHSV) during regeneration have also been studied. The developed adsorbents also show high attrition resistance and hence, can be effectively used in commercial application for CO_2 capture. These studies have been disclosed as Indian patent (Application No.: 866/MUM/**2014**).

6.2 Physico-chemical characterization of adsorbents

6.2.1 Surface area, pore volume and average pore diameter

Table 6.1(a) shows the BET surface area, total pore volume and average pore diameter of the fresh/ modified support materials e.g. γ-Al_2O_3, modified γ-Al_2O_3, and as such α-Al_2O_3. It is observed that during calcination of γ-Al_2O_3 alone (without metal carbonate loading) at high temperatures, both the surface area and pore volume decrease significantly and their average pore diameter increases drastically. This is due to the formation of macro-structure from changes in wall crystal structure of the support [102]. In increasing the calcination temperature, the water (free water, water of crystallization, interlayer water, etc.) is eliminated from γ-Al_2O_3 resulting in collapse of pore structures and produces large pores from small pores. The dehydrated alumina consists of a mixture of eta (ε), delta (δ), and theta (θ) alumina phases [104]. Figure 6.1 also shows the decrease in pore volume and increase in average pore diameter

with increase in calcination temperature. A broader pore size distribution (PSD) of meso-pores (100-250 Å) is seen from the calcination of γ-Al_2O_3 support. These broader meso-pores improves the dispersion of K_2CO_3 inside the pores, which facilitates the accessibility to CO_2 during adsorption. As explained earlier, a shift in average pore diameter from narrower to broader pores is observed due to collapsing of smaller meso-pores into larger meso-pores in γ-Al_2O_3 support. It is also observed that PSD pattern of 35KA(950) after 11 cycles is almost similar with respect to fresh adsorbent, which signifies the retention of active phase inside the pores. Similarly, from Table 6.1(b) and 6.1(c), it is seen that both the surface area and pore volume decreased with increase in K_2CO_3 loading due to the filling of pores during K_2CO_3 impregnation. It is also seen that the average pore diameter of K_2CO_3-based adsorbents supported on calcined/ alkali-treated calcined Al_2O_3 increases with the increase in calcination temperature of Al_2O_3 support. The larger average pore diameter of the support resulted from different calcination temperatures, helps to disperse similar amount of active component (i.e. K_2CO_3) inside the pores during impregnation. A shift in average pore diameter is shown in Figure 6.1 in case of 35KA(950) and 46KA(950), wherein average pore diameter of 46KA(950) is shifted 15 Å lower (i.e. 149 Å) as compared to 35KA(950). This is due to excess growth of K_2CO_3 for higher loading on the pores resulting in decrease in average pore diameter as shown in Figure 6.2b.

6.2.2 Acidity analysis

The acidity of γ-Al_2O_3, modified γ-Al_2O_3, and α-Al_2O_3 were measured using TPD of ammonia (NH_3), are reported in Table 6.1(a). It is seen that the total acidity (Lewis and Brönsted acidity) of γ-Al_2O_3 decreased significantly with increase in calcination temperature. For A(950) support, the acidity amounts reduced to 0.34 mmol NH_3/g from 0.55 mmol NH_3/g. Due to thermal dehydration, the surface hydroxyl groups and chemically bound internal hydroxyl groups in the support, are released as water from γ-Al_2O_3, which results in reduction of acid sites. These observations are consistent with the results reported by Maciver et al. [105]. During pretreatment of the support material, the different phases of transition alumina adsorb water that reduces Lewis acid sites (strong acid) and transform them into Brönsted sites (weak acid) [108]. Chen et al. [107] reported that during transient phase transformation of γ-Al_2O_3, Al^V coordinated state is responsible for creating Lewis acid sites. It is interesting to see that lesser the acidity of Al_2O_3, higher is the multi-cycle CO_2 adsorption capacity for K_2CO_3/Al_2O_3 adsorbents. For example, the acidity of 35KA(950) adsorbent is 0.34 mmol NH_3/g and its multi-

cycle CO_2 adsorption capacity is found to be 2.1 mmol CO_2/g of adsorbent, which is higher as compared to 34KA(700) (capacity 1.75 mmol/g as shown in Figure 6.11). This is due to the reduction of stable deactivating component $KAl(CO_3)_2(OH)_2$ formation during CO_2 adsorption. It is in good agreement with inferences from XRD, TGA and TPD analyses discussed in subsequent sections. It is also found from Table 6.1(a) that at almost same K_2CO_3 loading, adsorbents supported on α-Al_2O_3 show very low CO_2 adsorption capacity (0.43 *vs*. 2.1 mmol/g) although its total acidity is found to be very low (0.083 mmol NH_3/g). The reduced surface area and pore volume available for K_2CO_3/α-Al_2O_3 as seen in Table 6.1(c) results in poor dispersion of active K_2CO_3 ingredient inside the α-Al_2O_3 support, which ultimately leads to lower CO_2 adsorption capacity.

6.2.3 Attrition index (AI)

The attrition resistance for selected adsorbents was measured using ASTM D5757 method. The attrition index of modified supports/ adsorbents was found within the desired range (<10%). It is found from Table 6.1 that the attrition index slightly increases with the increase in calcination temperature of Al_2O_3 support. It may be due to the increase in average pore diameter and enhanced compactness of the calcined support material.

Table 6.1 Structural characteristic of modified support and prepared adsorbents

(a). Modified γ-Al_2O_3 supports

Adsorbents*	**Adsorbent name**	**K_2CO_3 loading (wt %)**	**Acidity (mmol NH_3/g)**	**Surface area (m^2/g)**	**Pore volume (cm^3/g)**	**Average pore diameter (Å)**	**AI (%)**
Fresh γ-Al_2O_3 (as such)	A	0	0.55	188	0.48	98	4.4
Modification of γ-Al_2O_3 (calcination of support material)							
γ-Al_2O_3 calcined at 700 ^oC	A(700)	0	0.53	152	0.45	120	4.8
γ-Al_2O_3 calcined at 900 ^oC	A(900)	0	0.41	100	0.42	170	5.1
γ-Al_2O_3 calcined at 950 ^oC	A(950)	0	0.34	86	0.38	178	5.3

Modification of γ-Al_2O_3 (1% NaOH treated followed by calcination of support material)							
γ-Al_2O_3 treated with 1% NaOH followed by calcination at 700 ^oC	A(Na700)	0	0.45	161	0.446	111	6.7
Fresh α-Al_2O_3 (as such)	B	0	0.083	8	0.22	37	5.3

(b). Prepared adsorbents using fresh and calcined Al_2O_3

Adsorbents*	**Adsorbent name**	**K_2CO_3 loading (wt %)**	**Acidity (mmol NH_3/g)**	**Surface area (m^2/g)**	**Pore volume (cm^3/g)**	**Average pore diameter (Å)**	**AI (%)**
40% K_2CO_3/ γ-Al_2O_3	40KA	40	ND	22	0.11	102	7.1
K_2CO_3/Al_2O_3 adsorbents (metal carbonate loading on calcined Al_2O_3)							
34% K_2CO_3/ γ-Al_2O_3	34KA(700)	34	ND	58	0.18	125	ND
31% K_2CO_3/ γ-Al_2O_3	31KA(900)	31	ND	43	0.16	155	ND
35% K_2CO_3/ γ-Al_2O_3	35KA(950)	35	ND	31	0.15	164	3.8
46% K_2CO_3/ γ-Al_2O_3	46KA(950)	46	ND	35	0.13	149	ND
36% K_2CO_3/ γ-Al_2O_3	36KA(Na700)	36	ND	53	0.15	120	7.2

(c). Prepared adsorbents using fresh α-Al_2O_3

Adsorbents*	**Adsorbent name**	**K_2CO_3 loading (wt %)**	**Acidity (mmol NH_3/g)**	**Surface area (m^2/g)**	**Pore volume (cm^3/g)**	**Average pore diameter (Å)**	**AI (%)**
K_2CO_3/Al_2O_3 adsorbents (metal carbonate loading on as such α-Al_2O_3)							
28% K_2CO_3/ α-Al_2O_3	28KB	28	ND	4	0.005	62	8.2
33% K_2CO_3/ α-Al_2O_3	33KB	33	ND	3	0.004	59	ND
* Abbreviation used for designated adsorbent are Na: Na_2CO_3, K: K_2CO_3, A: γ-Al_2O_3, B: α-Al_2O_3, as example, 36KA(Na700) means 36% K_2CO_3 impregnated on γ-Al_2O_3 wherein, support is treated with 1% NaOH solution and then calcined at 700 ^oC prior to impregnation. ND: Not determined.							

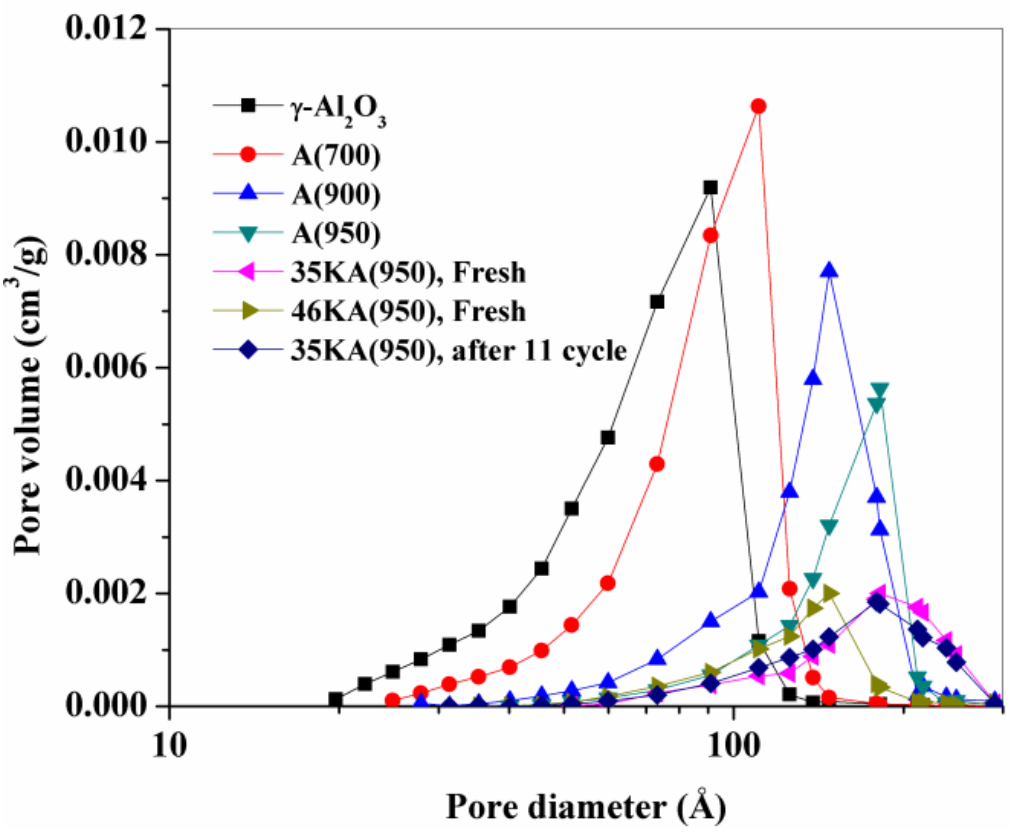

Figure 6.1 Pore size distribution (PSD) of modified alumina supports and adsorbents

6.2.4 SEM analysis

The morphological characteristics of K_2CO_3 loaded adsorbents are discussed using SEM images, which are shown in Figure 6.2. Under similar magnification, 46-wt% K_2CO_3 loaded adsorbent shows higher density of K_2CO_3 fibers compared to 35-wt% loaded adsorbent.

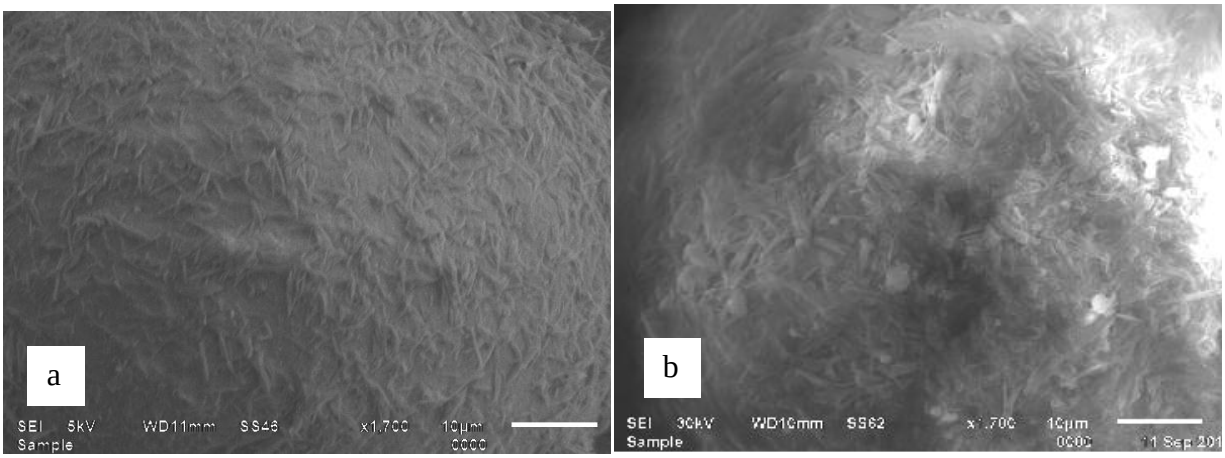

Figure 6.2 SEM images of K_2CO_3-based modified adsorbents: (a) 35KA(950), (b) 46KA(950)

The higher concentration of K_2CO_3 solution in the preparation of 46KA(950) exhibits high viscosity, which leads to poor dispersion into the pores of modified Al_2O_3. This results in formation of larger particles/ aggregates on the external surface.

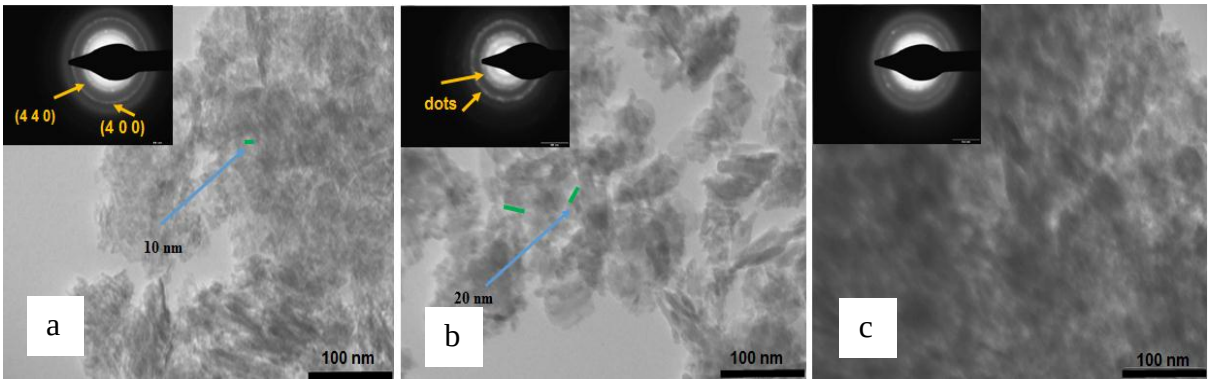

Figure 6.3 TEM images of (a) fresh γ-Al_2O_3, (b) calcined γ-Al_2O_3, (c) 35KA(950)

6.2.5 TEM analysis

Figure 6.3a is a TEM image of fresh γ-Al_2O_3 support, which indicates a semi-crystalline structure of γ-Al_2O_3. The average pore diameter observed in as-such γ-Al_2O_3 is found to be 10 nm, which is close to the average pore diameter obtained from BET analysis. The selected area electron diffraction (SAED) pattern of the uncalcined γ-Al_2O_3 support (as shown in inset of Figure 6.3a) shows concentric rings corresponding to (400) and (440) reflections at 2θ of 46.3 and 67.2 respectively. Figure 6.3b shows the TEM image of A(950) indicating an increase in average pore diameter (> 20 nm). As explained earlier, the average pore diameter is increased during calcination at higher temperatures due to the collapse of smaller meso-structure framework and increased the crystallinity. These results fully agree with the BET analysis data in Table 6.1a. Moreover, SAED of A(950) shown in Figure 6.3b indicates the dots in the concentric rings. These dots in A(950) appeared to be more as compared to fresh γ-Al_2O_3, which indicates more crystalline structure in calcined Al_2O_3.

The TEM image of 35KA(950) (shown in Figure 6.3c) indicates that K_2CO_3 is dispersed uniformly inside the broader meso-pores of calcined γ-Al_2O_3. The SEM image in Figure 6.2a confirms this observation. The SAED pattern (shown in inset) also indicates disappearance of dots pattern, which suggests that K_2CO_3 is dispersed inside the crystalline pores.

6.2.6 XRD analysis

While modifying γ-Al_2O_3 supports by calcination method or alkaline treatment followed by calcination, the XRD pattern shows that as the calcination temperature increases, the γ-Al_2O_3 phase transformed into mixture of metastable phases γ-Al_2O_3, δ-Al_2O_3 (JCPDS: 46-1131), θ-Al_2O_3 (JCPDS: 35-0121) at calcination temperature of 700 to 900 ^oC (as shown in Figure 6.4a) [105, 108-109].

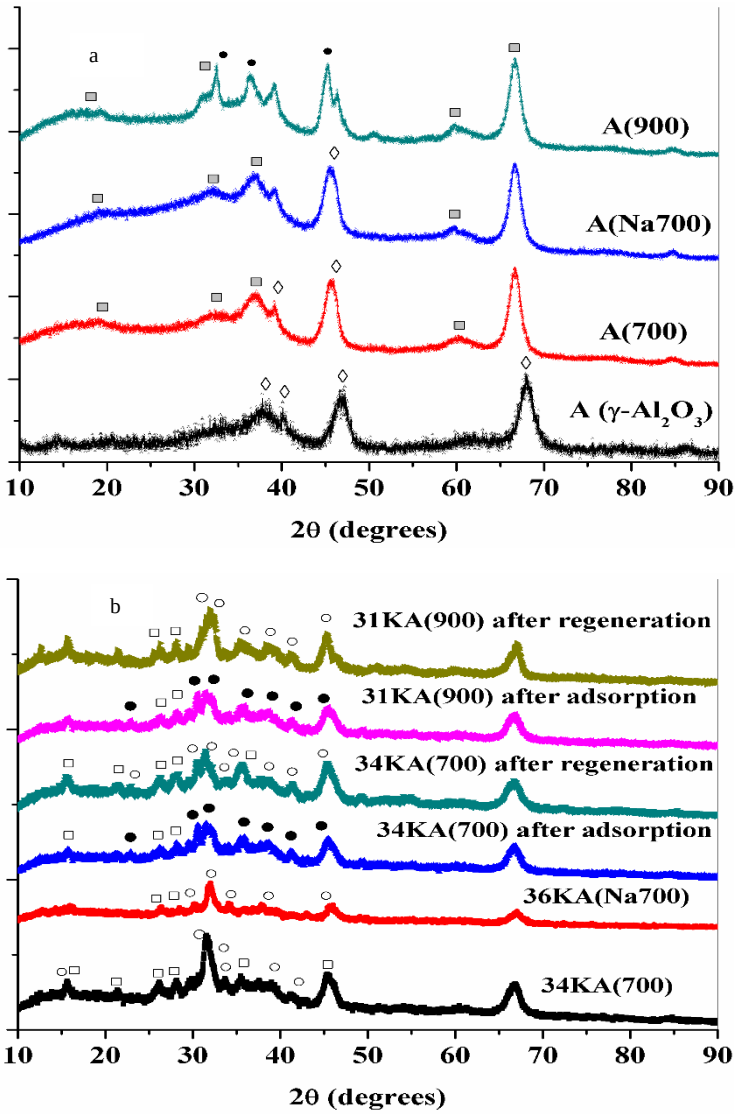

Figure 6.4 XRD patterns of (a) modified γ-Al_2O_3 support materials (b) adsorbents (fresh / adsorbed/ regenerated) (◊ γ-Al_2O_3, ■ δ-Al_2O_3, * θ-Al_2O_3, ○ K_2CO_3, ● $KHCO_3$, □ $KAl(CO_3)_2(OH)_2$)

The peaks appeared from the intermediate phases are difficult to identify from XRD pattern but appeared to be δ-phase obtained at 900 ^oC. The presence of remaining γ-phase also cannot

be ignored from the XRD. Based on XRD results, the estimated percentage value of a mix of δ-Al_2O_3 and θ-Al_2O_3 present in modified alumina was found to be nearly 46.5 wt% and remaining was γ-Al_2O_3. The structural differences of these forms involve the arrangement of Al cations in the interstices of the face-centered cubic (fcc) array of oxygen anions. The γ-Al_2O_3 has defect spinel structure, while δ-Al_2O_3 and θ-Al_2O_3 have tetragonal and monoclinic crystalline structures respectively [110]. The thermal dehydration of alumina will increase the crystallinity of Al_2O_3 [102-103, 111].

It is interesting to know how the calcination of Al_2O_3 support plays an active role on CO_2 adsorption capacity over multiple cycles. As discussed above, during calcination up to 950 ^oC, γ-Al_2O_3 undergoes phase transformation into a dominant mix of δ-Al_2O_3 and θ-Al_2O_3. As a result, calcined γ-Al_2O_3 becomes more crystalline (as sharp peaks appeared in the XRD results) and possessing less acidic sites. Due to this reduced acidity, the alkaline K_2CO_3 interacts to the lesser extent with the support to produce stable component like $KAl(CO_3)_2(OH)_2$ during adsorption and improves CO_2 capture capacity over multi-cycle testing.

The XRD patterns of some selected adsorbents in their fresh, after adsorption and regeneration are shown in Figure 6.4b. Both K_2CO_3 and $KAl(CO_3)_2(OH)_2$ phases were present in fresh adsorbents 34KA(700), 36KA(Na700). The major diffraction peaks present in these fresh K_2CO_3 based adsorbents at 2θ of 15.8, 26.1, 30.0, 31.7, 32.0, 32.1, 34.1, 42.8 and 48.9 are assigned to K_2CO_3 of monoclinic crystalline phase (JCPDS 71-1466), while peaks at 2θ of 15.9, 26.8, 28.0, 33.8, 35.9 and 45.8 are of $KAl(CO_3)_2(OH)_2$ (JCPDS 21-0979). It is observed that the intensity of stable species $KAl(CO_3)_2(OH)_2$ was comparatively lower in case of 36KA(Na700) than in 34KA(700). This may be due to the reduction of total acidity of γ-Al_2O_3, which has occurred while performing additional alkaline treatment, followed by calcination at 700 ^oC. The XRD peaks of 36KA(Na700) and 31KA(900) at their adsorbed and regenerated conditions confirm the presence of both $KHCO_3$ (JCPDS 70-1168) along with $KAl(CO_3)_2(OH)_2$ and K_2CO_3 along with $KAl(CO_3)_2(OH)_2$ respectively. The formation of stable component was found to be less as compared to 36KA(Na700) as the support material of 31KA(900) adsorbent was thermally treated at 900 ^oC to further reduce the strong acidity sites [105-106].

Similarly, XRD analysis of 35KA(950) was performed for fresh, after adsorption and after regeneration steps. As expected, the presence of both $KHCO_3$, and $KAl(CO_3)_2(OH)_2$ are observed after CO_2 adsorption and K_2CO_3 along with $KAl(CO_3)_2(OH)_2$ after adsorbent

regeneration (as shown in Figure 6.5). Interestingly, the intensity of stable species formation was observed to be lower as compared to other adsorbents. This is due to the reduced surface hydroxyl group of γ-Al_2O_3, which was calcined further at higher temperature. Therefore, the multi-cycle adsorption capacity for 35KA(950) increased as compared to other adsorbents.

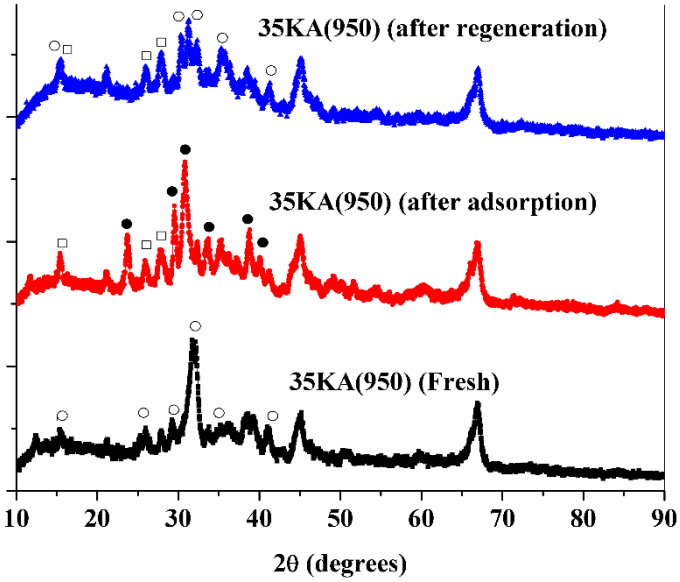

Figure 6.5 XRD patterns of 35KA(950) adsorbent (fresh / adsorbed/ regenerated) (○ K_2CO_3, ● $KHCO_3$, □ $KAl(CO_3)_2(OH)_2$)

6.2.7 FTIR analysis

The solid-state FTIR study was conducted for pure K_2CO_3 and three adsorbents *viz.* 31KA(900), 36KA(Na700) and 40KA in their fresh, adsorbed and regenerated conditions (as shown in Figure 6.6). The peaks appeared between 1060-1506 cm^{-1} were attributed to the presence of C=O bond in all the cases [112]. In both the products, peak appearing between 862-890 cm^{-1} region indicates the presence of CO_3^{2-} ions. The absorption peaks appearing between 2180-2230 cm^{-1} in these adsorbents, indicate the presence of Al(CO) species as reported by Iordan et al. [113]. The peaks observed between 3340-1943 cm^{-1} corresponds to O-H bond stretching band for adsorbed and regenerated species of all the products. It is observed that percent transmission (%T) for K_2CO_3/Al_2O_3 adsorbents is less in case of adsorbed samples, which indicates the presence of O-H group containing compounds. These peaks are consistent with O-H group frequency but are difficult to identify any definite state of potassium compounds. The O-H group frequency could be due to the presence of different O-H group

content in the form of $KHCO_3$, $KAl(CO_3)_2(OH)_2$, $K_2CO_3 \cdot 1.5\ H_2O$. It is also interesting to see that higher the calcination temperature used for adsorbent preparation, higher is the %T values for regenerated adsorbents. Moreover, lower %T was observed for regenerated 40KA adsorbent, which is prepared using uncalcined γ-Al_2O_3. It suggests the lesser chance of stable species e.g. $KAl(CO_3)_2(OH)_2$ formation during CO_2 adsorption on the adsorbents prepared after high temperature calcination of γ-Al_2O_3.

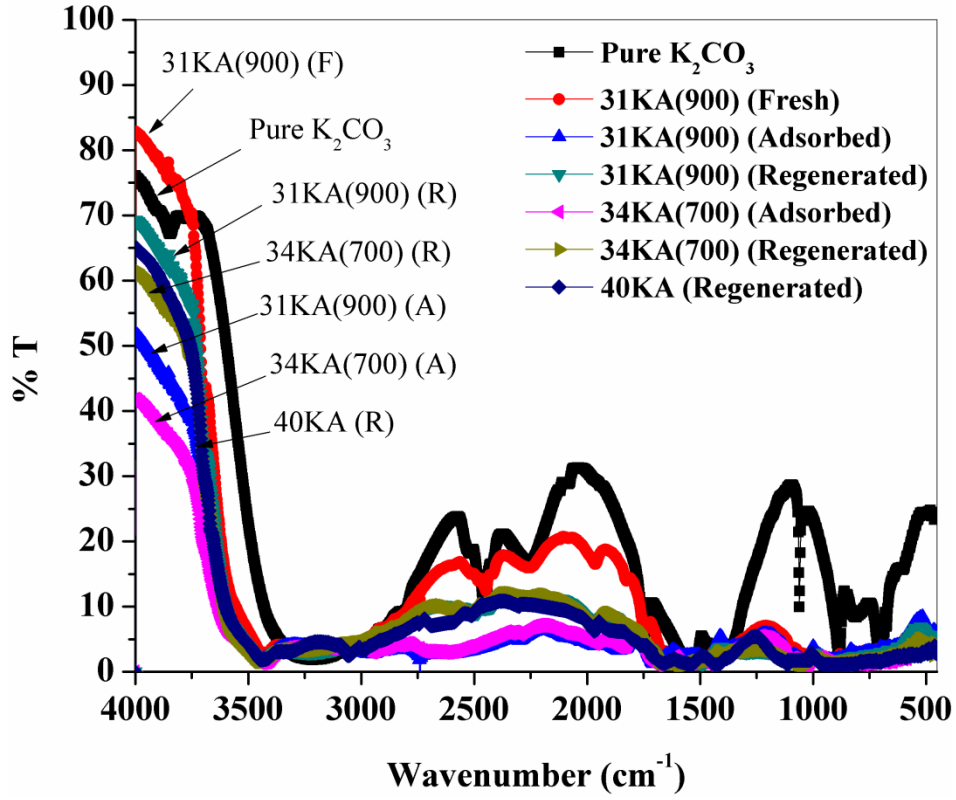

Figure 6.6 FTIR spectra of 31KA(900), 34KA(700) and 40KA after adsorption/ regeneration step

6.2.8 TG analysis

The thermal stability using TGA for some selected adsorbents *viz*. 36KA(Na700), 31KA(900) and 35KA(950) is shown in Figure 6.7. For all these fresh adsorbents, the first weight loss of 5.8-8.1wt% was found between 35 ^oC and 100 ^oC, which were the losses attributed to the loss of free surface water after preparation of adsorbents. The minor weight loss of around 1.6 wt% in the temperature range of 100-200 ^oC was attributed to the loss of molecular bound water. It may be $K_2CO_3.1 \cdot 5\ H_2O$, which was not detected in XRD analysis. The third weight loss ranging from 2.5-3.1 wt% was observed between 200-400 ^oC. This loss was primarily

attributed to the loss of stable deactivating component $KAl(CO_3)_2(OH)_2$ produced during preparation step. These results were consistent with XRD results shown in Figure 6.4b.

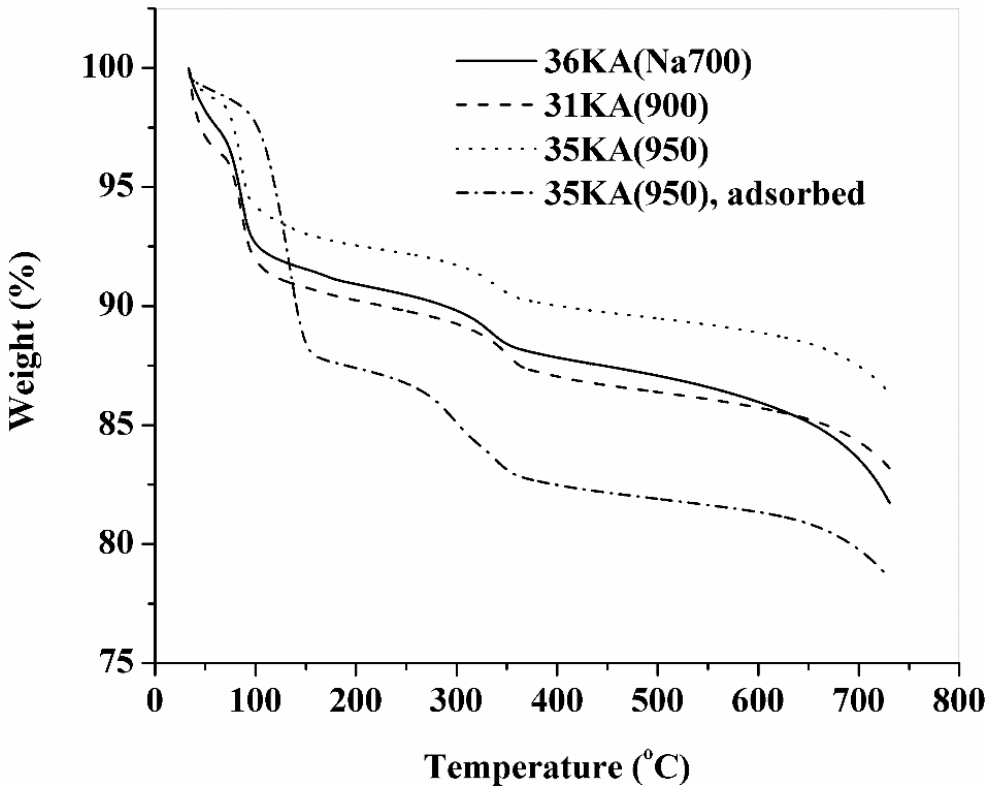

Figure 6.7 TG analyses of selected adsorbents

Similarly, TG analysis for 35KA(950) was performed after its adsorption step to analyze the adsorption characteristics. It was observed that the first weight loss between 35 and 100 ^oC was due to removal of free water. The major second weight loss in the range of 100-200 ^oC was 10.3 wt%, which indicated the decomposition of $KHCO_3$ into K_2CO_3. The minor weight loss of 4.8 wt% between 200 ^oC and 400 ^oC was attributed due to the decomposition of $KAl(CO_3)_2(OH)_2$ between 250-300 ^oC along with chemically bound water. XRD analyses also indicated the presence of this stable species $KAl(CO_3)_2(OH)_2$ in the adsorbed species of 35KA(950).

6.2.9 TPD analysis

TPD analysis was conducted to identify the presence of components formed during CO_2 adsorption. TPD data of K_2CO_3-based modified adsorbents after adsorption at 55 ^oC was compared with the unmodified alumina supported adsorbent, which is shown in Figure 6.8. It is seen that first two peaks appeared between 50 and 150 ^oC attributed to the phase transition (i.e. vaporization) of water and decomposition of $KHCO_3$ respectively. The third peak appeared

at 280-330 ^{o}C attributed to the decomposition of stable component $KAl(CO_3)_2(OH)_2$ [62-63, 114-115].

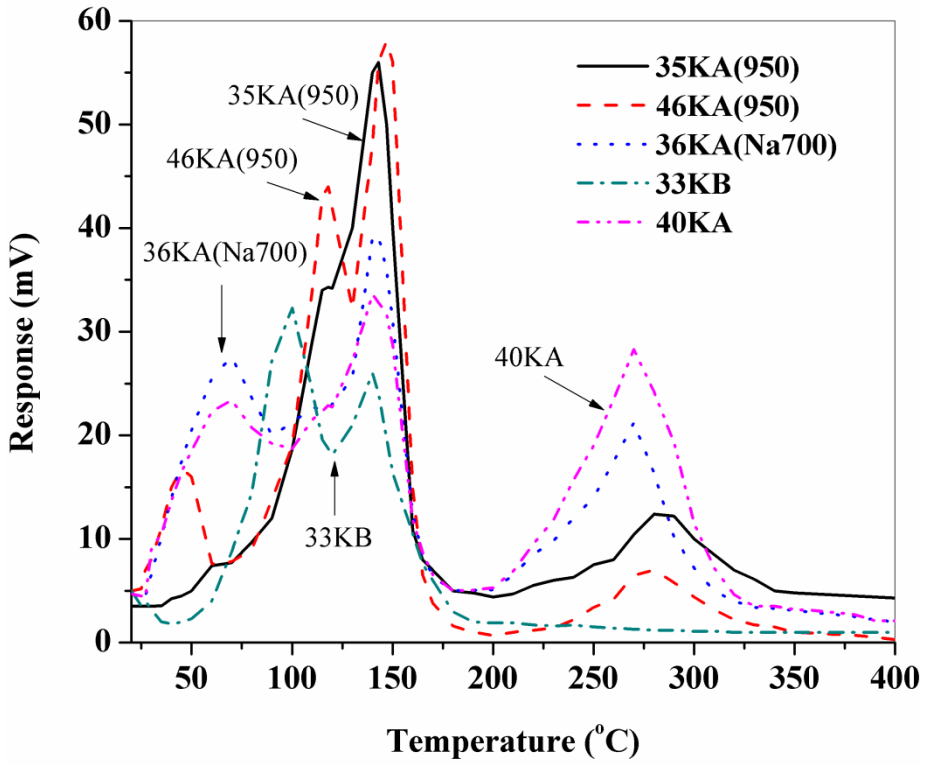

Figure 6.8 TPD profiles of selected adsorbents (after adsorption)

In case of 35KA(950) adsorbent, the intensity of stable component formation is less as compared to 36KA(Na700). As explained in the previous sections, higher calcination temperature drastically reduces the total acidity of the γ-Al_2O_3 support and hence, results in less interaction of support with the reactants during adsorption. Hence, 35KA(950) adsorbent requires lower temperature for regeneration (130 ^{o}C) and showed stable adsorption capacity after multi-cycle tests. In case of 40KA, which is prepared with unmodified γ-Al_2O_3 support, the intensity of stable component is more as compared to modified adsorbents. This is due to the interaction between the support (γ-Al_2O_3) and active phase (K_2CO_3) as a result of more acid sites. Therefore, the role of calcination temperature is very important on adsorbent regeneration temperature. For 33KB adsorbent, which is based on α-Al_2O_3 support, there was no such peak observed at 300 ^{o}C. As the acidity of sourced α-Al_2O_3 support is very low (0.083 mmol/g), the Lewis acidity part is almost reduced at 1200 ^{o}C. As a result, the chance of formation of stable component during adsorption is very low. For 46KA(950), the intensity of $KAl(CO_3)_2(OH)_2$ was very low because of formation of larger crystallites, which reduces the active sites for CO_2

adsorption. The same observation is noticed from SEM of 46KA(950) as shown in Figure 6.2b. As a result, the adsorption capacity was limited to 1.82 mmol CO_2/g of adsorbent.

6.3 CO_2 adsorption studies of K_2CO_3-based adsorbents using modified γ-Al_2O_3

CO_2 adsorption studies of potassium-based modified γ-Al_2O_3 and α-Al_2O_3 supported adsorbents were performed using simulated gas mixture of 8 vol% CO_2, 15 vol% H_2O and rest N_2 in a fixed bed system at 55-75 ^oC. Being an exothermic reaction, the adsorption capacity was found to be 2.38 mmol/g at 55 ^oC, but decreased to 1.90 mmol/g at 75 ^oC. The breakthrough curves for modified adsorbents are shown in Figure 6.9. It is observed that the breakthrough time for the adsorption on fresh support modified adsorbents varied from 23-30 minutes, while it varied from 15-23 minutes for multi-cycle tests at an adsorption/ regeneration temperature of 55 and 130 ^oC. The similar fresh adsorption capacities were observed for 31-36 wt% K_2CO_3-based adsorbents with support modified at different calcination temperatures. Therefore, the role of calcination on Al_2O_3 is required to explain the variation in fresh and multi-cycle CO_2 adsorption capacity.

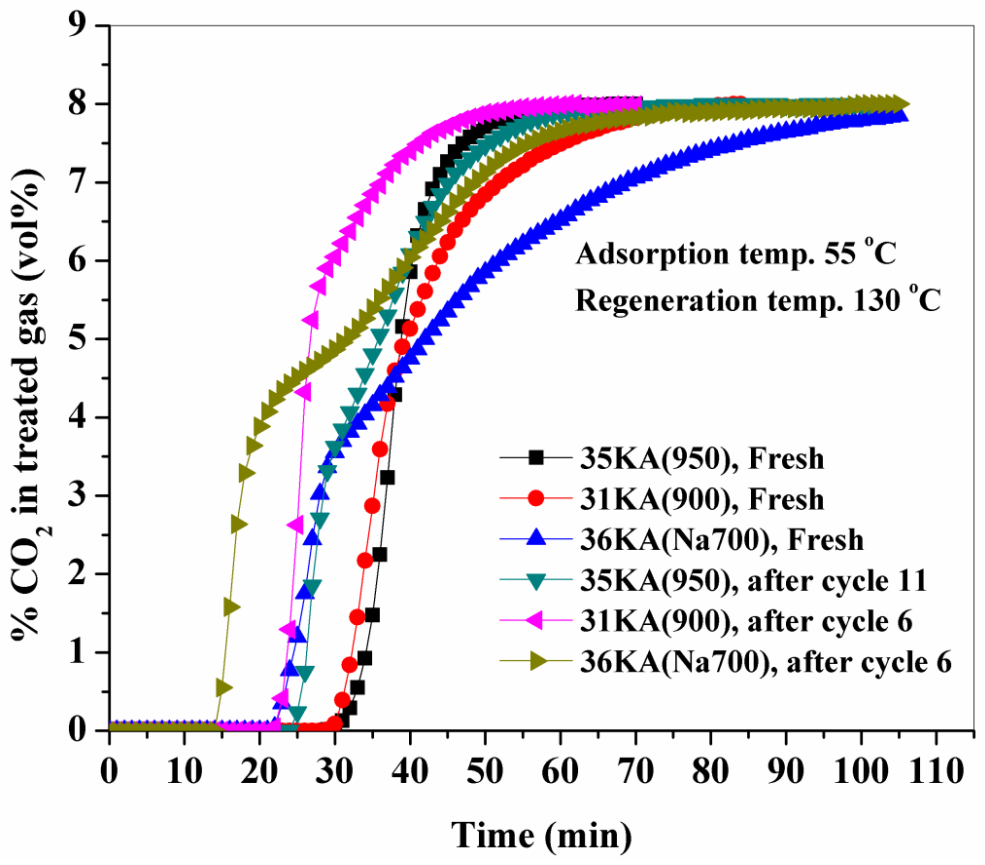

Figure 6.9 Breakthrough curves for CO_2 adsorption on selected adsorbents

From Figure 6.11, it is observed that there was a drop in 15% of adsorption capacity after fresh adsorption, and then it was stable during multiple tests. The first drop in adsorption capacity is due to remnant strong acidity sites in the support that cannot be decreased further unless calcination is carried out at higher temperature. Similar explanation is applied to describe the variation in breakthrough time for K_2CO_3/Al_2O_3 adsorbents, which are prepared using support calcined at different temperatures namely, A(Na700), A(900) and A(950). The XRD, TPD, FTIR data suggest the presence of stable component $KAl(CO_3)_2(OH)_2$ after significant acidity reduction, which causes the drop in adsorption capacity in first cycle.

From Figure 6.11, one can see the variation in CO_2 adsorption capacity on different modified supports based on calcination temperatures. In case of 46KA(950) prepared to load more K_2CO_3 with dissolution in water at higher temperature (70 ^oC), the adsorption capacity of fresh 46KA(950) was achieved as 2.11 mmol/g, which was 64% of theoretical CO_2 adsorption capacity and even lower than 35KA(950) (2.38 mmol/g). The lower adsorption capacity achieved with respect to 46 wt% K_2CO_3 loading is due to decreased accessibility of CO_2 as a result of the formation of large crystalline phase of K_2CO_3 outside the pores (Figure 6.2b), which blocks some of the broader meso-pores.

The 28KB and 33KB adsorbents with commercial α-Al_2O_3 support showed very low adsorption capacity of 0.52-0.62 mmol/g, which is much lower than the capacity reported by Lee et al. [20]. The decrease in CO_2 adsorption capacity in case of α-Al_2O_3-based adsorbents may be due to the reduced pore volume restricting CO_2 accessibility inside the pores.

6.4 Effect of adsorption temperature on CO_2 adsorption capacity

The effect of adsorption temperature on CO_2 adsorption was evaluated using 35KA(950) at three different temperatures ranging from 55-75 ^oC. From Figure 6.10, it is observed that the adsorption capacity decreased with increase in adsorption temperature. At 55 ^oC, the adsorption capacity was found as 2.38 mmol/g while at 75 ^oC, the capacity was 1.90 mmol/g of adsorbent.

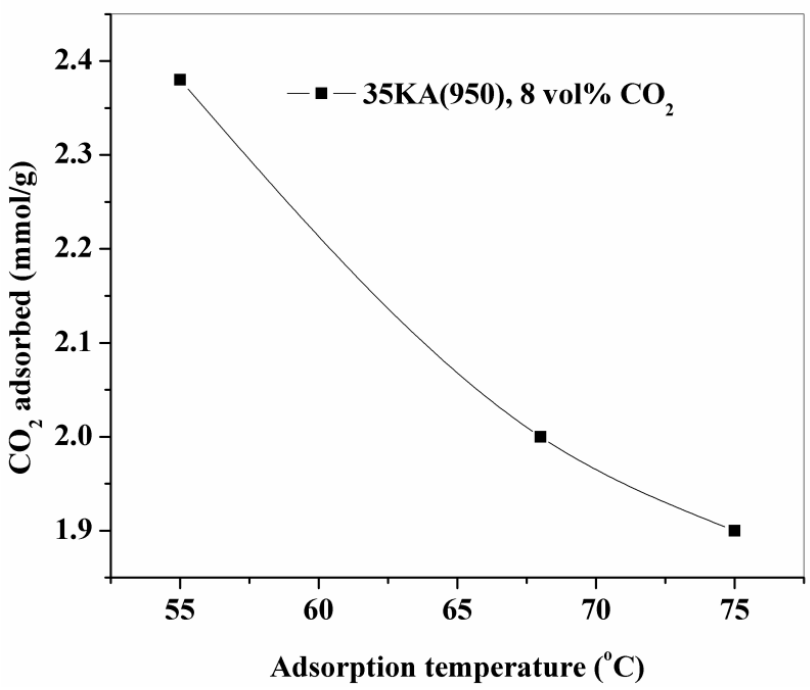

Figure 6.10 Effect of temperature on adsorption capacity of 35KA(950)

6.5 Effect of calcination temperature on stability of CO_2 adsorption capacity during multi-cycle

Figure 6.11 shows that the CO_2 adsorption capacity is higher for the adsorbents, wherein the support material was calcined at increased temperatures. In case of 35KA(950) adsorbent, the multi-cycle adsorption capacity was 2.1 mmol/g after 11 cycles while 34KA(700) has stable adsorption capacity of 1.75 mmol/g after 6 cycles. As explained earlier, this is due to the reduced total acidity in the support material caused by the calcination at higher temperature. At high temperature of calcination, γ-Al_2O_3 is transformed into metastable phases γ→δ→θ→α-Al_2O_3 [108]. At 700 ºC, the XRD of γ-Al_2O_3 showed a small peak at 2θ of 37.2, which is assigned to δ phase [107]. At 900 ºC and up to 950 ºC, XRD of pure γ-Al_2O_3 showed the presence of mixed phases of δ (JCPDS: 46-1131) and θ (JCPDS: 35-0121). These observations are in good agreement with those reported by Boumaza et al. [108]. During phase transformation, Al^{3+} ions are migrated from tetrahedral to octahedral sites and oxygen ions are distributed to face-centered cubic (fcc) lattice. Upon raising calcination temperature, the strong acidity (Lewis acidity) of γ-Al_2O_3 decreases [103, 105]. The water treatment of calcined γ-Al_2O_3 produces weak acid sites (Brönsted) [106]. That is why γ-Al_2O_3 calcined at 950 ºC forms less stable species $KAl(CO_3)_2(OH)_2$ during preparation and CO_2 adsorption, hence 35KA(950) can be regenerated at lower temperature of 130-150 ºC.

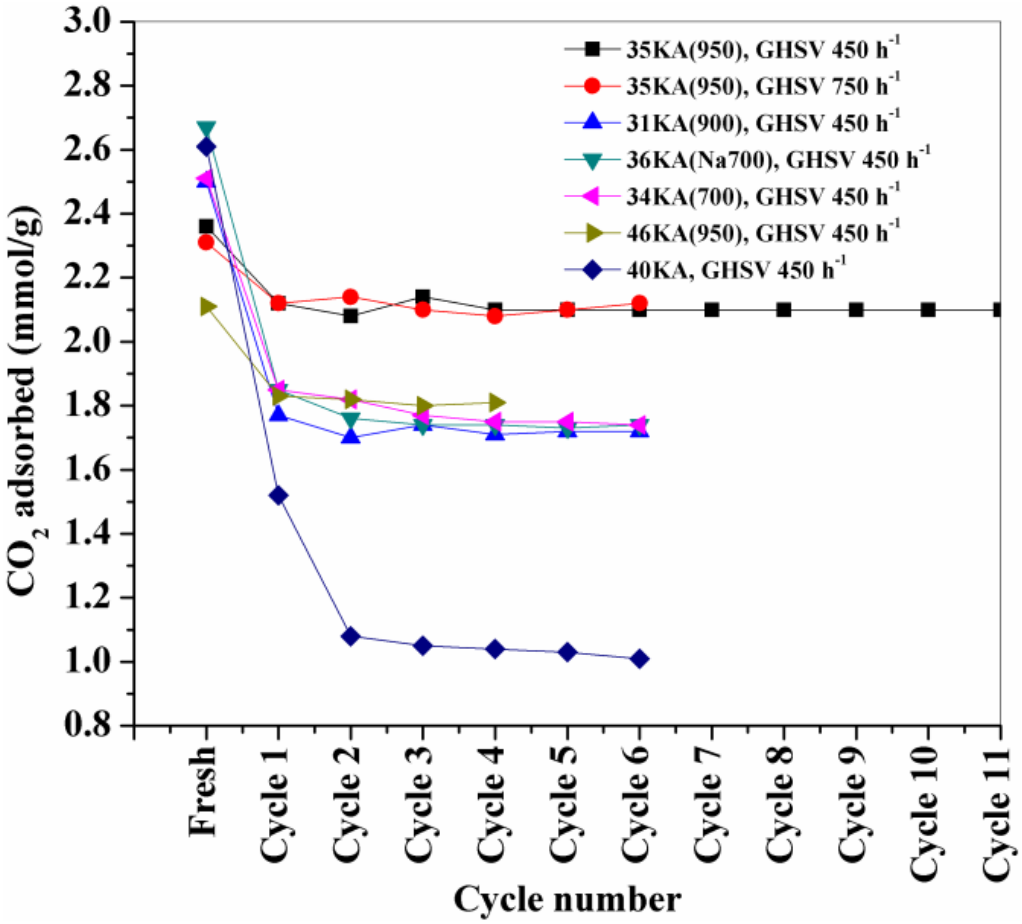

Figure 6.11 Multi-cycle stability of adsorbents (adsorption at 55 ^{o}C and regeneration at 130 ^{o}C, GHSV 450-750 h^{-1})

6.6 Regeneration of adsorbents and multi-cycle stability

The regeneration of adsorbents was carried out at 130-150 ^{o}C using N_2 as sweep gas at GHSV 450 h^{-1} and 750 h^{-1}. From Figure 6.11, it was observed that all K_2CO_3-based adsorbents prepared with modified-Al_2O_3, were regenerated 70-88% at 130 ^{o}C and stable after first cycle of adsorption/ regeneration, while the regeneration efficiency decreased drastically to 41% after multi-cycle tests for unmodified adsorbent at the same temperature. There was a good correlation between the support characteristics and adsorbent regeneration properties. According to the characteristics of support materials, higher the calcination temperature applied for dehydration, higher is the regeneration efficiency at constant regeneration temperature and GHSV. For 36KA(Na700), 34KA(700) and 31KA(900) adsorbents, the stable CO_2 adsorption capacity was found after second cycle of adsorption/ regeneration. 35KA(950) adsorbent showed excellent regeneration properties over multiple cycle tests. The stable

adsorption capacity after 11 cycles was found to be 2.1 mmol/g. In case of 35KA(950), formation of $KAl(CO_3)_2(OH)_2$ during adsorption was very low, hence resulted higher multi-cycle adsorption capacity and required lower temperature for regeneration. These results were consistent with XRD, TPD and TG analysis. The specific reason for higher regeneration efficiency for all these modified adsorbents is linked with the thermal dehydration of γ-Al_2O_3 support at high temperatures, resulting in lower acidity of supports caused by transformation of its structural properties. During adsorption on fresh adsorbents, the residual strong Lewis acid sites produced deactivating component, resulted in a drop in CO_2 adsorption capacity after first cycle.

To study the effect of GHSV on regeneration properties, the regeneration of 35KA(950) adsorbent was performed at 750 h^{-1}. Figure 6.11 shows the results of regeneration of 35KA(950) up to sixth cycle. The stable adsorption capacity of 35KA(950) adsorbent during multiple cycles was 2.1 mmol/g with regeneration carried out at GHSV of 450 and 750 h^{-1}. It was found that higher the GHSV during regeneration with N_2, lesser is the time required for regeneration. Around 30% of the total regeneration time was reduced with increase in GHSV (as shown in Table 6.2). This is due to the increase in CO_2 concentration gradient over the adsorbent surface during regeneration. To study the extent of regeneration efficiency, the 35KA(950) was regenerated at 150 ^oC and the regeneration efficiency reached to almost 98% of its original fresh adsorption capacity.

Table 6.2 Regeneration performance of 35KA(950) at different GHSV

Adsorbent	**Regeneration temperature (^oC)**	**Regeneration GHSV on N_2 (h^{-1})**	**Multi-cycle adsorption capacity (mmol/g)**	**Regeneration time (min)**
35KA(950)	130	450	2.1	140
	130	750	2.1	100

6.7 Conclusions

In this work, an improved regeneration properties of various potassium-based γ-Al_2O_3 adsorbents were studied. The γ-Al_2O_3 as a support material was pretreated by (i) thermal treatment and (ii) alkaline treatment followed by calcination to reduce the formation of stable component like $KAl(CO_3)_2(OH)_2$ during CO_2 adsorption. The presence of such component in the adsorbents exhibits low adsorption capacity over multiple cycles and require high

temperatures for regeneration (>300 ^{o}C). The adoption of aforementioned strategies for improving regeneration properties not only increased multi-cycle stability of adsorption capacity, but also decreased the regeneration temperature drastically from 300 ^{o}C to 130 ^{o}C. From the experimental results, it was concluded that γ-Al_2O_3 calcined at 950 ^{o}C significantly reduced the surface acidity and hence decreased the formation of $KAl(CO_3)_2(OH)_2$ to much extent. Among all the K_2CO_3-based adsorbents, 35KA(950) showed excellent adsorption and regeneration performance. CO_2 adsorption capacity of 35KA(950) was found to be 2.1 mmol/g after 11 cycle tests at 55 ^{o}C. The adsorbent was almost completely regenerated at 130 ^{o}C over multiple cycles. All these results are consistent with XRD, TPD and TG analysis. The specific reason for this improved regeneration is linked with acidity of modified γ-Al_2O_3 support material of different transient phases. The thermal dehydration of γ-Al_2O_3 at 950 ^{o}C produced a dominant mix of δ and θ phases, resulted in prevention of stable component formation during CO_2 adsorption. CO_2 adsorption capacity for 35KA(950) was maximum at 55 ^{o}C and can be regenerated up to ~98% at 150 ^{o}C. There was approximately 30% reduction of total regeneration time at GHSV of 750 h^{-1}. Also, the dissolution of K_2CO_3 in de-ionized water at elevated temperature (70 ^{o}C) could not permit higher loading to achieve high adsorption capacity as K_2CO_3 forms as crystals/aggregates on the outside of the support, which reduce active sites for CO_2 adsorption. Even then, all the K_2CO_3-based adsorbents showed high attrition resistance (<10%), which indicates large applicability in commercial fluidized bed CO_2 capture process.

Chapter 7

Circulating Fluid Bed Studies for Continuous CO_2 Capture from Flue Gas using K_2CO_3/Al_2O_3 Adsorbent

7.1 Introduction

The results obtained from continuous CO_2 adsorption-regeneration in circulating fluid-bed reactors at pilot scale level are discussed. Many scientific literatures have described the performance of various solid-based adsorbents for CO_2 capture in fixed-bed mode. These adsorbents showed excellent CO_2 adsorption capacities at various operating conditions but their regeneration requires relatively higher regeneration temperature (> 200 ^oC). To increase the efficiency of adsorptive capture route, many researchers have investigated the potassium-based adsorbent in continuous fluidization system under atmospheric pressure, where adsorption takes place in one fluidized-bed reactor at 50-80 ^oC and regeneration takes place in another fluidized-bed reactor at 120-300 ^oC. The CO_2 capture with dry regenerable solid sorbents is the reversible reaction between potassium carbonate and potassium bicarbonate in a thermal-swing process carried out in fluidized bed reactor. K_2CO_3 reacts with H_2O during activation process and transforms to K_2CO_3. $1.5H_2O$, and further reaction with CO_2 during adsorption process transforms to potassium bicarbonate ($KHCO_3$) and further decomposition at higher temperature to potassium carbonate (K_2CO_3) are represented by following reaction:

$$K_2CO_3 + H_2O = K_2CO_3.\ 1.5\ H_2O \qquad \Delta H=-103\ kJ/mol \qquad (7.1)$$

$$K_2CO_3.\ 1.5\ H_2O + CO_2 = 2KHCO_3 + 0.5\ H_2O \qquad \Delta H=-38\ kJ/mol \qquad (7.2)$$

Based on this reaction, the experiments were conducted in an existing fluid catalytic cracking (FCC) pilot plant. A spray-dried alumina supported adsorbent with 35 wt% K_2CO_3 loading was used to study the effect of various operating parameters on the CO_2 removal efficiency in both batch (non-circulating) and in continuous circulating mode. Multiple adsorption-regeneration cycles were done in two separate fluidized beds, with continuous circulation of the adsorbent between the two beds, in order to investigate the effect of adsorption and regeneration temperature, water vapor content in simulated inlet flue gas stream, gas-hourly space velocity (GHSV) and mode of adsorbent regeneration. The effects of several operating parameters have been widely discussed in both batch fluidization and circulating fluidization mode. The performance evaluation results from the CO_2 capturing adsorbent in fluidized bed system at pilot scale were very promising and encouraging to scale up the trials further to demonstration level. This work is unique as it was tested at pilot scale level to evaluate the adsorption-regeneration performance of stabilized K_2CO_3/Al_2O_3 adsorbent. Moreover, adsorbent regeneration with pure CO_2 as sweep gas is reported for the first time. The entire studies have been disclosed as Indian patent (Application No.: 1963/MUM/2015).

7.2 Experimental

7.2.1 Solid adsorbent preparation

A 50-kg inventory of 35-wt% potassium carbonate-based adsorbents used in this study was prepared in house by the incipient wet impregnation method on meso-porous γ-Al_2O_3 support. The adsorbent was prepared using five major conventional steps namely, dissolution of K_2CO_3 in de-ionized water, incipient wet impregnation, drying, grinding and sieving. The details of adsorbent preparation method are described in recently filed patent [98, 104] and Section 3.2 of Chapter 3.

7.2.2 Adsorbent characterization

7.2.2.1 Physical characterization

The nitrogen adsorption–desorption method was used to determine BET surface area and total pore volume of the adsorbents using Micromeritics ASAP 2020 apparatus. The physical properties of solid adsorbent (35% K_2CO_3/Al_2O_3) used in this study is presented in Table 7.1. The average particle size was measured using Malvern Mastersizer 2000 and was found between 75 and 80 µm. Attrition resistance of these adsorbents was measured as Attrition Index (AI) by ASTM D5757 method.

The XRD analysis was performed to identify phases present in the spent and regenerated adsorbents using X-ray diffraction (XRD, X'Pert Pro, PANalytical) using CuKα radiation at room temperature. The analysis was performed at a scanning rate of 0.02°/min between 10° and 90°.

The thermal stability of selected spent and regenerated adsorbents was carried out using thermo gravimetric analyzer (TGA: Universal V4.5A TA Instruments) using N_2 as carrier gas at the heating rate of 10 °C/min. TG analyses provided the decomposition of the species formed during adsorption-regeneration, which helped to explain adsorption-regeneration characteristics of the adsorbents.

It is well known from the literature that the adsorption and desorption capacities were greatly affected by the microscopic structure of adsorbent [65]. Therefore, alumina support with large surface area and pore volume was used to load potassium carbonate, to improve the CO_2 capture capacity. Also, AI of 35% K_2CO_3/Al_2O_3 adsorbent is much smaller than that of

commercial FCC catalyst (AI ≈ 20%). Hence, the adsorbent with high chemical reactivity and high attrition resistance are appropriate for multi-cycle use with solid in continuous circulating mode between adsorber and desorber.

7.2.3 Experimental set-up

Figure 7.1 shows a schematic diagram of existing pilot plant for fluid catalytic cracking unit (FCC) at Reliance Industries Limited (RIL), which was used for CO_2 capture experiments. This unit consists of (i) riser, (ii) stripper, (iii) combustor, (iv) regenerator, (v) cyclone separators, (vi) two-interconnected stand-pipes with slide valves for controlling catalyst circulation, (vii) CO_2 infra-red analyzer, (viii) filters for collection of fines (abraded adsorbent particle). In this unit, regenerator and riser-stripper assembly were used as adsorber and desorber respectively. In the subsequent sections, the adsorber and desorber terms imply their respective meaning. Both adsorber and desorber are operated in bubbling fluidization flow regime. The bubbling fluidized mode operation is expected to provide efficient adsorption of CO_2 in the adsorber and efficient desorption in the regenerator.

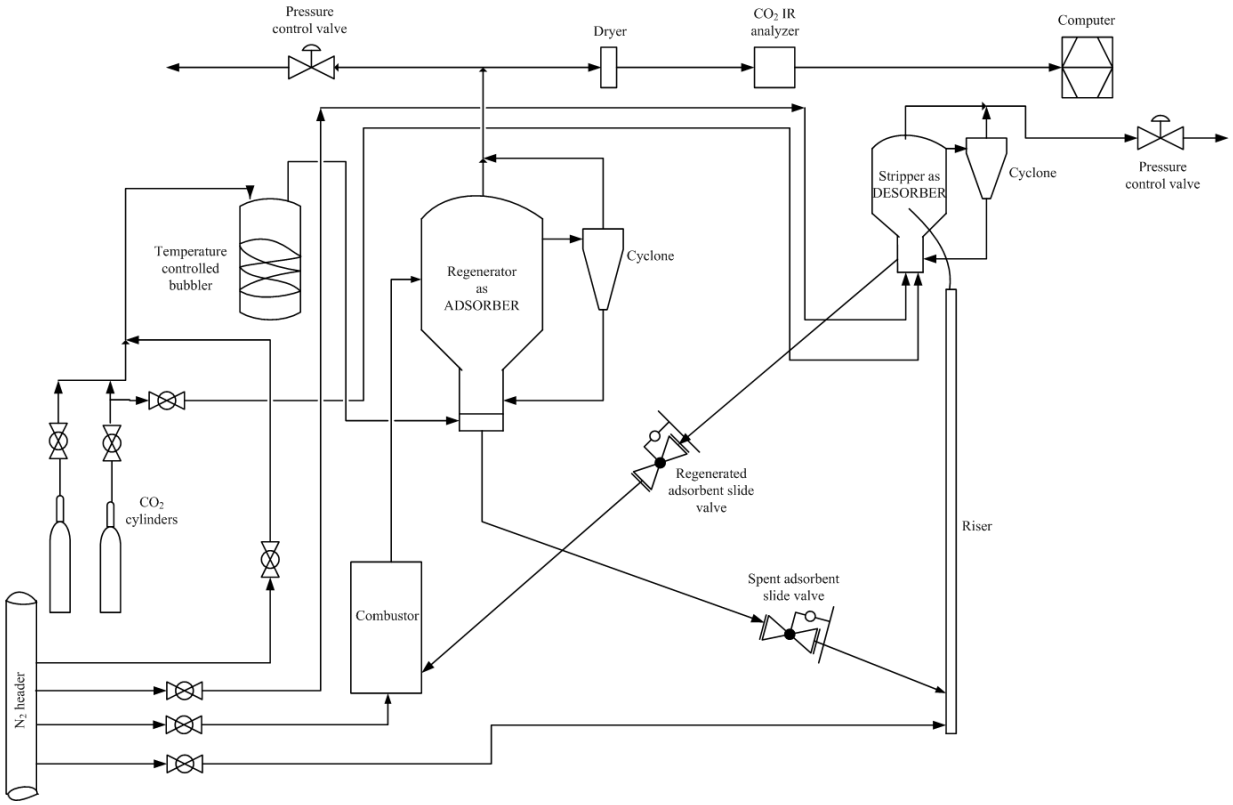

Figure 7.1 Schematic representation of existing FCC pilot plant at RIL used for dry sorbent CO_2 capture process (Patent Application No.: 1963/MUM/2015).

All reactors and inter-connected lines are surrounded by electric heating elements, which are controlled remotely by PLC-based control system. The insulation on the adsorber side and the stand-pipes between desorber and adsorber are removed to control the temperature rise due to exothermic heat of carbonation reaction.

The simulated flue gas composition: 8-10 vol% CO_2, 10-23 vol% H_2O and balance N_2 was fed through pre-calibrated mass flow controllers (MFCs) into the adsorber. The nitrogen was supplied through N_2 header, CO_2 from high purity gas cylinder and water vapor was supplied from temperature controlled gas bubbler filled with water. In some experimental runs, steam was also supplied using steam generating unit with high precision metering pump, to study the effect of different modes of water vapor injection into the adsorber. The gas mixture (N_2 and CO_2) is passed through the gas bubbler to saturate the gas stream with H_2O which was confirmed by measuring the humidity level. The entire feed gas lines are insulated and temperature-controlled to avoid condensation of water vapors in downstream lines. In the adsorber, CO_2 in presence of H_2O reacts with supported K_2CO_3 adsorbent coming from the desorber, at temperature between 50 and 80 ^oC according to forward reaction shown in equation (2.1). The potassium bicarbonate ($KHCO_3$) formed in the adsorber is regenerated at 130-200 ^oC with N_2/ CO_2 as sweep gas as shown by backward reaction in equation (2.1).

The CO_2 removal efficiency (η) is estimated by the given equation

$$\eta = \frac{\left(C_{CO2_{in}} - C_{CO2_{out}}\right) \times 100}{C_{CO2_{in}}} \qquad (7.3)$$

Where, $C_{CO2\ in}$ = inlet CO_2 concentration in feed simulated gas, vol%, $C_{CO2\ out}$ = outlet CO_2 concentration in treated simulated gas, vol%. Similarly, gas residence time (t_{gas} in seconds) and adsorbent residence time (t_{solid} in minutes) in adsorber (A) and desorber (D) are estimated by the following equation

$$t_{gas} = \frac{V_{A\ or\ D}}{v_{A\ or\ D}} \times 3600 \qquad (7.4)$$

$$t_{solid} = \frac{W_{solid}}{SCR} \times 60 \qquad (7.5)$$

Where, $V_{A\ or\ D}$ is the volume of adsorber (A) or desorber (B) in m^3 and $v_{A\ or\ D}$ is the volumetric flow in (m^3/h) in adsorber and desorber. W_{solid} and SCR are expressed as weight of adsorbent

(kg) and solid circulation rate (kg/h) respectively. The CO_2 removal efficiency is strongly influenced by increasing both gas-solid residence time in the reactors.

The CO_2 in the gas out of the adsorber was continuously measured by online IR analyzer. A computer collects all the electrical signals from pressure transducers, thermocouples, level controllers, MFCs and gas analyzer. Furthermore, there is an adsorbent collection point just below the adsorbent charging point in the adsorber where adsorbent can be withdrawn and their residual capture capacity by thermo-gravimetric analysis can be measured.

Non-circulating Fluidization Mode: The experiments were carried out to study the effect of parameters such as adsorption-regeneration temperature, GHSV etc. Initially, 16 kg solid adsorbent was charged in the adsorber to examine the CO_2 capture characteristics. The gas flow rate and the gas velocity in the adsorber were varied between 2.0-11.0 m^3/h and 0.08-0.19 m/s respectively. During desorption, GHSV was varied from 100 to 650 h^{-1}.

Continuous Fluidization Mode: During the continuous circulation mode, the adsorbent is circulated between adsorber and desorber through solid transfer standpipes. The flow regime for the fluidization in two reactors was maintained as bubbling regime. The flows of spent adsorbent to the desorber and regenerated adsorbent to the adsorber are regulated by slide valves in the spent adsorbent and regenerated adsorbent lines respectively. The pressure maintained in the adsorber and desorber was 1.75 and 1.80 bar respectively. For circulating fluidized bed studies, the initial inventory of 25 kg of K_2CO_3/Al_2O_3 adsorbents was charged into the adsorber. Temperatures in the adsorber and desorber were stabilized at target values by circulating the adsorbent initially without injecting H_2O and CO_2. The steady and constant adsorbent circulation between adsorber and desorber was ensured by stable differential pressure between the two reactors. The adsorbent was pretreated with saturated water vapor for 20 min and thereafter CO_2 was injected into the adsorber. In each run, measurements of the gas composition from both reactors was made by online IR analyzer and also the intermittently collected gas samples were analyzed offline by gas chromatograph. This was done by diverting the solids to a dead volume for a certain period of time. These solids were then subjected to analysis together with other solid samples that were extracted directly from the riser ports. It is to be noted that the total solid adsorbents were flushed with N_2 for 2 h to remove any free water between the two consecutive runs. Regeneration of adsorbents was performed with N_2 and with CO_2 as a sweep gas between 130 to 200 ^oC to study the regeneration characteristics. For each set of experimental run, the regeneration efficiency was calculated in terms of percent CO_2

removed, i.e. difference between inlet and outlet CO_2 concentration in the adsorber. This difference also indicates the amount of CO_2 captured during carbonation in a given operating conditions.

7.3 Results and discussion

7.3.1 Physico-chemical properties

The physical properties of solid adsorbent (35% K_2CO_3/Al_2O_3) used in this study is presented in Table 7.1. It is the modified adsorbent, which showed excellent multi-cycle CO_2 adsorption capacity in fixed bed adsorption-regeneration studies. This adsorbent was prepared in bulk quantity of 47-kg for pilot plant studies. The properties measured showed similar properties as obtained for laboratory scale adsorbent.

Table 7.1 Physical properties of 35% K_2CO_3/Al_2O_3 adsorbent

Properties	**Unit**	**Values**
BET surface area	m^2/g	35.2
Total pore volume	cm^3/g	0.146
Average pore diameter	nm	19.8
Bulk density	g/cm^3	0.96
Attrition index	%	4.33

Figure 7.2 shows the XRD analysis of the spent and regenerated adsorbent samples collected at stable circulation of the experiment. The experiment was conducted with H_2O/CO_2 ratio of 1.91 in simulated flue gas adsorption at 87 ^oC and desorption at 150 ^oC. It is observed from XRD analysis that both the K_2CO_3. 1.5 H_2O (JCPDS 73-0470) and $KHCO_3$ (JCPDS 70-1168) phases are present in the samples. It indicates that the adsorbent is partially regenerated in this circulating fluidized bed system.

Figure 7.3 shows the thermo-gravimetric analysis (TGA) of the regenerated adsorbent sample (experiment carried out with flue gas containing H_2O/CO_2 ratio of 1.91). It was observed that approximately 2.15-wt% of weight loss during 110-150 ^oC, which were the losses due to the decomposition of K_2CO_3. 1.5 H_2O and $KHCO_3$. The presence of these hydrated species was also observed through XRD analysis (Figure 7.2). TG analysis of spent adsorbent sample (experiment carried out with flue gas containing H_2O/CO_2 ratio of 1.91), shows approximately 2.16-wt% weight loss between 110 and 150 ^oC, which indicatively dictates the adsorption

capacity of 0.53 mmol CO_2/g of adsorbent (~25% capacity utilization at 3.5 min solid residence time.

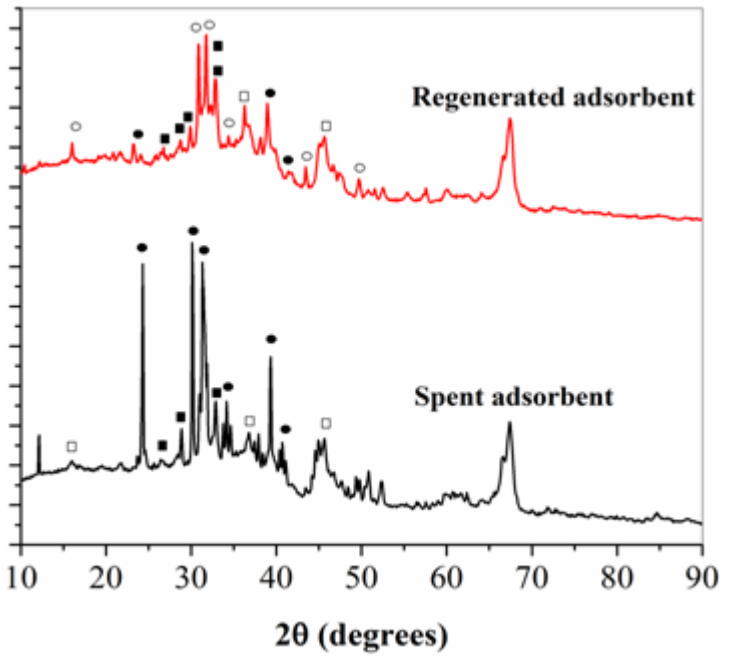

Figure 7.2 XRD analysis of the spent and regenerated adsorbents (○ K_2CO_3, ■ $K_2CO_3 \cdot 1.5\ H_2O$, ● $KHCO_3$, □ $KAl(CO_3)_2(OH)_2$).

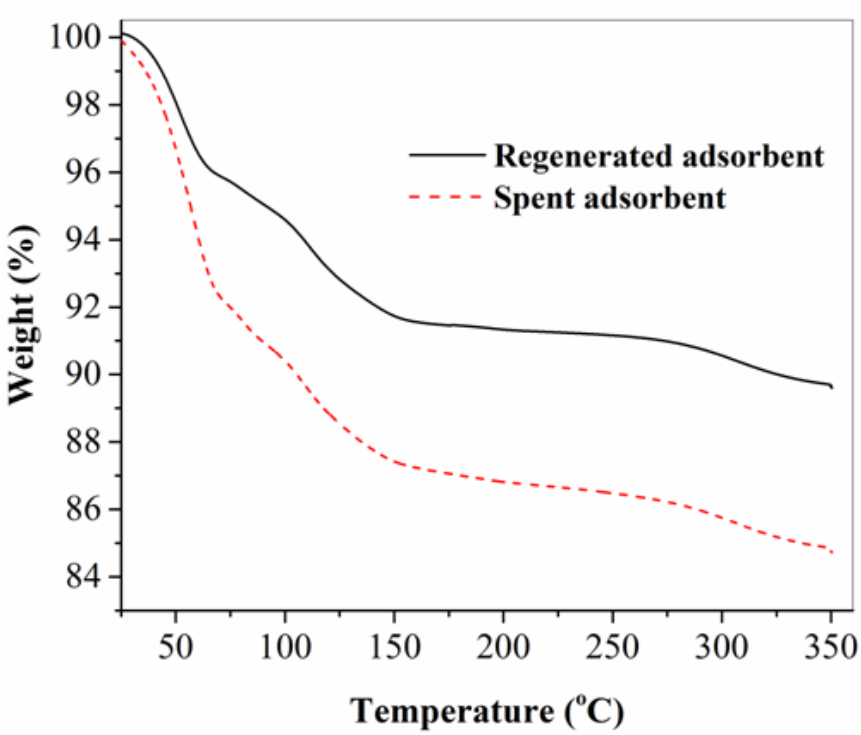

Figure 7.3 Thermo gravimetric analysis (TGA) of the spent and regenerated adsorbents

7.3.2 CO_2 adsorption in non-circulating fluidization study

7.3.2.1 Effect of adsorption temperature

The experiments were carried out at four different temperatures *viz*. 50, 60, 65 and 70 ^oC to study the effect of adsorption temperature (T_{ads}) on CO_2 removal as well as CO_2 adsorption capacity. During these experiments, adsorber was isolated from the desorber using the slide valve for solids. Figure 7.4a shows profile for CO_2 adsorption capacity with adsorption temperature in a fixed bubbling fluidized-bed reactor with 16 kg adsorbent at constant gas velocity of 0.16 m/s. It was observed that at 65 ^oC, the percent CO_2 removal from the feed gas mixture was 26.04% and the adsorption capacity for CO_2 to be 0.9 mol/kg adsorbent. At higher adsorption temperature, CO_2 capture capacity decreases due to exothermic heat liberation from forward reaction. Hence, shift in reaction equilibrium to backward direction, favors decomposition of bicarbonate species (equation (2.1)). In our non-circulating fluidization studies, there was no cooling facility to control the exothermic heat generated during carbonation reaction. Hence, the adsorption capacity has been related to the average of the temperatures experienced by the adsorbent during the run. For example, when reaction was performed at 70 ^oC, the temperature rose up to 113.4 ^oC. Hence, an average of the temperatures (~86.7 ^oC) was considered for the observed adsorption capacity. This observation is in good agreement with those reported by RTI group [15].

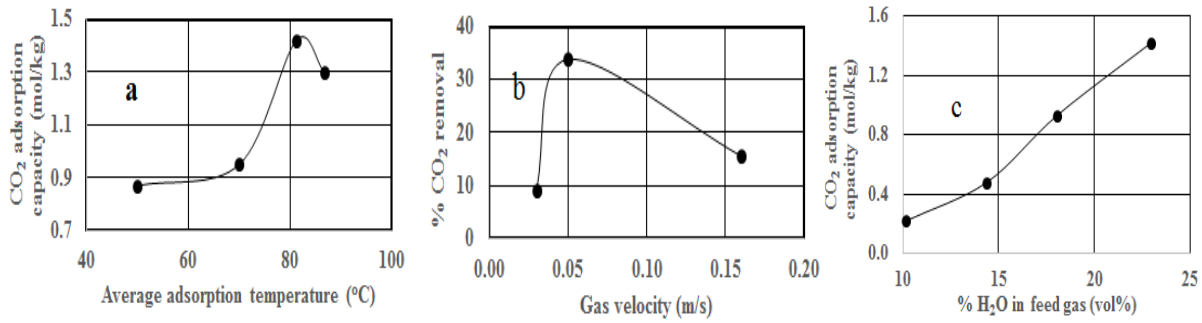

Figure 7.4 Effects of parameters (a) adsorption temperature (b) water vapor content in simulated flue gas (c) gas velocity on CO_2 adsorption capacity (also removal efficiency)

As stated above, low temperature was preferred for the adsorption reaction due to reaction kinetics. Care was taken to operate the adsorption reaction well above the dew point of water to prevent water condensation.

7.3.2.2 Effect of H_2O concentration in simulated flue gas

Figure 7.4b shows the effect of water vapor concentration in simulated flue gas stream at a constant temperature of 65 ^oC and total flow of 3.3 m^3/h. The experiments were carried out with four different water vapor contents *viz*. 10.2%, 14.4%, 18.1% and 23% (by volume) to study its effect on CO_2 removal. The water vapor was fed into the reactor by direct steam injection using steam generator. It was interesting to note that as the water vapor concentration in simulated flue gas increases, the CO_2 adsorption increases significantly. For example, at H_2O/CO_2 ratio of 1.25 in simulated flue gas, the adsorption capacity was found to be as low as 0.2 mol CO_2/kg adsorbent, while at 3.11 ratio the capacity significantly increased to 1.42 mol CO_2/kg adsorbent. This is about 71% of adsorption capacity achieved in fixed-bed reactor studies (2.0 mol/kg). The substantial increase in adsorption capacity is due to the availability of active sites like $K_2CO_3 \cdot 1.5\ H_2O$ due to the presence of water vapor during adsorption. The reactive species $K_2CO_3 \cdot 1.5\ H_2O$ then convert to $KHCO_3$ by reacting with CO_2. This observation is consistent with the results reported by other researchers [65, 71, 98].

7.3.2.3 Effect of gas velocity on CO_2 removal

Figure 7.4c shows the effect of gas superficial velocity (U_o) on CO_2 removal, where percent CO_2 removal increased up to 34% at a gas velocity of 0.05 m/s for constant composition of gases. When the gas velocity was further increased to 0.16 m/s, the percent CO_2 removal dropped significantly to 15.8%. The highest removal efficiency at 0.05 m/s can be explained by the existence of an optimum residence time for the gas within the experimental range of 40 s and 7 s at the gas velocities of 0.03 m/s and 0.16 m/s respectively (using equation (7.4)). This velocity of gas streams provides an effective bubbling fluidization regime, wherein all particles are in sufficient gas-solid contact in the adsorber. It is observed that sufficient gas-solid contacts during carbonation reaction is required to give good CO_2 removal, which is consistent with the result reported by Yi et al. [71].

7.3.3 CO_2 adsorption in a continuous fluidization study

7.3.3.1 CO_2 removal adsorption curves in bubbling fluidized beds using direct steam injection

As discussed in experimental section, FCC regenerator vessel was used as adsorber and riser-stripper as desorber. The modifications were necessary to achieve desirable residence time for the adsorbent in both adsorber and desorber. Several key parameters, such as H_2O concentration in simulated flue gas, regeneration temperature, gas velocity, and method of injecting water vapor in the adsorber was studied.

Simulated flue gas enters from the bottom of the bubbling-bed adsorber wherein CO_2, N_2 mixture and steam (produced from the existing steam generator) are co-fed in the adsorber bottom while the solid adsorbent flows down the adsorber countercurrent to the flue gas flow. The treated flue gas from the adsorber is passed through the cyclone separators and analyzed in the infra-red analyzer. The solid fines captured in the cyclones are recycled back into the adsorber and while the spent adsorbents are sent to the bubbling-bed desorber through the circulation slide valve and the riser. The regenerated adsorbents from desorber are recirculated to the adsorber through regenerated adsorbent slide valve and subsequently lifted pneumatically by additional flow of N_2 through an existing vessel (FCC combustor).

Figure 7.5 shows the CO_2 adsorption profile for circulating fluidized bed for more than 13 h operation. The continuous adsorption-regeneration was conducted at constant gas velocity of 0.11 m/s in the adsorber at average temperature of 75 ^oC. It is seen that CO_2 removal was 58.3% at H_2O/CO_2 ratio of 1.67 vol/vol % in simulated flue gas and 31.3% when the ratio was 1.14 (from equation (7.3)). The solid circulation rate (SCR) was maintained at 40 kg/h. Depending on adsorbent circulation rate and adsorbent inventory in the adsorber and desorber, the adsorbent residence times were maintained at 7.3 and 3.6 min in adsorber and desorber respectively (using equation (7.5)).

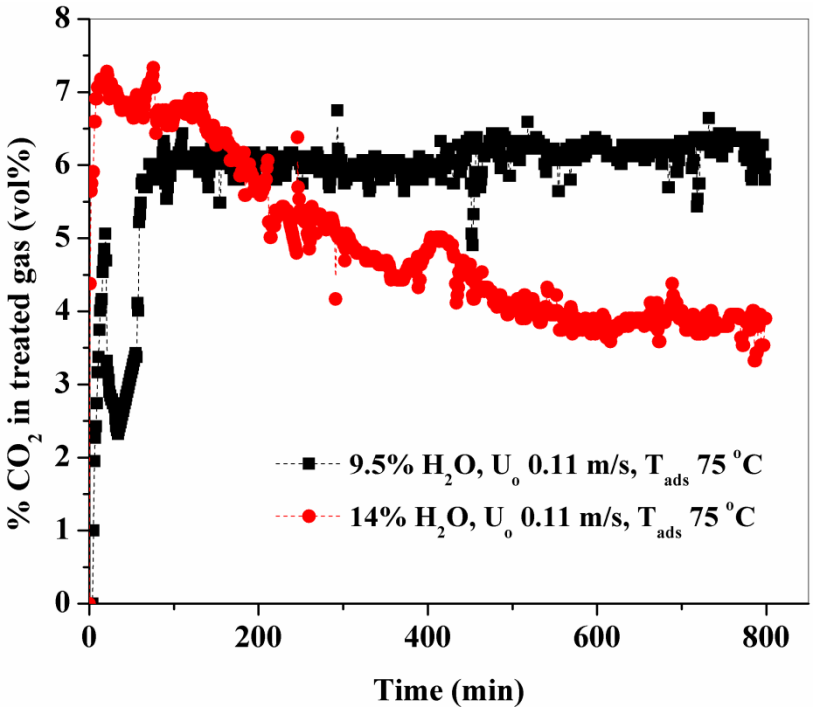

Figure 7.5 Effect of direct steam injection on CO_2 adsorption

The temperature rise due to the exothermic heat liberated during carbonation was controlled by removing insulation from the heat-generating sections i.e. adsorber and corresponding standpipes. It is interesting to note that direct steam injection in the simulated flue gas resulted in difficulties in adsorbent circulation. This was due to the condensation of water vapor in the adsorber and its subsequent take up by the hygroscopic K_2CO_3/Al_2O_3 adsorbent. Hence, the mode of water vapor injection inside the reactor is critical in establishing smooth continuous circulation of adsorbent in pilot plant set up.

7.3.3.2 CO_2 removal in bubbling fluidized beds using bubbler for controlling water in flue gas

A set of experiments were carried out to see the effect of water vapor injection in the adsorber using a temperature-controlled gas bubbler. An existing surge vessel was used as gas bubbler. This make-shift gas bubbler arrangement was wrapped with tape-heater and insulated to avoid heat losses. The simulated flue gas was bubbled through water in the bubbler and fed to the adsorber through a heated line. An insulated line bypassing the bubbler was connected to flush the closed loop adsorber-desorber system with N_2. The temperature of water in the bubbler was controlled based on its thermocouple reading.

Figure 7.6 shows the effects of various H_2O/CO_2 ratios in the flue gas studied in the experimental runs carried out at constant adsorption-desorption temperature, gas velocity and solid circulation rate. The adsorption and desorption temperatures were maintained at 80 ^oC and 150 ^oC respectively. The gas velocity to the adsorber was kept at 0.11 m/s, while the solid circulation rate maintained at 40 kg/h. It is interesting to note that higher the H_2O/CO_2 ratio in the adsorber, higher is the CO_2 removal. Hence, the role of water vapor during carbonation is critical to maximize the CO_2 removal from a given simulated flue gas stream. It is explained by the formation of more active sites ($K_2CO_3.1.5\ H_2O$) on the adsorbent. It is also observed that CO_2 removal was higher with water vapor injected through the bubbler than with direct injection of steam. Figure 7.5 and 7.6 show higher removal of CO_2 with water vapor injected through the bubbler at similar H_2O/CO_2 ratio (in the range of 1.67-1.71) in the simulated flue gas. This is attributed to better mixing of water vapors with the gas in the bubbler and its more uniform contacting subsequently with adsorbent in the adsorber.

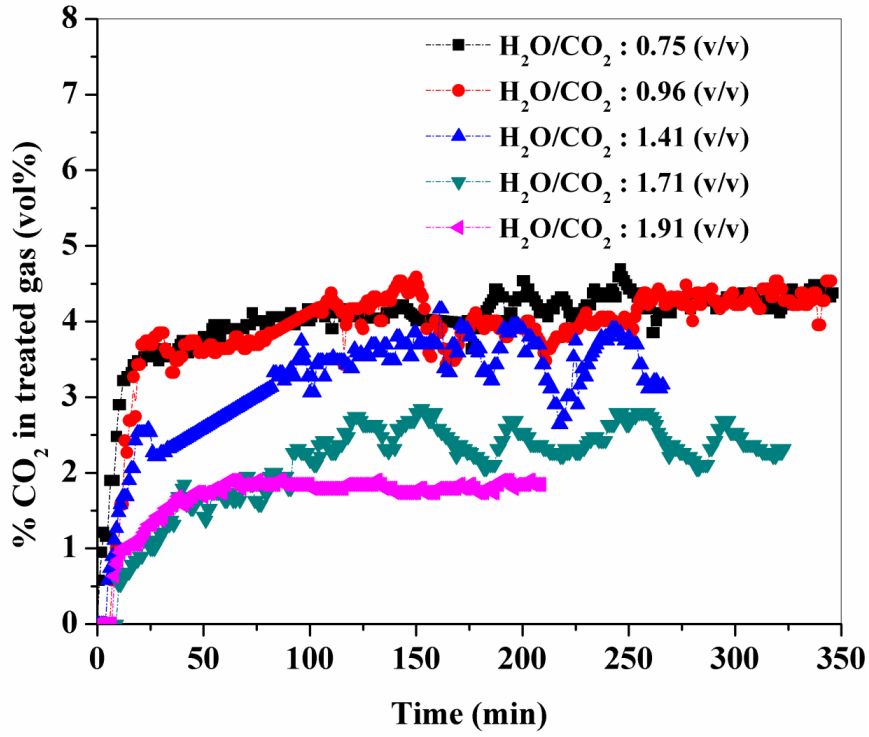

Figure 7.6 CO_2 outlet concentration in flue gas with adsorbent in continuous circulating mode for CO_2 capture with different water vapor concentration using gas bubbler arrangement (flue gas composition: CO_2 (dry basis) 10 vol %; adsorption and regeneration temperature: 80 ^oC and 150 ^oC; gas velocity in adsorber: 0.11 m/s; solid circulation rate: 40 kg/h)

Figure 7.7 shows the temperature and pressure profiles across the adsorber and desorber during continuous CO_2 removal process for 4 h. The temperatures in adsorber and desorber were measured using thermocouple at bottom position. During steady-state circulation without CO_2 feeding, the adsorber temperature was maintained at 70 ^oC. When CO_2 was fed into the adsorber, the temperature was increased to around 82 ^oC due to exothermic heat generation. The temperature in the adsorber, during 4 h continuous operation, was maintained at around 80 ^oC by heat loss through the adsorber and standpipe wall surface. The insulation of the equipment was removed for the purpose. The spent adsorbent at 80 ^oC was circulated to the desorber. The temperature in the desorber was maintained at 150 ^oC by electrical heating of the desorber. Differential pressures across the adsorber and desorber as measured between bottom and top positions is shown in Figure 7.7. The pressure drop across the adsorber and across the desorber were maintained constant, although some fluctuations in pressure drop across desorber were observed due to slight disturbance in solid circulation. These results show a stable continuous operation with the adsorbent in circulating fluidized bed reactors.

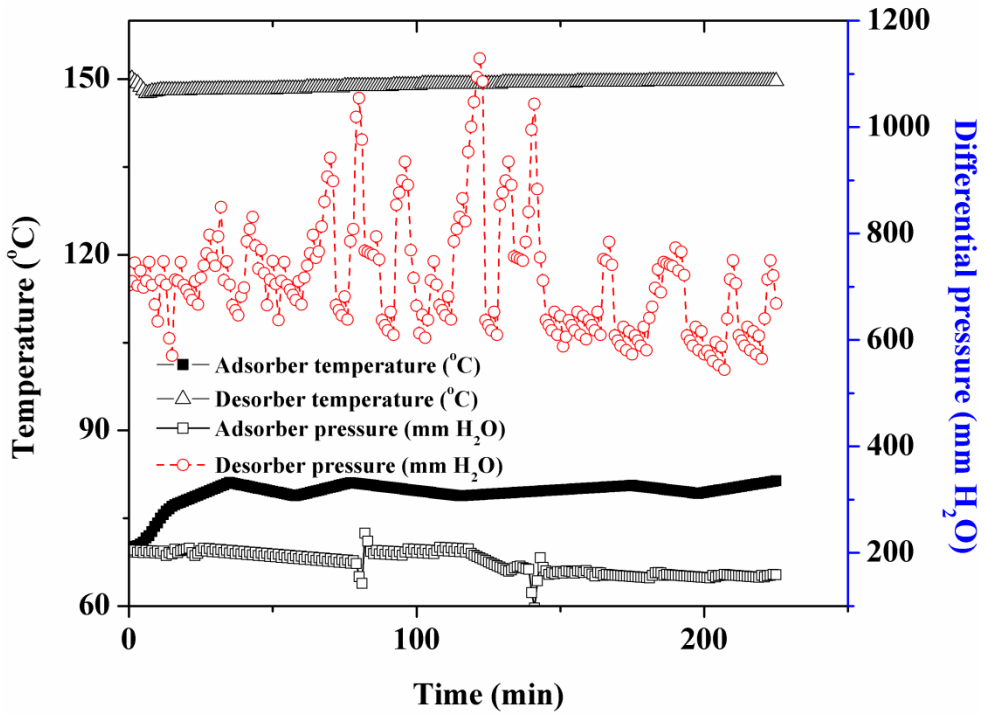

Figure 7.7 Temperature and pressure profiles in adsorber and desorber during continuous operation

The water vapor content in the simulated flue gas was varied by changing the gas bubbler temperature. The water vapor content in flue gas at saturated conditions increases with increase in bubbler temperature. Figure 7.8 shows the effect of water vapor content in simulated flue

gas on CO_2 removal at constant adsorption-desorption temperature, gas velocity and solid circulation rate. These experiments were performed at water vapor content of 6.36, 8.05, 11.33, 13.46 and 14.77 vol% at 75 ^oC. The adsorbent was regenerated at 150 ^oC and gas velocity and solid circulation rate were maintained at 0.11 and 40 kg/h respectively. As discussed earlier, CO_2 removal rate increases with increase in water vapor content in simulated flue gas in the continuous circulating mode also.

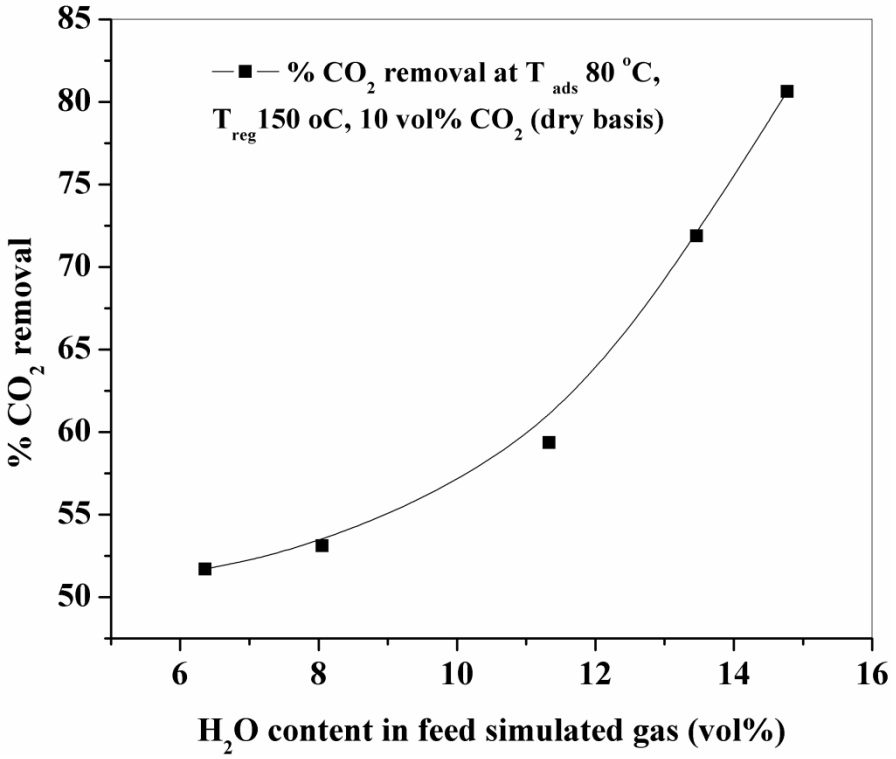

Figure 7.8 Effect of water vapor content on CO_2 removal using gas bubbler (flue gas composition: CO_2 10 vol % on dry basis; adsorption and regeneration temperature: 80 ^oC and 150 ^oC; gas velocity in adsorber: 0.11 m/s; solid circulation rate: 40 kg/h)

It is seen from the Figure 7.8 that at water vapor content of 6.36% vol., the CO_2 removal was 51.7%, while CO_2 removal of 80.6% was achieved with 14.77 vol% water vapor content. Therefore, water vapor content in simulated flue gas plays a significant role to achieve higher CO_2 removal. This is explained by the fact that CO_2 and K_2CO_3 in presence of excess water vapor results in formation of more active species during carbonation reaction. The results also showed appreciable removal of CO_2 at lower water vapor content in simulated flue gas. These observations are consistent with the observations reported by Kim et al (KIER) [72]. Experiments with still higher concentration of H_2O was not performed as the temperature rise during carbonation was excessive and difficult to control by natural convective cooling from bare surfaces of adsorber. Also, at higher temperatures, desorption of CO_2 from decomposition

of $KHCO_3$ is expected to be higher than the adsorption of CO_2. Thus water vapor content in simulated flue gas plays a crucial role in enhancing CO_2 removal efficiency. This can be explained in detail with the concept of partial regeneration of adsorbents during circulating fluidized bed studies. This circulating fluidized bed process includes the partial regeneration of adsorbents in which partially regenerated adsorbents from the desorber possesses hydrated active species in the form of K_2CO_3. 1.5 H_2O. The XRD data as shown in Figure 7.2 shows the presence of these species in the partially regenerated adsorbents. The partially regenerated adsorbents are transported through standpipes. The hydrated active species then facilitate in enhancing reaction kinetics by using low amount of H_2O fed into the adsorber. As a result, higher CO_2 removal efficiency (>80%) was achieved using a low H_2O/CO_2 ratio (of 1.91) in simulated flue gas. Similar TG analysis of spent and regenerated adsorbents using a simulated flue gas stream of H_2O/CO_2 ratio of 1.91 is shown in Figure 7.3. From the TGA of the regenerated adsorbent sample, it was observed that approximately 2.15-wt% of weight loss during 110-150 ^oC, are the losses due to the decomposition of K_2CO_3. 1.5 H_2O and $KHCO_3$. The presence of these hydrated species was also observed through XRD analysis (Figure 7.2). TG analysis of spent adsorbent sample shows approximately 2.16-wt% weight loss between 110 and 150 ^oC, which shows the adsorption capacity of 0.53 mmol CO_2/g of adsorbent (~25% capacity utilization at 3.5 min solid residence time. At this coverage, the isosteric heat requirement for CO_2 adsorption is estimated as 27 kJ/mol, which is within the heat requirement for physisorption. Hence, overall energy demand is required to be low for continuous CO_2 removal in an energy-integrated circulating fluidized bed process as reported in the patent filed (3190/MUM/2013).

Figure 7.9 shows the effect of gas velocity in adsorber on CO_2 removal in circulating fluidized bed process. The experiments were conducted at different gas velocities *viz*. 0.06, 0.08 and 0.11 m/s in the adsorber with constant CO_2 and H_2O compositions (H_2O/CO_2 ratio = 1.6) of simulated flue gas at constant adsorption-regeneration temperature and with constant solid circulation rate. It is seen that the increase in inlet gas velocity reduces CO_2 removal. This is due to decrease in gas-solid contact time in the adsorber. At low inlet gas velocity of 0.06 m/s, the CO_2 removal was found to be 76.6%, while it reduced to 66.7% at 0.11 m/s.

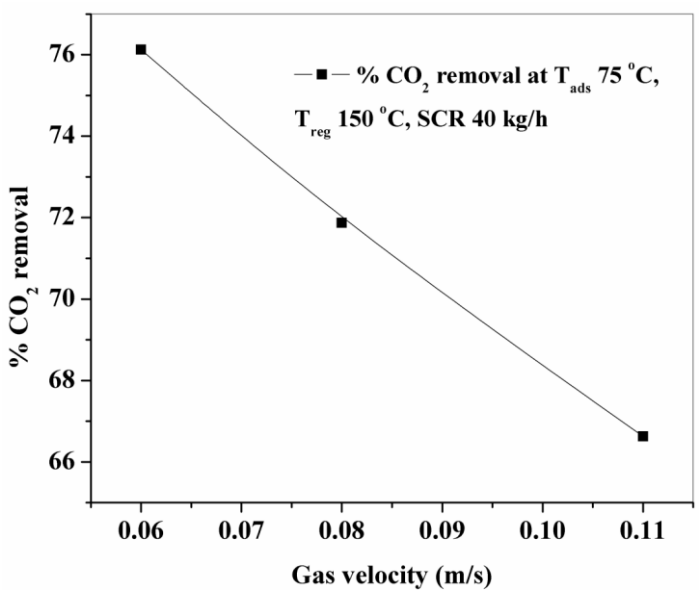

Figure 7.9 Effect of gas velocity on CO_2 removal using gas bubbler (flue gas composition: CO_2 (dry basis) 10 vol %; adsorption and regeneration temperature: 75 ^oC and 150 ^oC; gas velocity in adsorber: 0.11 m/s; solid circulation rate: 40 kg/h)

Figure 7.10 shows the effect of regeneration temperature (T_{reg}) on CO_2 removal in continuous adsorption-regeneration process. The experiments were conducted at carbonation temperature of 75 ^oC with a simulated flue gas composition of CO_2 7.96%, H_2O 14.98% on wet basis. The solid circulation rate was maintained at 40 kg/h. The adsorbents were regenerated at three different temperatures *viz*. 130, 150 and 200 ^oC to study the effect of regeneration temperature on CO_2 removal. It is seen from Figure 7.10 that as the temperature for regeneration increases, the CO_2 removal increases from 71.87% to 81.33%. This is due to the easier decomposition of $KHCO_3$ (saturated adsorbent) at higher temperature. It is interesting to note that even at 130 ^oC, appreciable removal of the CO_2 (71.87%) occurs and the removal at higher temperatures of 150 ^oC and 200 ^oC increases to only 80.06 and 81.33% respectively. It is also possible to achieve higher percent CO_2 removal at 130 ^oC by providing sufficient solid residence time in the desorber. This is the first time it is reported that continuous CO_2 removal is performed with lower temperature differential between adsorption and desorption (40-50 ^oC). Since, there is almost no change in percent CO_2 removal efficiency with desorption temperature of 150-200 ^oC, hence, 150 ^oC can be considered as an optimum temperature for desorption. At this temperature, the adsorbent is partially regenerated with a fractional coverage of 0.25. Figure 7.2 shows the XRD analysis of spent and regenerated adsorbent samples collected at stable circulation condition, wherein, both the K_2CO_3. 1.5 H_2O and $KHCO_3$ phases are observed to

be present in the samples. This signifies that the adsorbent is partially regenerated in this circulating fluidized bed system.

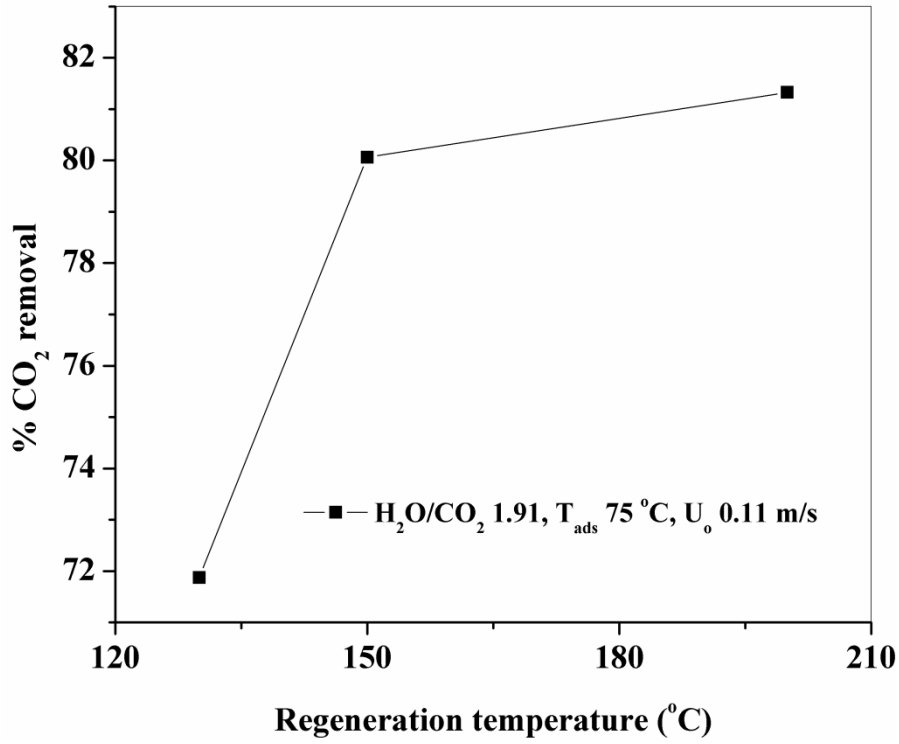

Figure 7.10 Effect of regeneration temperature on CO_2 removal using gas bubbler

It suggests that the adsorbent used in this study is efficiently regenerated so as to give more than 85% removal of CO_2 from feed flue gas which is similar to those reported in our previous studies in fixed bed reactor system [98, 104]. Moreover, there is a very minor difference in CO_2 removal (i.e. 80.06 and 81.33%) observed at regeneration temperatures of 150 and 200 ^oC. This observation in circulating fluid-bed process corresponds to about 98% regeneration efficiency reported in our previous work for fixed bed reactor. Thus the adsorbent is almost completely regenerated at 150 ^oC due to improved regeneration properties of the adsorbent.

Figure 7.11 shows the effect of sweep gases on CO_2 removal during regeneration. The adsorption and regeneration temperature was maintained at 75 ^oC and 150 ^oC respectively. The gas compositions in simulated flue gas was kept at 8.47% CO_2, 13.06% H_2O and rest N_2 and fed in the reactor maintained to keep gas velocity of 0.11 m/s. The sweep gases used in regeneration at 150 ^oC were N_2 and CO_2 at constant flow rate. To maximize the purity of captured CO_2, an important aspect for scale up and commercialization of this CO_2 capture process, the regeneration was initially conducted with N_2 as sweep gas and then switched over

to CO_2 to study the effect of sweep gas on CO_2 removal. The experiment was conducted for more than 6 h. CO_2 removal efficiency with N_2 was observed to be 76.25% while it reduced to 50.7% with CO_2 as regeneration sweep gas. The introduction of CO_2 as sweep gas decreases the regeneration of the adsorbent at the given temperature due to the low concentration gradient of CO_2 at the solid-gas interface; the adsorbent being present in a new chemical equilibrium state with CO_2 as sweep gas. In order to achieve higher removal efficiencies, the regeneration needs to be carried out at higher temperature and the additional energy would be required for full regeneration [69]. Further, steam or CO_2 or a combination of these can be used as sweep gas in regenerator. In parallel, the purity of CO_2 is also as important as CO_2 removal efficiency, foreseeing its utilization aspects.

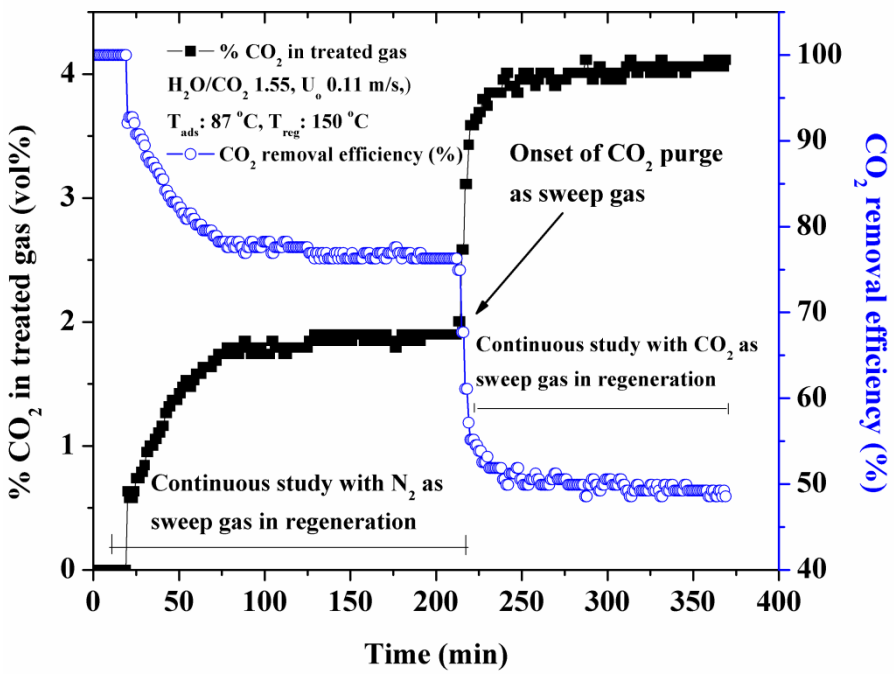

Figure 7.11 Effect of regeneration sweep gases (N_2 and CO_2) on CO_2 adsorption profile

7.4 Conclusions

The fluid-bed process for CO_2 capture using 35% K_2CO_3/Al_2O_3 adsorbent was investigated in an existing pilot plant unit designed for FCC process. The effect of process parameters such as adsorption and desorption temperature, gas velocity, feed water vapor content, mode of water vapor injection in the adsorber, mode of sweep gas during regeneration on CO_2 removal efficiency were studied with the adsorbent in non-circulating fluidized (bubbling bed) and in circulating fluidized (bubbling bed) modes. The CO_2 removal achieved in non-circulating fluidized bed mode was 71% of the adsorption capacity in fixed bed. In circulating fluidized

bed capture process the mode of injecting water vapor in the adsorber bed had significant impact on the extent of CO_2 removal. Introducing water vapor injection using temperature controlled gas bubbler arrangement provides higher CO_2 removal efficiency as compared to direct injection of steam as bubbling of flue gas through water avoids any local condensation of water in the flue gas feed line, adsorber and in the adsorbent loop. The circulating fluidized bed process was stable at carbonation temperature of 75-80 ^oC. An increase in water vapor content in the simulated flue gas and low gas velocity provide higher CO_2 removal efficiency. The adsorbent had showed CO_2 removal ranging from 52 to 81% for H_2O/CO_2 ratio within the range 0.75 to 1.91 studied with regeneration at 150 ^oC. The adsorbent is regenerable up to 85% efficiency at 130 ^oC, which is comparable with efficiency in fixed bed. The studies on effect of sweep gases like CO_2 and N_2 during regeneration of the adsorbent are important for scaling the process up to commercial level. The percent CO_2 removal using N_2 as sweep gas is 76.25%, while it is reduced to 50.7% with CO_2 as sweep gas. Moreover, lowering of temperature difference between adsorption and regeneration (50-70 ^oC) would be helpful in reducing energy demand for the process. The results of this study on continuous CO_2 adsorption-regeneration provide definite indications towards the efficacy and scalability of the dry regenerable adsorbent process for capturing CO_2. This process also provides partial regeneration of adsorbents in the desorber, which helps to retain hydrated active species K_2CO_3. 1.5 H_2O in the regenerated adsorbent. This active species provides less energetic sites for CO_2 adsorption in circulating fluidized bed process at a low temperature differential between adsorption and desorption. This is the first time it is reported that continuous CO_2 removal is performed with lower temperature differential between adsorption and desorption (40-50 ^oC). These studies are disclosed as an Indian patent (Application No.: 1963/MUM/2015).

Chapter 8

Energy-Integrated Process for CO_2 Capture

8.1 Introduction

CO_2 capture from flue gas stream is a major concern in the view of environmental aspects. The amount of CO_2 present in flue gas can be reduced by methods such as burning less coal, improving the efficiency of coal-fired power plants and capturing, followed by storing the captured CO_2. Among the various CO_2 capture techniques such as pre-combustion, post-combustion and oxy-combustion, post-combustion is the most promising technique as it can be retrofitted with existing process plant.

Amine absorption technique, is only the conventional technique for CO_2 capture. However, the absorption techniques are associated with several drawbacks such as (i) limitation in the rate of absorption of CO_2 due to diffusional resistance through the liquid phase; (ii) high energy requirement for amine regeneration (2.5 – 4.0 GJ/ton CO_2); (iii) oxidative degradation and acidification of solvent due to the presence of oxygen in the flue gas thereby making it corrosive in addition to causing loss in the available alkalinity for CO_2 capture; (iv) loss of amine due to its appreciable volatility results in equilibrium losses of amine to the treated gas; and (v) thermal degradation of amine rendering it unsuitable for continued use and hence, the requirement for substantial amounts of fresh make-up amine. Further, it is observed that the amine absorption process is restricted to CO_2 capture at ambient temperatures. Furthermore, capturing CO_2 using the absorption technique requires energy in the form of electricity or steam or both [8, 116] that is supplied by process plants like power plants which reduces the overall efficiency of the power plant by up to 14% using heat integration [128].

Therefore, there is an increased interest in developing less expensive and/or energy integrated processes for capturing CO_2. The adsorption processes, generally employing solid adsorptive material that fall under the post combustion category, serve as an alternative to the absorption based process. This is because replacing water by solid support greatly reduces the energy required for CO_2 capture due to the lower heat capacity of solid supports as compared to water. Published literature on CO_2 capture by the adsorption technique shows considerable CO_2 capture capacity. However, the high temperature and resource requirements for the regeneration of the capture media influence the overall cost and time efficiency of the process.

US Patents 7731782 [122] and 7947120 [123] disclose adsorption processes that employ zeolite for CO_2 capture and utilize the heat of compression of the resulting CO_2 rich stream in

the desorption step. Here, the CO_2 rich stream is compressed after the adsorption-desorption step and the heat generated is used for matching the heat demand, resulting in significant requirement of energy to carry out the process.

World Patent WO 2012083108 [124] discloses sodium carbonate enriched sorbent based adsorption process for CO_2 capture. The method utilizes the exothermic heat from the adsorber via heat exchange with LPG or propane as the working fluid for production of power. This requirement of additional LPG or propane adds to the costs and inventory.

US Patent 5917136 [125] discloses a pressure swing adsorption process for CO_2 capture that uses modified alumina adsorbents. The modified adsorbents have CO_2 sorption capacities of about 0.11-0.29 mmol/g, however, they are of expensive nature.

Most of the above mentioned processes for capturing CO_2 from air or flue gas stream utilize heat from an external source together with the heat made available by compressing the desorbed vapor product (pure CO_2). However, this type of heat utilization does not significantly improve the cost-efficiency of the process.

The process makes use of dry regenerable solid sorbent to remove CO_2 from refinery flue gas stream available at relatively high temperature. The use of moderate temperature flue gas in the CO_2 capture step has the potential to reduce efficiency penalties with respect to generic amine absorption methods. In principle, the combustion flue gas is put in contact with the sorbent in a suitable reactor to allow the gas-solid reaction of CO_2 with the sorbent (usually the carbonation of an alkali metal carbonate). Hence, the development of an energy efficient and economic process as well as system for the removal of CO_2 present in flue gases that overcomes the drawbacks associated with the above prior arts is required.

8.2 Generic amine absorption process

The idea of separating CO_2 from flue gas started in the 1970s – not out of concern about greenhouse gas emissions but as a source of potential economically valuable CO_2, mainly for enhanced oil recovery. Taking a clue from industries that needed to remove acid gas impurities (e.g. H_2S and CO_2) from their flow stream, the power industry started to explore the use of chemical absorbents, specifically monoethanolamine (MEA) solvent, to capture CO_2. Typical amine absorption process for CO_2 capture uses 30 wt.% MEA with chemical inhibitors to prevent amine degradation and equipment corrosion. The advantages and disadvantages of

MEA absorption technology is described in Table 8.1. Despite the cost and inefficiency, amine scrubbing is now a key technology for post-combustion capture. The major players in MEA-based technology for CO_2 capture amine process are namely: MHI, Fluor Daniel Inc., Dow Chemical Co., Kerr-McGee Chemical Corp. and ABB Lummus Crest Inc., Typically, about 75% to 90% of the CO_2 is captured using these technologies, producing a nearly pure (> 95%) CO_2 product stream. Table 8.2 shows a comparison of the various commercial amine absorption and other processes. One of the most critical parameters needs to be discussed in the absorption based CO_2 capture processes is the regeneration energy requirement of the spent absorbent. From Table 8.2, it is seen that MEA-based absorption process requires twice of regeneration energy as compared to solid-based adsorption processes. The specific reason for this higher regeneration requirement in case of absorption route is energy requirement for vaporization of water in absorbing media. Moreover, direct cooling of flue gas (from 200 ^oC to 40 ^oC) in direct contact cooler (DCC) is also considered to be heat losses and thereafter, flue gas carries more water vapour in absorber, which also demands more regeneration energy in the stripper. In addition, amine degradation is more prominent in the absorber in presence of oxygen in flue gas, which increases the make-up solvent rate in the absorber. Based on these energy and reliability issues, the conventional amine absorption process is very difficult to make a cost-effective energy-integrated process for CO_2 capture.

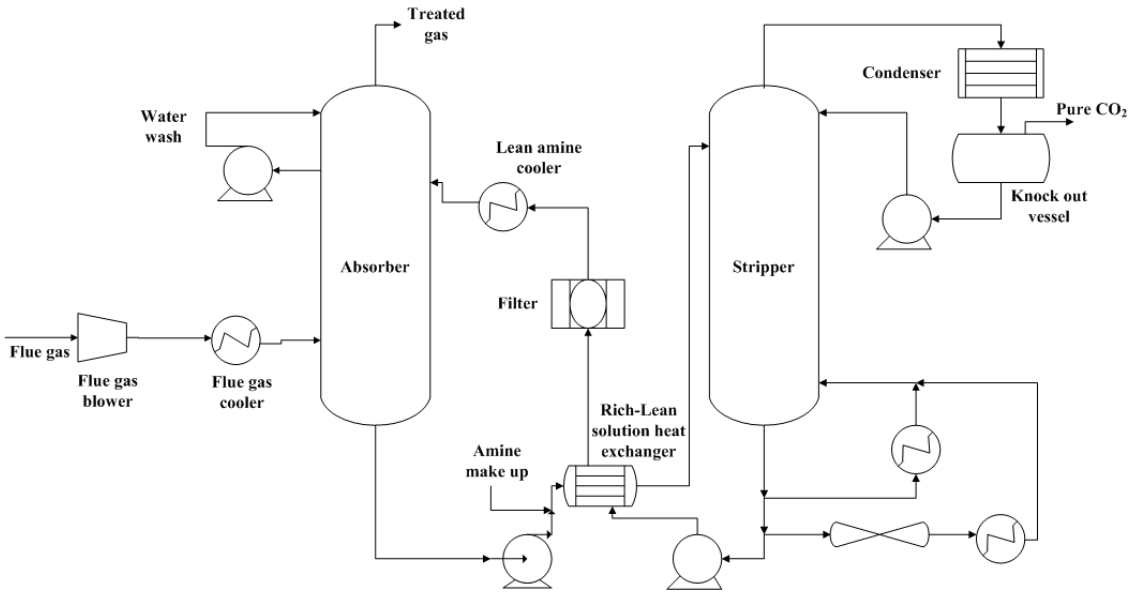

Figure 8.1 Schematic of MEA solvent absorption process for CO_2 capture [2]

The amine process has four main elements as shown in Figure 8.1 *viz.* (i) flue gas cooling and compression, (ii) CO_2 absorption, (iii) CO_2 regeneration using steam stripping columns, and

(iv) compression of pure CO_2. Amines in the water solution react with CO_2 in the absorber, forming chemical compounds that separate CO_2 from the gas mixtures at a higher rate than the natural CO_2 absorption in pure water. The MEA, which is a primary amine, produces the carbamate ion when it reacts with CO_2. The main advantages in using MEA/water solutions are its high CO_2 loading (0.5 mole CO_2/mole MEA ~ 0.108 kg CO_2/kg solution). Its main drawback is the stability of the carbamate ion that makes the regeneration more heat demanding to regenerate the solvent. Flue gases containing acid gases such as SO_2 and NO_2 react with MEA to form heat-stable salts that reduce the CO_2 absorption capacity of the solvent and raise the MEA make-up to cover additional losses. Thus, very low concentrations of these gases (typically 10 ppm) are desirable to avoid excessive loss of solvent.

Table 8.1 Advantages and disadvantages of MEA absorption technology

S. No.	**Advantages**	**Disadvantages**
1	It is demonstrated technology with some commercial plants around the world.	It has a high stripping energy requirement. The steam used to run the reboiler contributes significantly to OPEX. During amine regeneration, part of water gets vaporized while stripping out the CO_2 from amine. This increases the heat demand by more than double of the theoretical heat of desorption for amine-CO_2 system.
2	The solvent has reasonable rates of absorption/desorption but requires a significant amount of packing.	Significant solvent vapor losses are experienced because of the higher vapor pressure of the amine. This can be overcome with a water wash section at the top of the column.
3	It possesses a high solution capacity and high alkalinity so it can readily react with acid components such as CO_2.	The loaded amine causes corrosion to carbon steel equipment and hence, stainless steel will have to be used or corrosion inhibitors added to the solvent.
4	It can be reclaimed easily relative to other amines.	The amine suffers from both oxidative and thermal degradation. This requires make-up solvent and introduces an additional cost component for solvent make-up.

The flue gas entering the absorber bottom flows up counter-currently to the lean amine solution. The CO_2 in the flue gas reacts chemically with the lean MEA while the purified gas is vented

to the atmosphere, and the solvent enriched by CO_2 is pumped from the absorber to a lean-rich heat exchanger (L-R HeX). The rich amine solution is preheated in the lean-rich exchanger by the hot lean solution returning from the stripper on its way back to the absorber. The rich amine solution enters the top of the stripper where it flows counter-currently to the stripping steam generated in the reboiler. Steam and solvent vapors move up the stripper and condense as CO_2 is liberated. Uncondensed steam and CO_2 leave the top of the stripper and then enter the reflux condenser. The condensate is returned to the system while CO_2 is removed. The lean solution is pumped from the bottom of the stripper directly to the L-R HeX. The solvent leaves the L-R HeX after giving up heat to the rich solution and then enters a cooler, where its temperature is further lowered before being returned to the absorber.

In spite of primacy for gas absorption using alkanolamine solutions for CO_2 capture, this process suffers from number of shortcomings. For example, it generates severe corrosion of the equipment, and the regeneration of amine solutions is highly energy intensive. These drawbacks have been widely documented, prompting a search for alternative technologies. One viable route is adsorption which, compared to other separation processes, is recognized to be attractive to complement or replace the current absorption technology due to its low energy requirement and higher CO_2 capture capacity.

Table 8.2 Common chemical solvents used in CO_2 capture absorption processes [8, 117-121, 128-130]

Key Parameters	**Absorption Process**					**Ammonia Process**		**Carbonate Process**	
	Generic Amine Process	Econamine Process	KM-CDR MHI (KS-1/2/3)	Cansolv Process	Siemens	ECO_2 Process	Chilled Ammonia Process	Benfield Process	UNO MK 3
Process Licensor	Dow, Exxon, Lurgi, Union Carbide	Fluor	Mitshubishi Heavy Industries	Shell	Siemens	Powerspan Clean Energy Tech	Alstom	Eickmeyer, Exxon, Lurgi, Union Carbide, Vetrocoke,	CO2CRC
Sorbent /Solvent	MEA	30% wt. MEA + inhibitors	Sterically hindered MEA + promoter	Tertiary amine (DIPA+ MDEA) + promoter	Aq. Amino Acid Salts	Ammonium Carbonate	Ammonium Carbonate	20-40 %wt. K_2CO_3	20-40 %wt. K_2CO_3
Absorption temp. (C)	35 - 50	35 - 50	35 - 50	35-40	40-45	25 - 60	0 – 10	50 – 70	50 – 80
Abs capacity (RL:LL)	0.4 : 0.25 mol/mol	0.4 : 0.25 mol/mol	0.545 : 0.25 mol/mol	0.4 -0.75 : 0.2 mol/mol	0.4 –0.05 mol/mol	0.9 kg /kg NH_3	1.2 kg /kg NH_3	NA	NA
Regeneration temp. (C)	100- 110	100-110	100 - 110	100 - 110	90-105	100-125	100-125	100 - 120	150
Heat of Reaction (kcal/kg CO_2)	470	470	350	245	215	145	145		
Regeneration Energy (kcal/kg CO_2)	1075 -1565	775-955	585-650	475	550-830	645-670	400-530	680-850	480-600
Steam requirement (ton/ton CO_2)	2.0	2.3	1.2 – 1.5	1.25	1.2	1.53	1.94	NA	NA
Electricity (kWh/ton CO_2)	70	40	11	20	41	46	NA	NA	NA

Cooling water (ton/ton CO_2)	70 – 105	70-105	NA	NA	35 - 45	NA	NA	NA	NA
Solvent /Sorbent consumption (kg/ton CO_2)	1.0 – 3.0	1.6	0.35	< 0.1	0.1	0.2	1000 – 3000 ppm	NA	NA
Corrosion (milli-inch / yr)	More than sec/tert amine 76 - 93	8.9	3.1 - 3.9	Non corrosive wrt. MEA	Non corrosive wrt. MEA	Non corrosive wrt. MEA	Non corrosive wrt. MEA	NA	NA
Impurities handled	SOx: <20 ppm NOx: 10 ppm	SOx in FG = 10-40 ppmw	NA	NA	NA	SOx & NOx reacts to form fertilizer	NE (saleable byproduct)	NA	NA
Thermal Degradation	> 150C (2.5 - 6% per week)	Less than MEA	90% less than MEA (>200C)	NA	Higher stability	Very stable	NA	NA	NA
Oxidative degradation	Forms NH_3 & -COOH	Less than MEA	90% less than MEA	NA	Higher stability	Very stable	NA	NA	NA
Polymerization	Polycarba-mate ineffective < 100 ^oC	NA	NA	NA	NA	NA	NA	NA	NA
Solvent/Sorbent Cost ($/kg)	1.3 – 3.9	2.3	1.75	NA	6.15	0.175 –0. 25	NA	NA	NA
Others						Difficult regeneration of NH_3 from its carbonate salts.			

NA: Not available

8.3 Base-case study with MEA absorption process

The simulations were developed in ProMax (ProMax *ver* 3.2) as open loop simulations in order to perform parametric simulations. ProMax uses Electrolyte ELR-Peng Robinson property package. TSWEET kinetics was used to estimate the kinetic effects of CO_2-MEA system in the absorber and desorber. In ASPEN, simulations were not converged in a closed-loop model for CO_2 capture plant, wherein, ProMax converged closed-loop model simulations. The simulations were designed to incorporate a number of design specifications on the reboiler duty and the heat exchangers in order to converge in a closed loop. The flow sheet model used to simulate the system for MEA is shown in Figure 8.2.

The flow sheet is composed of three distinct sections and all are interlinked by cross-connector in ProMax. Section A is the flue as cooling and absorption section. Section B consists of L-R HeX and CO_2 desorption unit while Section C refers to the CO_2 compression section. In Section A and B, the Electrolyte-ELR model was used to model the system while in Section C the Peng-Robinson equation was used.

Figure 8.2 (a-c) depicts the operation and Table 8.3 summarizes the performance study of a typical amine based absorption plant for recovery of CO_2 from flue gas. The flue gas is pressurized through blower so as to overcome the pressure-drop in the direct contact cooler (DCC) and the absorption column. Before the flue gas enters the absorption column, it is cooled in DCC by circulating cooling water. The outlet temperature of DCC is set at 40 ^oC as this allegedly maximizes CO_2 absorption. It is found that increasing temperature from 20 ^oC to 40 ^oC, increased CO_2 uptake due to an increase in the rate of the reaction between CO_2 and MEA and increasing temperature from 40 ^oC to 65 ^oC, decreased CO_2 absorption because of Henry's constant increasing with temperature.

(a) MEA Absorption Unit

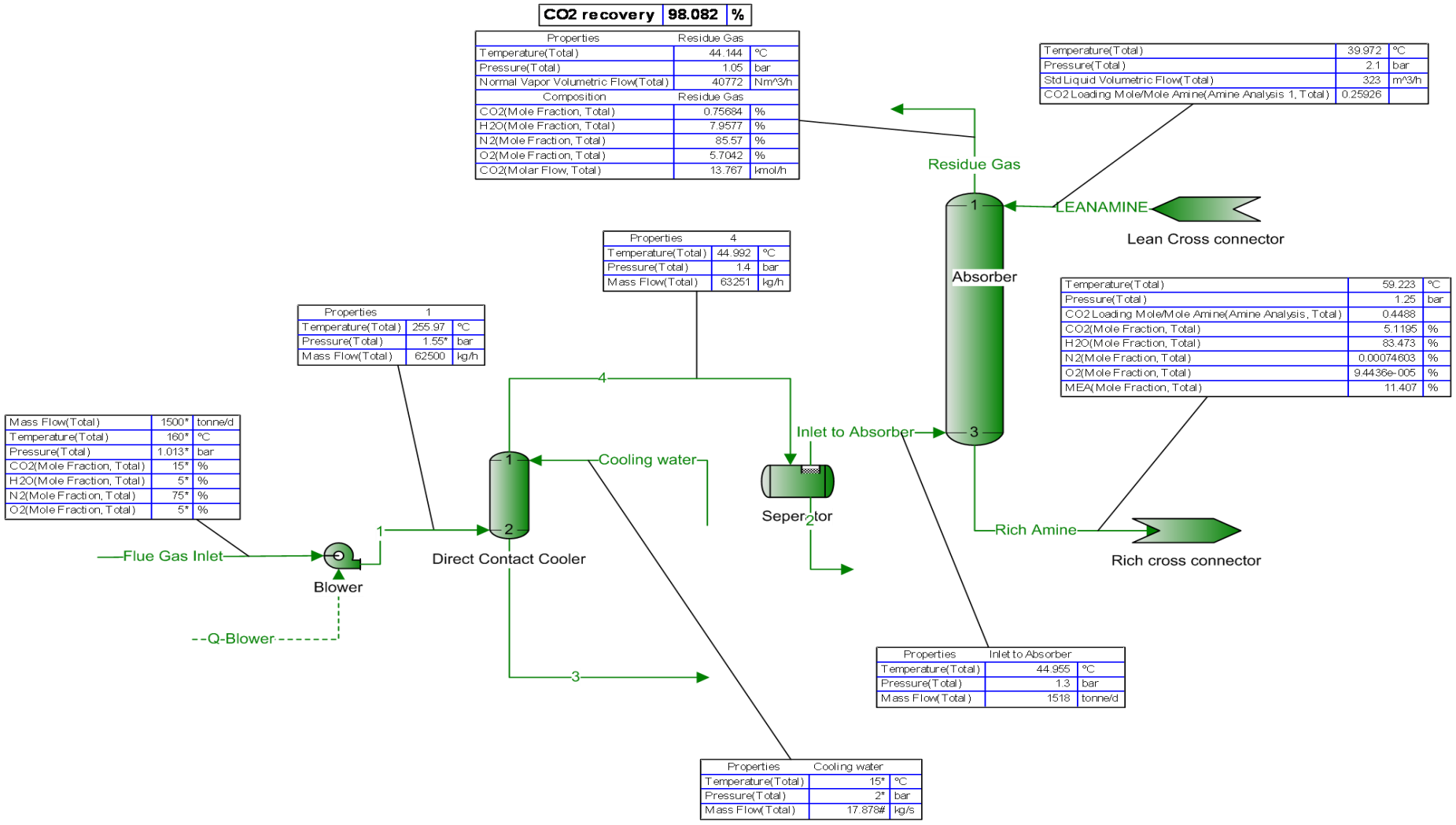

(b) MEA Regeneration Unit

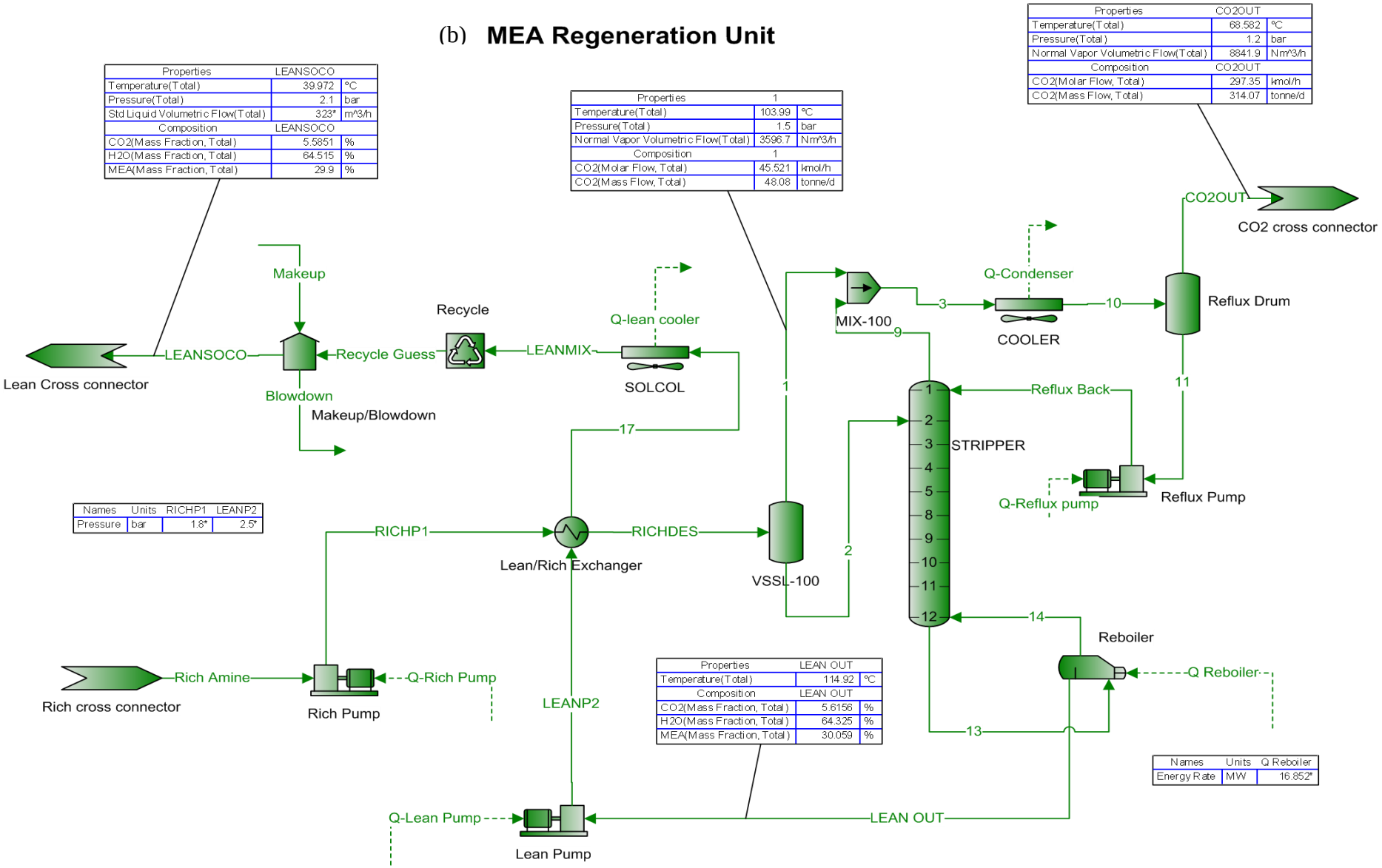

(c) CO_2 Compression

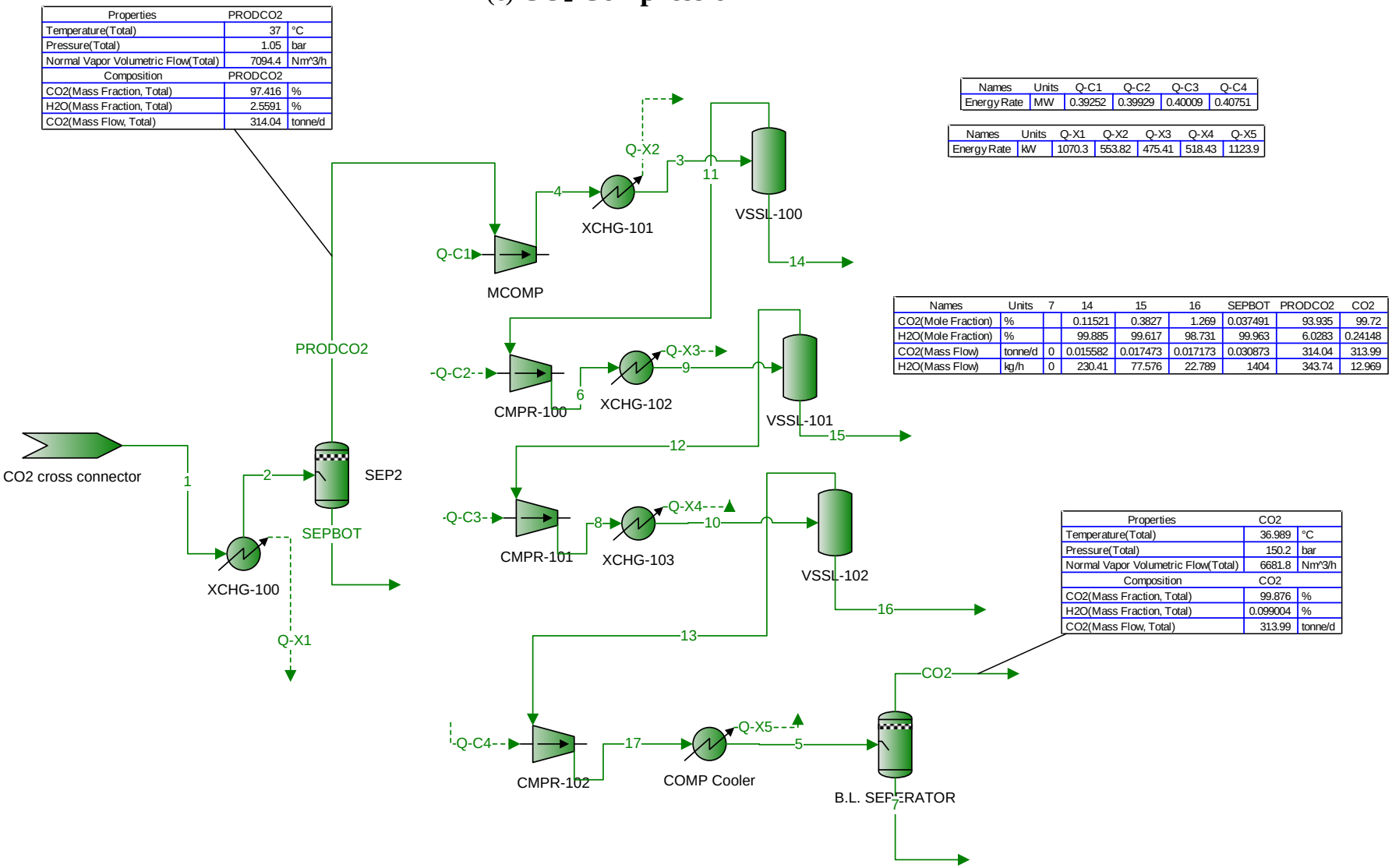

Figure 8.2 MEA absorption process for CO_2 Capture in ProMax (a) MEA absorption unit, (b) MEA regeneration unit and (c) CO_2 compression

Table 8.3 ProMax simulation performance study for amine based absorption for 13.125 TPH CO_2 capture

Flue Gas Parameters	
Composition (vol%)	CO_2: H_2O: N_2: O_2 = 15: 5 : 75: 5
Temperature and Pressure	160 ^oC, 1.013 bar
Flow rate	62.5 TPH
Unit Operation Model	
Blower	
Flue gas pressure (OUT)	1.55 bar
Flue gas temperature (OUT)	255 ^oC
Direct Contact Cooler	
Cooling water required (IN)	64.36 TPH
Temperature and Pressure of flue gas (OUT)	44.99 ^oC, 1.4 bar
Mass flow rate of flue gas (OUT)	63.2 TPH
Separator	
Temperature and Pressure of flue gas (OUT)	44.95 ^oC and 1.3 bar
Flow rate of flue gas (OUT)	63.2 TPH
Absorber	
Lean amine solution stream (IN)	
Flow rate, Temperature, Pressure	320.59 TPH, 39.97 ^oC, 2.1 bar
Lean amine loading	0.259 mol CO_2/mol amine or 0.056 kg CO_2/kg solution
Composition	CO_2 : H_2O : MEA = 5.58 : 64.58 : 29.9
Rich amine solution stream (OUT)	
Flow rate, Temperature, Pressure	333.69 TPH, 59.22 ^oC, 1.25 bar
Rich amine loading	0.44 mol CO_2/mol amine or 0.0947 kg CO_2/kg solution
Composition	CO_2 : H_2O : MEA = 9.28 : 61.98 : 28.72 (rest N_2 & O_2)
Treated flue gas (OUT)	
Flow rate, Temperature, Pressure	50.15 TPH, 44.14 ^oC, 1.05 bar
Rich Pump	
Rich amine (OUT)	
Flow rate, Temperature, Pressure	333.69 TPH, 59.23 ^oC, 1.8 bar

Lean-Rich Heat Exchanger (L-R HeX)	
Lean amine from stripper (IN)	
Flow rate, Temperature, Pressure	318.85 TPH, 114.92 ^{o}C, 1.6 bar
Composition	CO_2 : H_2O : MEA = 5.61 : 64.32 : 30.05
Lean amine from L-R HeX (OUT)	
Flow rate, Temperature, Pressure	318.85 TPH, 62.95 ^{o}C, 2.3 bar
Composition	CO_2 : H_2O : MEA = 5.61 : 64.32 : 30.05
Solvent Cooler	
Lean amine from solvent cooler (OUT)	
Flow rate, Temperature, Pressure	318.85 TPH, 40 ^{o}C, 2.1 bar
Composition	CO_2 : H_2O : MEA = 5.61 : 64.32 : 30.05
Intermediate Flash Separator	
Rich amine (OUT)	
Flow rate, Temperature, Pressure	329.61 TPH, 103.9 ^{o}C, 1.5 bar
Composition	CO_2 : H_2O : MEA = 8.79 : 62.12 : 29.07
Stripper	
Stripper Bottom (Lean amine) (OUT)	
Flow rate, Temperature, Pressure	346.18 TPH, 113.67 ^{o}C, 1.6 bar
Composition	CO_2 : H_2O : MEA = 5.97 : 66.26 : 27.76
Reboil Stream (IN)	
Flow rate, Temperature, Pressure	27.33 TPH, 114.91 ^{o}C, 1.6 bar
Composition	CO_2 : H_2O : MEA = 10.10 : 88.9 : 0.987
Stripper overhead (OUT)	
Flow rate, Temperature, Pressure	23.13 TPH, 101.05 ^{o}C, 1.45 bar
Composition	CO_2 : H_2O : MEA = 47.96 : 52.03 : 0.0032
Stripper reflux (IN)	
Flow rate, Temperature, Pressure	123.76 TPH, 68.59 ^{o}C, 2.03 bar
Composition	CO_2 : H_2O : MEA = 0.104 : 99.82 : 0.065
Stripper condenser	
Stream (IN)	
Flow rate, Temperature, Pressure	27.21 TPH, 101.47 ^{o}C, 1.45 bar
Composition	CO_2 : H_2O : MEA = 48.13 : 51.82 : 0.0297
Stream (OUT)	
Flow rate, Temperature, Pressure	27.21 TPH, 70 ^{o}C, 1.3 bar

Composition	CO_2 : H_2O : MEA = 48.13 : 51.82 : 0.0297
Lean Pump	
Lean amine (OUT)	
Flow rate, Temperature, Pressure	333.69 TPH, 114.93 ^oC, 2.5 bar
Composition	Same as stripper bottom
COMPRESSOR	
Stream (IN)	
Flow rate, Temperature, Pressure	13.43 TPH, 37 ^oC, 1.05 bar
Composition	CO_2 : H_2O : MEA = 99.87 : 0.021 : 0.003
Pure CO_2 (OUT)	
Flow rate, Temperature, Pressure	13.09 TPH, 36.96 ^oC, 150 bar
Composition	CO_2 : H_2O : MEA = 99.87 : 0.021 : 0.003

8.4 Proposed energy-integrated CO_2 capture process

The amine based absorption is energy intensive due to large amount of heat required for the regeneration of amine solution. In order to get rid of process related glitch, the below mentioned process is claimed to be more energy-saving in terms of process utility consumption. This process has been applied for patent in India (3190/MUM/2013). The development of heat integrated process involves harnessing the heat associated with flue gas stream at 160 ^oC, 1 bar in fluidized bed reactor system.

Till now, the patent landscape indicates the CO_2 capture studies in fixed bed reactor using zeolite adsorbent with heat integration [125] and fluidized bed reactor using supported alkali carbonate adsorbent without heat integration [126]. This process has its unique innovativeness in carrying out the reaction in fluidized bed reactor system as shown in Figure 8.3.

The process includes compressing the flue gas available at 160 ^oC and 1 bar to 1.6 bar through blower to raise the flue gas temperature to 238 ^oC. In order to reduce the flue gas temperature to carbonation reaction temperature, it is allowed to exchange its heat with heat transfer fluid like **Dowtherm** in heat exchanger **HeX-A**. The solid adsorbents allow such heat exchanger for flue gas cooling, while amine-based solvent would not allow heat exchange due to vaporization and degradation of amine at high temperature. A similar heat transfer is proposed for heating and cooling the adsorbent bed in **regenerator** and **carbonator** respectively. The fluidized bed reactor is employed for the carbonation reaction *i.e.* adsorption of CO_2 which is exothermic

(ΔH = - 570 kcal/kg CO_2 as calculated) in nature. It is desirable to cool the adsorbent bed in the carbonator during adsorption to keep it isothermal and maximize the CO_2 loading. The fluidized condition in carbonator also assists in maintaining uniform temperature distribution in the reactor system. The cooling water coil in the carbonator provides rapid cooling to maintain fast kinetics and minimizes the total adsorption time. The treated gas exits from the top of carbonator at 70 ^oC.

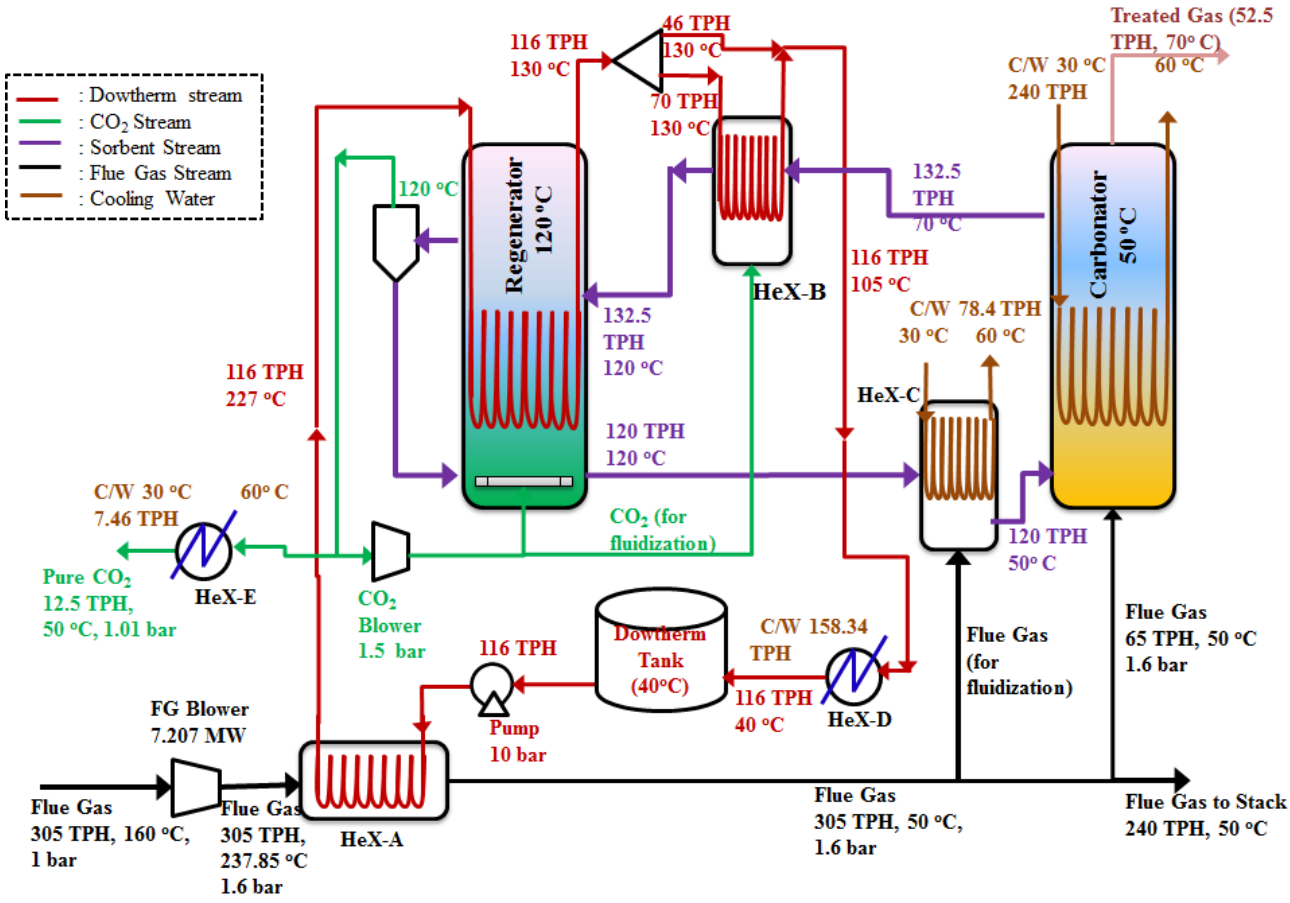

Figure 8.3 Schematic of proposed energy-integrated process for CO_2 capture (Patent Application No.: 3190/MUM/**2013**)

The spent sorbent at 70 ^oC from carbonator is heated to ~120 ^oC in sorbent heater (**HeX-B**) by circulating Dowtherm, and then is routed to regenerator. The regeneration reaction is carried out in another fluidized bed reactor called regenerator which is maintained at 120 ^oC by Dowtherm from **HeX-A**. The solid sorbents have the potential for significant energy savings over liquid solvents (in amine absorption process), because they avoid the need for the large quantities of water that must be repeatedly heated and cooled to regenerate the solvent solution. This reduces the cost of regeneration. Sorbent materials also have lower heat capacity than solvents and thus require less regeneration energy to change their temperature.

The pure CO_2 obtained at 120 ^oC is passed through cyclone separator and then cooled in **HeX-E** using cooling water. Some portion of pure CO_2 is pressurized to 1.5 bar and used as fluidizing media in regenerator and **HeX-B**. The regenerated adsorbent is cooled in **HeX-C** with cooling water to 50 ^oC for necessary carbonation reaction in carbonator. The heat exchanger **HeX-D** is used to cool Dowtherm from **HeX-B** to 40 ^oC for further use, as cooling media in **HeX-A**.

In this process, Dowtherm loop is significant heat carrier for sufficient heating required elsewhere in the process scheme. The heat exchangers used in this process scheme provide close temperature approach and also flexibility in heat transfer. Herein, in this process heat integration is important for the thermal efficiency of the process. The heat content in flue gas after blower operation should be efficiently harnessed by the Dowtherm to satisfy for necessary heat demand in regenerator. The operating conditions and performance estimates are shown in Table 8.4.

Table 8.4 Operating conditions and performance estimates for heat integrated CO_2 capture process

Flue Gas Parameters	
Composition (vol%)	CO_2: H_2O: N_2: O_2 = 21.57: 6.13 : 70.34: 1.96
Temperature and Pressure	250 ^oC, 1.013 bar
Flow rate	150 TPH
Unit Operation Model	
Blower	
Flue gas pressure (OUT)	1.6 bar
Flue gas temperature (OUT)	340 ^oC
Heat Exchanger (HeX-A)	
Dowtherm (IN): Flow rate, Temperature, Pressure	57 TPH, 40 ^oC, 10 bar
Dowtherm (OUT): Flow rate, Temperature, Pressure	57 TPH, 330 ^oC, 8.4 bar
Flue gas (OUT): Flow rate, Temperature, Pressure	150 TPH, 50 ^oC, 1.6 bar
Carbonator	
Flue gas (IN): Flow rate, Temperature, Pressure	65 TPH, 50 ^oC, 1.6 bar
Reaction temperature	50 ^oC

Treated gas (OUT): Flow rate, Temperature, Pressure	52.5 TPH, 70 ^{o}C, 1.4 bar
Spent adsorbent (OUT): (flow rate, temperature)	132.5 TPH, 70 ^{o}C
Cooling water (in heat transfer coil)	
Flow rate, temperature (in and out)	218 TPH, 32 ^{o}C (IN) and 60 ^{o}C (OUT)
Adsorbent Heater (HeX-B)	
Spent adsorbent (OUT): flow rate, temperature	132.5 TPH, 119 ^{o}C
Dowtherm (IN): Flow rate, Temperature, Pressure	57 TPH, 130 ^{o}C, 7 bar
Dowtherm (OUT): Flow rate, Temperature, Pressure	57 TPH, 80 ^{o}C, 6 bar
Regenerator	
Regenerated sorbent (OUT): flow rate, temperature	120 TPH, 120 ^{o}C
Dowtherm (IN): Flow rate, Temperature, Pressure	57 TPH, 330 ^{o}C, 10 bar
Dowtherm (OUT): Flow rate, Temperature, Pressure	57 TPH, 130 ^{o}C, 9 bar
Regeneration temperature	120 ^{o}C
Adsorbent Cooler (HeX-C)	
Regenerated sorbent (OUT): flow rate, temperature	120 TPH, 50 ^{o}C
Cooling water : Flow rate, Temperature	84 TPH, 32 ^{o}C (IN) and 60 ^{o}C (OUT)
Dowtherm Cooler (HeX-D)	
Dowtherm (IN): Flow rate, Temperature, Pressure	57 TPH, 80 ^{o}C, 6 bar
Dowtherm (OUT): Flow rate, Temperature, Pressure	57 TPH, 40 ^{o}C, 5 bar
Cooling water : Flow rate, Temperature	51 TPH, 32 ^{o}C (IN) and 60 ^{o}C (OUT)
CO_2 Product Cooler (HeX-E)	
Cooling water : Flow rate, Temperature	7 TPH, 32 ^{o}C (IN) and 60 ^{o}C (OUT)

8.5 Operating expenditure (OPEX) estimation for amine absorption process and energy- integrated CO_2 capture process

This section intends to establish a framework for quantifying the impacts of associated cost factors *viz.* steam and power consumption, cooling water requirement for carbon capture process by both conventional amine process and energy-integrated process. The Table 8.5 shows how operating parameters closely influence the cost figures and promotes new technology options. The major driving forces in reducing capture cost are the development of better sorbents with lower regeneration energy requirement and process energy integration.

Table 8.5 Cost comparison between MEA absorption process and energy-integrated CO_2 capture process (excluding compression and sorbent/solvent cost)

Factors	**Conventional MEA based absorption process for CO_2 capture**	**Energy-integrated CO_2 capture process**
Flue Gas	CO_2:15, H_2O:5, O_2:5, N_2:75 (vol%) at 160 ^oC and 1.013 bar	CO_2:16, H_2O:10, O_2:2, N_2:72 (vol%) at 250 ^oC and 1.013 bar
Target	314 TPD	300 TPD
Regeneration temperature ΔH_{Regen}	100 – 120 ^oC 700 kcal/kg CO_2	120 ^oC 570 kcal/kg CO_2
Rich Loading	0.097 (kg CO_2/kg solvent)	0.130 (kg CO_2/kg sorbent)
Electricity Power Consumption		
Blower/Pump	1.8 MW [a]	4 MW [a]
Steam Consumption		
Steam	2.05 ton /ton CO_2 [b]	0.0 ton/ton CO_2 [b]
Cold Utility Requirement		
Cooling water	59 ton/ton CO_2 [c]	29 ton/ton CO_2 [c]
OPEX	**54 $/ton CO_2**	**17 $/ton CO_2** [d]

Cost values:

[a] Power: 46$/MWhr

[b] Steam: 21.15 $/ton (16.5$/MWhr)

[c] Cooling water: 0.08 $/$m^3$

[d] 90% of cost calculated is due to power required in the flue gas blower which in turn depends on the heat of regeneration to be supplied in the regenerator for K_2CO_3 based adsorbent.

8.6 Innovative features of the energy-integrated circulating fluidized bed process

The proposed energy-integrated circulating fluidized bed process for CO_2 capture from flue gas streams has the unique innovativeness of utilization of heat of flue gas for meeting the energy required for thermal regeneration of adsorbent in the regenerator. The heat content in the flue gas after blower operation is efficiently harnessed by the Dowtherm in the flue gas cooler to meet the energy demand for adsorbent regeneration. Moreover, Dowtherm is a high boiling point heat transfer media having high heat capacity (1.5-2.5 kJ/kg.K) to capture heat from flue gas with low consumption of Dowtherm. In this proposed energy-integrated process, Dowtherm is circulated to utilize heat in the adsorbent heater (HeX-B) to heat the adsorbent from 70 ^oC to 130 ^oC. After harnessing of heat from flue gas, part of the flue gas (very small quantity) is used as a fluidization media in the adsorbent cooler and major quantity is diverted to the stack. This process is designed to facilitate a single compression system for capturing CO_2 from flue gas, wherein power requirement for the flue gas blower is estimated using ASPEN simulator as 7.2 MW. The proposed process excludes the utilization of steam for adsorbent regeneration and utility requirement is also less. As a result, cost for CO_2 capture is estimated as low as one-third of conventional amine absorption process.

8.7 Conclusions

The proposed energy-integrated process for CO_2 capture from flue gas stream is very cost-effective, energy-intensive process. The estimated cost per ton of CO_2 captured is found to be one third of the cost associated with conventional amine absorption process. Significant improvements on utility and power requirement helps to make heat integrated based CO_2 capture more economically competitive. An important feature of the study is analysis of key performance parameters that influence the cost economics. Understanding the nature of these impact, and the potential for reducing them, is crucial to projecting future costs and capabilities of new technologies for carbon capture.

Chapter 9

Conclusions and Recommendations

9.1 Conclusions

In this study, we explored various adsorbents and processes for capturing CO_2 from low CO_2 concentration (dilute) flue gas streams. The following main conclusions are obtained from this research work:

1. The CO_2 adsorption studies have been performed at 45 to 65 ^oC using 8 vol% of CO_2, 0-15 vol% of H_2O and rest N_2 in simulated flue gas mixture in a fixed bed system. The K_2CO_3-based adsorbents are prepared successfully using single- and multi-step incipient wet impregnation method. There is a significant enhancement in CO_2 adsorption capacity by employing multi-step as compared to single-step wetness impregnation approach by improving dispersion of active phase. Multi-step impregnation facilitates improved dispersion of active component on the alumina support resulting in higher specific surface area and pore volume of adsorbents, and significant improvement in the adsorption breakthrough time. The adsorbents with higher loading requires higher temperature (>300 ^oC) for regeneration due to the formation of stable component on the adsorbed species. The regeneration efficiency is also improved for MI prepared adsorbents due to the limited chance of blockage of meso-pores.

2. An improved regeneration properties of various K_2CO_3-based γ-Al_2O_3 adsorbents have been studied for the first time, to the best of author's knowledge. The modification of γ-Al_2O_3 as a support material by (i) thermal treatment and (ii) alkaline treatment followed by calcination helps to reduce the formation of stable component like $KAl(CO_3)_2(OH)_2$ during CO_2 adsorption. The presence of deactivating component e.g. $KAl(CO_3)_2(OH)_2$ in the adsorbents exhibits low adsorption capacity over multiple cycles and requires high temperatures for regeneration (>300 ^oC). The modification of supports as well as adsorbents helps to decrease the regeneration temperature drastically from 300 ^oC to 130 ^oC. γ-Al_2O_3 calcined at 950 ^oC significantly reduces the surface acidity and hence decreases the formation of $KAl(CO_3)_2(OH)_2$ to much extent. It is found that higher the calcination temperature, higher is the acidity reduction of the support material. The adsorbent gets almost completely regenerated at 130 ^oC over multiple cycles. There is approximately 30% reduction of total regeneration time at higher GHSV (750 h^{-1}). The dissolution of K_2CO_3 in de-ionized water at elevated temperature (70 ^oC) does not permit higher loading to achieve high adsorption capacity as K_2CO_3 forms crystals/aggregates on the outside of the support, which reduces active sites for CO_2 adsorption. All the K_2CO_3-

based adsorbents show high attrition resistance (<10%), which indicates large applicability in commercial fluidized bed CO_2 capture process.

3. A spray-dried alumina supported modified adsorbent with 35 wt% K_2CO_3 loading was used to study the effect of various operating parameters on the CO_2 removal efficiency in both batch (non-circulating) and in continuous circulating mode at pilot scale level. In circulating fluidized bed capture process the mode of injecting water vapor in the adsorber bed has significant impact on the extent of CO_2 removal. Introducing water vapor injection using temperature controlled gas bubbler arrangement provides higher CO_2 removal efficiency as compared to direct injection of steam as bubbling of flue gas through water avoids any local condensation of water in the flue gas feed line, adsorber and in the adsorbent loop. The circulating fluidized bed process is stable at carbonation temperature of 75-80 ^oC. An increase in water vapor content in the simulated flue gas at low gas velocity also provides higher CO_2 removal efficiency. The adsorbent shows CO_2 removal ranging from 52 to 81% for H_2O/CO_2 ratio within the range 0.75 to 1.91 studied with regeneration at 150 ^oC. The studies on effect of sweep gases like CO_2 and N_2 during regeneration of the adsorbent are important for scaling the process up to commercial level. The percent CO_2 removal using N_2 as sweep gas is 76.25%, while it is reduced to 50.7% with CO_2 as sweep gas. Lowering of temperature difference between adsorption and regeneration (50-70 ^oC) would be helpful in reducing energy demand for the process. This process provides partial regeneration of adsorbents in the desorber, which helps to retain hydrated active species K_2CO_3. 1.5 H_2O in the regenerated adsorbent. This active species provides less energetic sites for CO_2 adsorption in circulating fluidized bed process at a low temperature differential between adsorption and desorption. This is the first time it is reported that continuous CO_2 removal is performed with lower temperature differential between adsorption and desorption (40-50 ^oC).

4. The development of low cost energy-intensive process for CO_2 capture is performed in this work. Amine based absorption process was evaluated using ProMax equilibrium model to develop energy-integrated adsorptive CO_2 capture process. A cost comparison with conventional amine absorption process was made with the proposed developed process. The proposed energy-integrated process for CO_2 capture from flue gas stream is very cost-effective, energy-intensive process. The estimated cost per ton of CO_2 captured is found to be one third of the cost associated with conventional amine absorption process.

5. Like K_2CO_3, initially the Na_2CO_3-based adsorbents prepared by incipient wet impregnation method shows lower CO_2 adsorption capacity at flue gas temperature of 55 °C and CO_2 content of about 8 v/v% at 20-wt% Na_2CO_3 loading. It is found that the lower CO_2 adsorption capacity with these adsorbent systems is due to the effect of water content in flue gas streams. That is why the role of water content in feed simulated flue gas needs to be examined. Moreover, textural properties of the support material play an important role to achieve higher CO_2 adsorption capacity. Homogeneous dispersion of active phase needs to be assured to produce available active sites for CO_2 adsorption.

9.2 Recommendations

- Further study should be carried out to understand how K_2CO_3 is dispersed inside the Al_2O_3 pores by multi-step impregnation method using effective pore modeling. The analysis using high resolution transmission electron microscopy (HRTEM) could provide ample information about the thickness of K_2CO_3 inside the meso-pores during every successive impregnation.
- Further study should be undertaken to quantify the distribution of Lewis acidity (L, strong acidity) and Brönsted acidity (B, weak acidity) of the total acidity of the support material using pyridine-FTIR method. This study will provide the ratio of L/B distribution during varying calcination temperature, and their impact on stabilization of support material.
- For process design, the adsorption kinetic models for low temperature CO_2 adsorption should be investigated.
- Further study should be undertaken to assess the effects of various impurities (like, SO_x, NO_x, and particulate matter) on CO_2 adsorption-regeneration characteristics in achieving overall capture process.
- For a cost-effective demonstration of commercial CO_2 capture plant, further research should be undertaken based on the fouling studies of these K_2CO_3/Al_2O_3 adsorbents. This study will be helpful to evaluate the adsorbent thermal and hygroscopic properties in heat transfer equipment during simultaneous heating and cooling.
- Further study should be undertaken to develop high capacity adsorbent with hybrid adsorbent concept to minimize regeneration temperature and also further reduction of temperature differential between adsorption and desorption.

References

References

[1] National Aeronautics and Space Administration (NASA) Earth Observatory report GISS Surface Temperature Analysis, 2014, Accessed from http://data.giss.nasa.gov/gistemp/graphs_v3/

[2] Metz, B., Davidson, O., Coninck, H., Loos, M., Meyer L. Carbon Dioxide Capture and Storage, *IPCC Special Report*, **2005**.

[3] World Energy Outlook 2007 report, IEA **2007**, p-11.

[4] Energy Technology Perspectives 2012 report, IEA **2012**.

[5] IPCC workshop on carbon dioxide capture and storage, Regina, Canada, 18-21 November **2002**, *ECN publication*.

[6] Rossi, F., Olguı´n, E. J., Diels, L., and Philippis, R. D. Microbial fixation of CO_2 in water bodies and in drylands to combat climate change, soil loss and desertification. *N. Biotechnol*. **2015**, *32*, 109-120.

[7] Folger, P. Carbon Capture: A Technology Assessment, *Congressional Research Service* 7-5700, November 5, **2013**.

[8] Rao, A.B., Rubin, E.S. A technical, economic and environmental assessment of amine-based CO_2 capture technology for power plant greenhouse gas control. *Environ. Sci. Technol*. **2002**, *36*, 4467-4475.

[9] Brett, P., Spigarelli, S., Komar K. Opportunities and challenges in carbon dioxide capture, *J CO_2 Utilization*, **2013**, *1*, 69-87.

[10] Yang, H., Xu, Z., Fan, M., Gupta, R., Slimane, R., Bland, A., Wright, I. Progress in carbon dioxide separation and capture: A review. *J. Environ. Sci*. **2008**, *20*, 14-27.

[11] Choi, S., Drese, J.H., and Jones, C.W. Adsorbent materials for carbon dioxide capture from large anthropogenic point sources. *ChemSusChem*, **2009**, *2*, 796-854.

[12] Lee, S.C., Chae, H.J., Choi, B.Y., Jung, S.Y., Ryu, C.Y., Park, J.J., et al. The effect of relative humidity on CO_2 capture capacity of potassium-based sorbents. *Korean J Chem Eng.*, **2011**, *28*, 480-486.

[13] Zhao, C., Chen, X., Zhao, C. K_2CO_3/Al_2O_3 for capturing CO_2 in flue gas from power plants. Part 2: regeneration behaviors of K_2CO_3/Al_2O_3. *Energ. Fuel.* **2012**, *26*, 1406-1411.

[14] Lee, S.C., Choi, B.Y., Ryu, C.K., Ahn, Y.S., Lee, T.J., and Kim, J.C. The effect of water on the activation and the CO_2 capture capacities of alkali metal-based sorbents. *Korean J Chem Eng.*, **2006**, *23*, 374-379.

[15] Green, D.A., Nelson, T.O., Turk, B.S., Box, P., and Gupta, R.P. CO_2 capture from flue gas using dry regenerable solvents. *Final Technical Project Report, DOE Cooperative Agreement No.- DE-FC26-00NT40923, RTI*, **2007**.

[16] Hayashi H., Taniuchi J., Furuyashiki N., Sugiyama S., Hirano S., Shigemoto N., et al. Efficient recovery of carbon dioxide from flue gases of coal-fired power plants by cyclic fixed–bed operations over K_2CO_3-on-carbon. *Ind. Eng. Chem. Res.* **1998**, *37*, 185-191.

[17] Lee, S.C., Choi, B.Y., Lee, T.J., Ryu, C.K., Ahn, Y.S., and Kim, J.C. CO_2 absorption and regeneration of alkali metal-based solid sorbents. *Catal. Today*, **2006**, *111*, 385-390.

[18] Lee, S.C., Chae, H.J., Lee, S.J., Park, Y.H., Ryu, C.K., Yi, C.K., et al. Novel regenerable potassium-based dry sorbents for CO_2 capture at low temperatures. *J. Mol. Catal. B: Enzym.*, **2009**, *56*, 179-184.

[19] Lee, S.C., Kwon, Y.M., Ryu, C.Y., Chae, H.J., Ragupathy, D., Jung, S.Y., et al. Development of new alumina-modified sorbents for CO_2 sorption and regeneration at temperatures below 200 ^oC. *Fuel.*, **2011**, *90*, 1465-1470.

[20] Lee, S.C., Kwon, Y.M., Chae, H.J., Jung, S.Y., Lee, J.B., Ryu, C.K., et al. Improving regeneration properties of potassium-based alumina sorbents for carbon dioxide capture from flue gas. *Fuel.*, **2013**, *104*, 882-885.

[21] Zhao, C., Chen, X., Zhao, C. K_2CO_3/Al_2O_3 for capturing CO_2 in flue gas from power plants. Part 1: carbonation behaviors of K_2CO_3/Al_2O_3. *Energ. Fuel.* **2012**, *26*, 1401-1405.

[22] Zhao, C., Chen, X., Zhao, C. K_2CO_3/Al_2O_3 for capturing CO_2 in flue gas from power plants. Part 3: CO_2 capture behaviors of K_2CO_3/Al_2O_3 in a bubbling fluidized-bed reactor. *Energ. Fuel.* **2012**, *26*, 3062-3068.

[23] Aaron, D., Tsouris, C. Separation of CO_2 from flue gas: A review. *Separ. Sci. Technol.* **2005**, *40*, 321-348.

[24] Figueroa, J.D., Fout, T., Plasynski, S., McIlvried, H., Srivastava, R.D. Advances in CO_2 capture technology - the US Department of Energy's carbon sequestration program, *Int. J. of Greenhouse Gas Control*. **2008**, *2*, 9-20.

[25] Blomen, E., Hendriks, C., Neele, F. Capture technologies: Improvements and promising developments, *Energy Procedia*, **2009**, *1*, 1505-1512.

[26] Klara, S.M., Srivastava, R.D., McIlvried, H.G. Integrated collaborative technology development program for CO_2 sequestration in geologic formations - United States Department of Energy R&D. *Energy Conv Manage*, **2003**, *44*, 2699-2712.

[27] Garg, A., Shukla, P.R. Coal and energy security for India: Role of carbon dioxide (CO_2) capture and storage (CCS). *Energy*, **2009**, *34*, 1032-1041.

[28] Mall, I.D., Srivastava, V.C., Agarwal, N.K., Mishra, I.M. Adsorptive removal of malachite green dye from aqueous solution by bagasse fly ash and activated carbon-kinetic study and equilibrium isotherm analyses. *Colloids Surf. A: Physicochem. Eng. Aspects*, **2005**, *264*, 17–28.

[29] Mall, I.D., Srivastava, V.C., Agarwal, N.K., Mishra, I.M. Removal of congo red from aqueous solution by bagasse fly ash and activated carbon: Kinetic study and equilibrium isotherm analyses. *Chemosphere*. **2005**, *61*, 492-501.

[30] Sharma, M., Vyas, R.K., Singh, K. A review on reactive adsorption for potential environmental applications. *Adsorption*. **2013**, *19*, 161-188.

[31] Jain, S., Kumar, P., Vyas, R.K., Pandit, P., Dalai, A.K. Adsorption optimization of acyclovir on prepared activated carbon. *Can J Chem Eng*. **2014**, *92*, 1627-1635.

[32] Samanta, A.K., Zhao, A., Shimizu, K.H., Sarkar, P., Gupta, R. Post-combustion CO_2 capture using solid sorbents: A review. *Ind. Eng. Chem. Res*. **2012**, *51*, 1438-1463.

[33] Zhao, A., Samanta, A.K., Sarkar, P., Gupta, R. Carbon dioxide adsorption on amine-impregnated mesoporous SBA-15 sorbents: Experimental and kinetics study. *Ind. Eng. Chem. Res*. **2013**, *52*, 6480-6491.

[34] Steeneveldt, R., Berger, B., Torp, T.A. CO_2 capture and storage: Closing the knowing-doing gap. *Chem. Eng. Res. Des*. **2006**, *84*, 739-763.

[35] Thiruvenkatachari, R., Su, S., An, H., Yu, X.X. Post combustion CO_2 capture by carbon fibre monolithic adsorbents. *Prog. Energ. Combust*. **2009**, *35*, 438-455.

[36] Spigarelli, B.P., Kawatra, S.K. Opportunities and challenges in carbon dioxide capture, *J of CO_2 Utilization.* **2013**, *1*, 69-87.

[37] Dabrowski, A. Adsorption - from theory to practice. *Adv. Colloid Interfac*. **2001**, *93*, 135-224.

[38] Kentish, S.E., Scholes, C.A., Stevens, G.W. Carbon dioxide separation through polymeric membrane systems for flue gas applications. *Recent Patents on Chemical Engineering*, **2008**, *1*, 52-66.

[39] Sayari, A., Belmabkhout, Y. Stabilization of amine-containing CO_2 adsorbents: Dramatic effect of water vapor. *J Am. Chem. Soc*. **2010**, *132*, 6312-6314.

[40] Li, P., Zhang, S., Chen, S., Zhang, Q., Pan, J., Ge, B. Preparation and adsorption properties of polyethylenimine containing fibrous adsorbent for carbon dioxide capture. *J Appl. Polym. Sci*. **2008**, *108*, 3851-3858.

[41] Plaza, M.G., Pevida, C., Arias, B., Fermoso, J., Rubiera, F., Pis, J.J. A comparison of two methods for producing CO_2 capture adsorbents. *Energy Procedia*. **2009**, *1*, 1107-1113.

[42] Pevida, C., Drage, T.C., Snape, C.E. Silica-templated melamine-formaldehyde resin derived adsorbents for CO_2 capture. *Carbon* **2008**, *46*, 1464-1474.

[43] Thomas, W.J., Crittenden, B. Adsorption Technology and Design. *Elsevier Science & Technology Books*, ISBN: 0750619597, **1998**, 31-65.

[44] Fletcher, A.J. Porosity and Sorption Behavior. Accessed through http://personal.strath.ac.uk/ashleigh.fletcher/adsorption.htm#top.

[45] Maroto-Valer M. M., Lu, Z., Zhang, Y., Tang, Z. Sorbents for CO_2 capture from high carbon fly ashes. *Waste Manage*. **2008**, *28*, 2320-2328.

[46] Serna-Guerrero, R., Belmabkhout, Y., Sayari, A. Triamine-grafted pore-expanded mesoporous silica for CO_2 capture: Effect of moisture and adsorbent regeneration strategies. *Adsorption*, **2010**, *16*, 567-575.

[47] Dutta, B.K. Principles of Mass Transfer and Separation Processes, *Prentice Hall of India*, New Delhi. **2007**.

[48] Yang, R.T. Gas Separation by Adsorption Processes, *Imperial College Press*, London, **1997**.

[49] Xiao, P., Zhang, J., Webley, P., Li, G., Singh, R., Todd, R. Capture of CO_2 from flue gas streams with zeolite 13X by vacuum-pressure swing adsorption. *Adsorption*. **2008**, *14*, 575-582.

[50] Zhou, L., Wu, J., Li, M., Wu, Q., Zhou, Y. Prediction of multicomponent adsorption equilibrium of gas mixtures including supercritical components. *Chem. Eng. Sci*. **2005**, *60*, 2833-2844.

[51] Belmabkhout, Y., Serna-Guerrero, R., Sayari, A. Adsorption of CO_2 from dry gases on MCM-41 silica at ambient temperature and high pressure. 1: Pure CO_2 adsorption. *Chem. Eng. Sci*. **2009**, *64*, 3721-3728.

[52] Caskey, S.R., Wong-Foy, A.G., Matzger, A.J. Dramatic tuning of carbon dioxide uptake via metal substitution in a coordination polymer with cylindrical pores. *J Am. Chem. Soc*. **2008**, *130*, 10870-10871.

[53] Li, Y., Zhao, C., Chen, H., Liang, C., Duan, L., Zhou, W. Modified CaO-based sorbent looping cycle for CO_2 mitigation. *Fuel*. **2009**, *88*, 697-704.

[54] Yue, M.B., Sun, L.B., Cao, Y., Wang, J., Wang, Y., Yu, Q., Zhu, J.H. Promoting the CO_2 adsorption in the amine-containing SBA-15 by hydroxyl group. *Microporous Mesoporous Mater.* **2008**, *114*, 74-81.

[55] Abanades, J.C. The maximum capture efficiency of CO_2 using a carbonation/calcination cycle of $CaO/CaCO_3$. *Chem Eng J*. **2002**, *90*, 303-306.

[56] Jadhav, P.D., Chatti, R.V., Biniwale, R.B., Labhsetwar, N.K., Devotta, S., Rayalu. S.S. Monoethanol amine modified zeolite 13X for CO_2 adsorption at different temperatures. *Energ. Fuel*. **2007**, *21*, 3555-3559.

[57] Chatti, R., Bansiwal, A.K., Thote, J.A., Kumar, V., Jadhav, P., Lokhande, S.K., et al. Amine loaded zeolites for carbon dioxide capture: Amine loading and adsorption studies. *Microporous Mesoporous Mater*. **2009**, *121*, 84-89.

[58] Xu, X., Zhao, X., Sun, L., Liu, X. Adsorption separation of carbon dioxide, methane and nitrogen on monoethanol amine modified [beta]-zeolite. *J. Nat. Gas Chem*. **2009**, *18*,167-172.

[59] Plaza, M.G., Pevida, C., Arenillas, A., Rubiera, F., Pis. J.J. CO_2 capture by adsorption with nitrogen enriched carbons. *Fuel*. **2007**, *86*, 2204-2212.

[60] Somy, A., Mehrnia, M.R., Amrei, H.D., Ghanizadeh, A., Safari, M. Adsorption of carbon dioxide using impregnated activated carbon promoted by zinc. *Int. J. of Greenhouse Gas Control*. **2009**, *3*, 249-254.

[61] Chen, C., Yang, S.T., Ahn, W.S., Ryoo, R. Amine-impregnated silica monolith with a hierarchical pore structure: Enhancement of CO_2 capture capacity. *Chem. Commun*. **2009**, *24*, 3627-3629.

[62] Zhao, C., Chen, X., Zhao, C., Liu, Y. Carbonation and hydration characteristics of dry potassium-based sorbents for CO_2 capture. *Energ. Fuel*. **2009**, *23*, 1766-1769.

[63] Zhao, C., Chen, X., Zhao, C. CO_2 absorption using dry potassium-based sorbents with different supports. *Energ. Fuel*. **2009**, *23*, 4683-4687.

[64] Zhao, C., Chen, X., Zhao, C. Carbonation behavior of K_2CO_3 with different microstructure used as an active component of dry sorbents for CO_2 capture. *Ind. Eng. Chem. Res*. **2010**, *49*, 12212-12216.

[65] Zhao, C., Chen, X., Zhao, C. Multiple cycles behavior of K_2CO_3/Al_2O_3 for CO_2 capture in a fluidized-bed reactor. *Energ. Fuel*. **2010**, *24*, 1009-1012.

[66] Zhao, C., Chen, X., Zhao, C. Carbonation and active-component-distribution behaviors of several potassium-based sorbents. *Ind. Eng. Chem. Res*. **2011**, *50*, 4464-4470.

[67] Zhao, C., Chen, X., Zhao, C. Carbonation behavior and the reaction kinetic of a new dry potassium-based sorbent for CO_2 capture. *Ind. Eng. Chem. Res*. **2012**, *51*, 14361−14366.

[68] Zhao, C., Xiaoping, C., Edward, J.A., Xi, J., Lunbo, D., et al. Capturing CO_2 in flue gas from fossil fuel-fired power plants using dry regenerable alkali metal-based sorbent. *Progr Energ Combust Sci*. **2013**, *39*, 515-534.

[69] Seo, Y., Jo, S.H., Ryu, C.K., Yi, C.K. Effects of water pretreatment time and reaction temperature on CO_2 capture characteristics of a sodium-based solid sorbent in a bubbling fluidized bed reactor, *Chemosphere*. **2007**, *69*, 712-718.

[70] Park, Y., Jo, S.H., Park, K.W., Park, Y.S., and Yi, C.K. Effect of bed height on the carbon dioxide capture by carbonation/regeneration cyclic operations using dry potassium-based sorbents. *Korean J Chem. Eng*. **2009**, *26*, 874-878.

[71] Yi, C.K., Jo, S.H., Seo, Y.W., Park, S.D., Moon, K.H., Yoo, J.S., Lee, J.B., Ryu, C.K. Feasibility test for CO_2 capture by dry sorbents in two fluidized bed reactors, *4th Annual Conference on Carbon Capture and Sequestration*, DOE/NETL, **2005**.

[72] Kim, K-C, Park, Y.C., Jo, Sung-Ho, Yi, C.K. The effect of CO_2 or steam partial pressure in the regeneration of solid sorbents on the CO_2 capture efficiency in the two-interconnected bubbling fluidized-beds system, *Korean J. Chem. Eng*., **2011**, *28*, 1986-1989.

[73] Wu, Y., Chen, X., Dong, W., Zhao, C., Zhang, Z., Liu, D., Liang, C. K_2CO_3/Al_2O_3 for capturing CO_2 in flue gas from power plants. Part 5: Carbonation and failure behavior of K_2CO_3/Al_2O_3 in the continuous CO_2 sorption−desorption system, *Energy Fuels*, **2013**, *27*, 4804-4809.

[74] Jaiboon, O., Chalermsinsuwan, B., Mekasut, L., Piumsomboon, P. Effect of flow patterns/regimes on CO_2 capture using K_2CO_3 solid sorbent in fluidized bed/circulating fluidized bed, *Chem. Eng. Journal*, **2013**, *219*, 262-272.

[75] Jaiboon, O., Chalermsinsuwan, B., Mekasut, L., Piumsomboon, P. Effect of regeneration temperature on the composition and carbon dioxide sorption ability of a K_2CO_3/Al_2O_3 solid sorbent in a bubbling fluidized bed reactor. *Chem. Eng. Commun.* **2015**, *202*, 361-365.

[76] Li, P., Ge, B., Zhang, S., Chen, S., Zhang, Q., Zhao, Y. CO_2 capture by polyethylenimine-modified fibrous adsorbent. *Langmuir*. **2008**, *24*, 6567-6574.

[77] Chang, F.Y., Chao, K.J., Cheng, H.H., Tan, C.S. Adsorption of CO_2 onto amine-grafted mesoporous silicas. *Sep. Purif. Technol*. **2009**, *70*, 87-95.

[78] Arenillas, A., Smith, K.M., Drage, T.C., Snape, C.E. CO_2 capture using some fly ash-derived carbon materials. *Fuel*. **2005**, *84*, 2204-2210.

[79] Belmabkhout, Y., Serna-Guerrero, R., Sayari, A. Adsorption of CO_2-containing gas mixtures over amine-bearing pore-expanded MCM-41 silica: Application for gas purification. *Ind. Eng. Chem. Res*. **2009**, *49*, 359-365.

[80] Chang, A.C.C., Chuang, S.S.C., Gray, M., Soong, Y. In-situ infrared study of CO_2 adsorption on SBA-15 grafted with Î³-(aminopropyl)triethoxysilane. *Energy Fuels*. **2003**, *17*, 468-473.

[81] Sanz, R., Calleja, G., Arencibia, A., Sanz-Pérez, E.S. CO_2 adsorption on branched polyethyleneimine-impregnated mesoporous silica SBA-15. *Appl. Surf. Sci*. **2010**, *256*, 5323-5328.

[82] Park, K.W., Park, Y.S., Park, Y.C., Jo, S.H., Yi, C.K., Study of CO_2 carbonation-regeneration characteristics of potassium-based dry sorbents according to water vapor contents of inlet gas and regeneration temperature in the cycle experiments of bubbling fluidized-bed reactor. *Korean Chem. Eng. Res*. **2009**, *47*, 349-354.

[83] Li, L., Zhang, B., Wang, F., Zhao, N., et al. Study of the novel KMgAl sorbents for CO_2 capture. *Energ. Fuel*. 2013, 27, 5388-5396.

[84] Wang, W., Song, M. Multistep impregnation method for incorporation of high amount of titania into SBA-15. *Mater. Res. Bull*. **2006**, *41*, 436-447.

[85] Zhao, C., Chen, X., Zhao, C., Wu, Y., Dong, W. K_2CO_3/Al_2O_3 for capturing CO_2 in flue gas from power plants. Part 4: Abrasion characteristics of K_2CO_3/Al_2O_3 sorbents. *Energ. Fuel*. **2012**, *26*, 3062-3068.

[86] Choi, J.H., Yi, C.K., Jo, S.H. A model on an entrained bed-bubbling bed process for CO_2 capture from flue gas, in: Proceedings of the 13th International Conference on Fluidization-New Paradigm in Fluidization Engineering, *Eng. Conf. Int*. Korea, **2010**.

[87] Yi, C.K., Jo, S.H., Seo, Y., Lee, J.B., Ryu, C.K. Continuous operation of the potassium-based dry sorbent CO_2 capture process with two fluidized-bed reactors, *Int. J. of Greenhouse Gas Control*. **2007**, *1*, 31-36.

[88] Langmuir, I. The adsorption of gases on plane surfaces of glass, mica and platinum. *J. Am. Chem. Soc.* **1918**, *40*, 1361-1402.

[89] Barrett, E.P., Joyner, L.G., Halenda, P.P. The determination of pore volume and area distributions in porous substances. I. Computations from nitrogen isotherms. *J. Am. Chem. Soc.* **1951**, *73*, 373–380.

[90] Freundlich, H. Colloid and Capillary Chemistry, *Methuen, London*, **1926**, 114-122.

[91] Liu, Z., Wang, L., Kong, X., Li, P., Yu, J., Rodrigues, A.E. Onsite CO_2 capture from flue gas by an adsorption process in a coal-fired power plant. *Ind. Eng. Chem. Res.* **2012**, *51*, 7355–7363.

[92] Wang, L., Yang, Y., Shen, W., Kong, X., Li, P., Yu, J., Rodrigues, A.E. Experimental evaluation of adsorption technology for CO_2 capture from flue gas in an existing coal-fired power plant. *Chem Eng Sci*. **2013**, *101*, 615–619.

[93] Do, D.D. Adsorption Analysis: Equilibria and Kinetics, *Imperial College Press*, London, **1998**.

[94] Gargiulo, N., Pepe, F., Caputo, D. Modeling carbon dioxide adsorption on polyethylenimine-functionalized TUD-1 mesoporous silica, *J. Colloid Interface Sci.* **2012**, *367*, 348-354.

[95] Aksoylu, A.E., Akin, A.N., Sunol, S.G., Önsan, Z.I. The effect of metal loading on the adsorption parameters of carbon dioxide on coprecipitated nickel-alumina catalysts. *Tr. J. of Chemistry*, **1996**, *20*, 88-94.

[96] Naumov, S. Hysteresis phenomena in mesoporous materials. Dissertation report, *Leipzig University*, **2009**, 51-66.

[97] Vincent, R.C., Merril, R.P. Concentration profile in impregnation of porous catalysts. *J. Catal*., **1974**, *35*, 206-217.

[98] Sengupta, S., Reddy, S.A., Dongara, R., Das, A.K., Bhunia, H., Bajpai, P.K. Improvement in regeneration properties and multi-cycle stability for K_2CO_3/Al_2O_3 adsorbents for CO_2 capture from flue gas. *Energ. Fuel*. **2014**, *28*, 5354-5362.

[99] Rozita, Y., Brydson, R., and Scott, A.J. An investigation of commercial gamma-Al_2O_3 nanoparticles. *Journal of Physics: Conference Series*, **2010**, *241*.

[100] Jong, K.P. Synthesis of Solid Catalysts. *WILEY-VCH Verlag GmbH & Co. KGaA*, Weinheim. **2009**, 59-69.

[101] Li, G., Xiao, P., Webley, P. Binary adsorption equilibrium of carbon dioxide and water vapor on activated alumina, *Langmuir*. **2009,** *25*, 10666-10675.

[102] Sun, Z-X., Zheng, T-T., Bo, Q-B., Du, M., Forsling, W. Effects of calcination temperature on the pore size and wall crystalline structure of mesoporous alumina. *J. Colloid Interface Sci*. **2008**, *319*, 247-251.

[103] Trueba, M., Trasatti, S.P. γ-alumina as a support for catalysts: a review of fundamental aspects. *Eur. J. Inorg. Chem.* **2005**, 3393-3403.

[104] Reddy, S.A., Sengupta, S., Dongara, R., Das, A.K., Amte, V., et al. Stabilized inorganic oxide supports and adsorbents derived therefrom for carbon dioxide capture. Indian Patent Appl. 866/MUM/**2014**.

[105] Maciver, D.S., Tobin, H.H., Barth, R.T. Catalytic aluminas I. surface chemistry of eta and gamma alumina. *J. Catal*. **1963**, *2*, 485-497.

[106] Elio Santacesaria, E., Gelosa, D., Carra, S. Basic behavior of alumina in the presence of strong acids. *Ind. Eng. Chem., Prod. Res. Dev.* **1977**, *16*, 45-47.

[107] Chen, F.R., Davis, J.G., Fripiat, J.J. Aluminum coordination and Lewis acidity in transition aluminas. *J. Catal*. **1992**, *133*, 263-278.

[108] Boumaza, A., Favaro, L., Le´dion, J., Sattonnay, G., Brubach, J.B., Berthet, P., et al. Transition alumina phases induced by heat treatment of boehmite: an X-ray diffraction and infrared spectroscopy study. *J Solid State Chem*. **2009**, *182*, 1171-1176.

[109] Eklund, P., Sridharan, M., Singh, G., Bøttiger, J. Thermal stability and phase transformations of γ-/amorphous Al_2O_3 thin films. *Plasma Process. Polym*. **2009**, *6*, 907-911.

[110] Lippens, B.C., DeBoer, J.H. Study of phase transformations during calcination of aluminum hydroxides by selected area electron diffraction. *Acta Cryst*. **1964**, *17*, 1312-1321.

[111] Yang, X., Sun, Z., Wang, D., Forsling, W. Surface acid-base properties and hydration/ dehydration mechanisms of aluminum (hydr)oxides. *J. Colloid Interface Sci*. **2007**, *308*, 395-404.

[112] Gasc, F., Thiebaud-Roux, S., Mouloungui, Z. Methods for synthesizing diethyl carbonate from ethanol and supercritical carbon dioxide by one-pot or two-step reactions in the presence of potassium carbonate. *J. Supercrit. Fluids*. **2009**, *50*, 46-53.

[113] Iordan, A., Zaki, M.I., and Kappenstein, C. Formation of carboxy species at CO/Al_2O_3 interfaces. Impacts of surface hydroxylation, potassium alkalization and hydrogenation as assessed by in situ FTIR spectroscopy. *Phys. Chem. Chem. Phys.*, **2004**, *6*, 2502-12.

[114] Okunev, A.G., Sharonov, V.E., Gubar, A.V., Danilova, I.G., Paukshtis, E.A., Moroz, E.M., et al. Sorption of carbon dioxide by the composite sorbent potassium carbonate in porous matrix. *Russ. Chem. Bull. Int Ed*. **2003**, *52*, 359-363.

[115] Okunev, A.G., Sharonov, V.E., Aistov, Y.I., Parmon, V.N. Sorption of carbon dioxide from wet gases by K_2CO_3–in-porous matrix: influence of the matrix nature. *React. Kinet. Catal. Lett*. **2000**, *71*, 355-362.

[116] Rao, A.B., Rubin, E.S., Keith, D.W., Morgan, M.G. Evaluation of potential cost reductions from improved amine-based CO_2 capture systems. *Energy Policy*. **2006**, *34*, 3765–3772.

[117] Folger, P. Carbon Capture: A Technology Assessment, *Congressional Research Service* 7-5700, July 19- **2010**.

[118] IEA Greenhouse Gas R&D Programme report, Evaluation of novel post-combustion CO_2 capture solvent concepts. Technical study, Report no. 2009/14.

[119] DOE/NETL Advanced CO_2 Capture R&D Program: Technology Update May **2013**.

[120] Endo, T., Kajiya, Y., Nagayasu, H., Iilima, M., Ohishi, T., Tanaka, H., Mitchell, R. Current status of MHI CO_2 capture plant technology, large scale demonstration project and road map to commercialization for coal fired flue gas application, *Energy Procedia*. **2011**, *4*, 1513-1519.

[121] Reddy, S., Gilmartin, J. 2008. *Econamine FG Plus*^{SM} *Technology for Post-Combustion* CO_2 *Capture.* Presented at the Seventh Annual Conference on Carbon Capture and Sequestration, Pittsburgh, PA, May 5-8, **2008**.

[122] Kelley, B.T., Deckman, H.W., Hershkowitz, F., Northrop, P.S., Ravikovitch, P.I. Temperature swing adsorption of CO_2 from flue gas utilizing heat from compression. US Patent US 7731782 B2, **2010**.

[123] Deckman, H.W., Kelley, B.T., Hershkowitz, F., Chance, R.R., Northrop, P.S., Corcoran Jr., E.W. Temperature swing adsorption of CO_2 from flue gas using a parallel channel contractor. US Patent, US 7947120 B2, **2011**.

[124] Gupta, R.P., Jamal, A. Heat recovery from sorbent-based CO_2 capture. World Patent, WO 2012083108 A3, **2012**.

[125] Gaffney, T.R., Golden, T.C., Mayorga, S.G., Brzozowski, J.R., Talyer, F.W. CO_2 pressure swing adsorption process using modified alumina adsorbents. US Patent, US 5917136, **1999**.

[126] Grover, B.S. Process and apparatus recovery for CO_2 from flue gas with thermocompression. US Patent 8137439, **2012**.

[127] Yi, C.K., Jin, G.T., Sun, D.W., Bae, D.H., Park, J.H., Ryu, H.J. and Lee, S.Y. Carbon dioxide capturing device including water vapor pretreatment apparatus. US Patent 8241408, **2012**.

[128] Harkin, T., Hoadley, A., Hooper, B. Process integration analysis of a brown coal-fired power station with CO_2 capture and storage and lignite drying, *Energy Procedia*, **2009**, *1*, 3817–3825.

[129] Harkin, T., Hoadley, A., Hooper, B. Reducing the energy penalty of CO_2 capture and compression using pinch analysis. *J Clean. Prod.* **2010**, *18*, 857-866.

[130] Anderson, C., Harkin, T., Ho, M., Mumford, K., Qader, A., Stevens, G., Hooper, B. Developments in the CO2CRC UNO MK 3 Process: A multi-component solvent process for large scale CO_2 capture, *Energy Procedia*, **2013**, *37*,225 – 232.